Microplastics in Coastal Marine Habitats and Food Webs

by

Garth Aidan Covernton

B.Sc., University of British Columbia, 2012

A Dissertation Submitted in Partial Fulfillment of the
Requirements for the Degree of

DOCTOR OF PHILOSOPHY

in the Department of Biology

We acknowledge with respect the Lekwungen peoples on whose traditional territory the university stands and the Songhees, Esquimalt and W̱SÁNEĆ peoples whose historical relationships with the land continue to this day.

Microplastics in Coastal Marine Habitats and Food Webs

by

Garth Aidan Covernton
B.Sc., University of British Columbia, 2012

Supervisory Committee

Dr. John Dower, Co-Supervisor
Department of Biology and School of Earth and Ocean Sciences

Dr. Sarah Dudas, Co-Supervisor
Department of Biology and Fisheries and Oceans Canada

Dr. Francis Juanes, Departmental Member
Department of Biology

Dr. Helen Gurney-Smith, Departmental Member
Department of Biology, Fisheries and Oceans Canada

Dr. Chris Pearce, Outside Member
Department of Geography, Fisheries and Oceans Canada

Abstract

Microplastic particles (MPs) are widely distributed in aquatic environments and present a potential risk to marine life. This thesis considers several issues relating to methodologies for sampling and analyzing MPs and the sources and fate of these particles in the marine environment, wild and farmed shellfish, and food webs of southern coastal British Columbia, Canada.

Chapter 1 introduces MPs as a contaminant, methodologies for studying them, and reviews what is known about their source, fates, and ecotoxicology in marine environments. Chapter 1 also outlines the goals of this thesis.

Chapter 2 compares the potential MP concentration estimates provided by two different seawater sampling methods. Jar samples filtered to 8-µm yielded MP concentrations averaging approximately 8.5 times higher than bucket samples filtered to 63 µm, per L of water (at the site level), driven largely by differences in the number of microfibres. An analysis of MP concentrations and mesh sizes reported in the literature suggests that using a 300–350-µm mesh may underestimate total MP concentrations by one to four orders of magnitude compared with samples filtered through much smaller mesh sizes (*e.g.*, less than 100 µm), and despite the effect of sample volume. Particles less than 300 µm in diameter make up a large component of MPs commonly found in fish and invertebrates. As such, common sampling practices fail to adequately measure a biologically relevant class of MPs, thereby undermining the ability to quantify ecological risk.

Chapter 3 determines the influence of shellfish aquaculture activity, and its use of plastic equipment, on MPs in bivalves and their environment by comparing MP concentrations in Manila clams (*Venerupis philippinarum*) and Pacific oysters (*Crassostrea gigas*) grown on

commercial shellfish beaches with those grown on non-aquaculture beaches from six areas. MP concentrations in water and sediment were also determined in four of the areas. MP concentrations did not differ between shellfish aquaculture and non-aquaculture sites for either bivalve species or for sediment and water samples. Beach sediment type had a minor effect, with more gravelly or sandier beaches associated with higher MP concentrations in oysters or clams, respectively. Oysters on sites using many synthetic anti-predator nets had more MPs than those on sites without any plastic, but analysis of particles using Fourier-transform infrared spectroscopy suggested a predominance of textile fibres including nylon and polyester, which are not typically used in shellfish aquaculture.

Chapter 4 uses stable isotope food web analysis and hierarchical Bayesian generalized linear mixed models to explore whether bioaccumulation and biomagnification are occurring in coastal marine food webs at three locations. Bioaccumulation was higher for smaller-bodied suspension feeding animals such as bivalves. However, biomagnification was not occurring in animal digestive tracts, and trophic dilution was demonstrated in fish livers. Trophic transfer was shown to occur between prey and predator for rockfish, but higher concentrations in full stomachs compared with empty ones suggested rapid excretion of ingested MPs.

Chapter 5 supplies some general conclusions on the status of MPs in the British Columbian environment, as well as risks to seafood consumers. It also explores future work that will be needed to understand the complex ecotoxicology of MPs.

Table of Contents

List of Tables

List of Figures

Acknowledgements

I would like to acknowledge the help I have had with my research from many different people, without whom this work would not have been possible.

I would first like to thank my supervisors John Dower and Sarah Dudas for their guidance, as well as my committee members Chris Pearce, Helen Gurney-Smith, and Francis Juanes for their help over the years.

For collaboration on many of these projects and help coordinating fieldwork I would like to thank my fellow graduate student Kieran Cox. For technical help in the lab and field, I would like to thank Brenna Collicutt, Wendy Fleming, Hailey Davies, Shaye Tudor, Nelson Perks, and Brittany Buirs. For volunteer help in the lab and field, I would like to thank Maddie Beange, Morgan Black, Jenna Bright, Quinn Deo, Maggie Dietterle, Lauren Farmer, Raquel Greiter Loerzer, Colleen Haddad, Aurora Kalmari, Alessia Kockel, Abbie Mabey, Matt Miller, Layla Olefs, Jessica Qualley, Chrissy Schellenberg, Caitlin Smith, and Mykah Stonely.

I would especially like to thank Chelsea Rochman for inviting me to visit her lab in Toronto for four months to conduct the Raman spectroscopy for Chapter 4, and her lab group for making me feel so welcome there.

I would also like to acknowledge the various members of the UVic Ecostats group over the years for allowing me a place to learn and develop much of my statistical knowledge.

Dedication

I dedicate this work to my parents, Tom Covernton and Laurie Greenwood. Your unwavering support since my childhood has made so many things possible for me. Thank you for always supporting whichever path in life I chose to throw myself down, be it making loud rock music in your garage and attending my late-night shows at random bars in Vancouver or pursuing a career in science.

I also dedicate this to my friend Evan French, who lost his years-long battle with brain cancer in 2019. We were not always close, or even in the same city, yet I always felt we had such a special connection that shone through when we were together. From our shared love of trashy science fiction and action movies to our attitudes, humour, and philosophies of life. You went calmly, and gently, as you always did. I will never meet another like you, and I think of you every day.

Chapter 1: General Introduction

1.1 Introduction to microplastics

Microplastics (MPs) are a ubiquitous contaminant that have been found to occur in every environmental compartment that has been examined (Zhang *et al.* 2019b, Hale *et al.* 2020). In this thesis, I define MPs as being 1-5000 µm in length along their longest dimension, which is common in the field (Hartmann *et al.* 2019). MPs are further categorized by source as either primary, meaning that they were manufactured to size for a particular function, or secondary, meaning that they were produced *via* fragmentation and degradation of larger plastic objects, including textiles. MPs are also categorized on the basis of colour, and shape – generally fragments, foams, films, and lines or fibres (GESAMP 2019). Fibrous MPs are sometimes also referred to as microfibres, although this term may also include semi-synthetic (*e.g.,* viscose) fibres, as well as anthropogenic natural fibres like cotton, wool, and silk (Barrows *et al.* 2018, Singh *et al.* 2020). Here, I only consider synthetic microfibres as MPs. MPs are complex contaminants, and toxicity can vary greatly depending on their size, shape, polymeric composition (*e.g.*, polypropylene, high density polyethylene, low density polyethylene, polyvinyl chloride, polyurethane), chemical additives (*e.g.*, flame retardants, plasticizers, UV stabilizers), and contaminants that have been sorbed from the environment, including heavy metals, pesticides, pharmaceuticals, and persistent organic pollutants (Rochman *et al.* 2019).

1.2 Sources and pathways of microplastics into marine environments

MPs reach marine environments through a variety of pathways. They can be transported from land into the ocean either directly, or indirectly *via* freshwater runoff, by sewage and storm-drain effluent, aerial dispersal, or as macroplastics that then degrade *in situ* due to UV and mechanical weathering (Andrady 2011, Dris *et al.* 2016, Sutton *et al.* 2016, Gies *et al.* 2018).

Synthetic microfibres are one of the most omnipresent forms of MPs that have been found in the environment using current methodologies, and are thought to primarily originate from textiles (Browne *et al.* 2011, Barrows *et al.* 2018). These microfibres are released into the environment due to textile production, use, care, and disposal, with release of microfibres during laundering and eventual transit through sewage treatment (if present) being a well documented process (Liu *et al.* 2019). Although sewage treatment can effectively remove up to 10.2-99.9% of MPs (Cheng *et al.* 2021), the particles are often transferred into sludge, which may then be applied to agricultural land and cause entry of MPs into terrestrial systems, as well as release to aquatic environments *via* soil erosion and runoff (Zhang *et al.* 2020a, Crossman *et al.* 2020). MPs, including microfibres, are also transported by aerial dispersal and have been documented in even the most remote of environments (Dris *et al.* 2016, Bergmann *et al.* 2019, Napper *et al.* 2020). Runoff-associated synthetic rubber dust created during vehicle tire wear is another emerging and substantial source of at MPs into aquatic environments, with what may be the greatest potential for toxicity among MP types due to the presence of many associated contaminants, including additives and heavy metals (Ryberg *et al.* 2019, Lee *et al.* 2020, Tian *et al.* 2021).

1.3 Fate of microplastics within the marine environment

Once they reach the marine environment, MPs are transported by wind and currents, with dispersal distances varying according to particle size, shape, and density and minimal biodegradation occurring (Wang *et al.* 2016). MPs will either sink or float depending on whether their polymer density is greater or less than that of seawater, and their shape will further modulate sinking rates, with fibrous particles having lower sinking velocities than spherical particles (Van Melkebeke *et al.* 2020). Both empirical and modeling evidence suggests that many MPs released from coastal areas, especially in bays and estuaries, are likely to remain

trapped in these areas and eventually deposited into the sediment (Zhang *et al.* 2020b, Harris 2020). MPs less dense than seawater travel further than denser particles, explaining their pervasive occurrence in the global ocean and accumulation in areas where currents converge (Lima *et al.* 2021). However, such particles will eventually be biofouled or ingested by animals and then excreted as part of faeces, both of which increase their density and cause greater sinking rates and eventual deposition into sediment, although further resuspension may occur (Fazey and Ryan 2016, Pabortsava and Lampitt 2020, Harris 2020, Kvale *et al.* 2020, Carl *et al.* 2021). As such, it is becoming evident that MPs in the oceans eventually become sequestered in sediment, with floating plastics thought to enter the sediment within 3 years (Koelmans *et al.* 2017).

1.4 Ingestion of microplastics by marine animals

Many animals have been shown to contain MPs within their digestive tracts, with the size, shape, and number of particles ingested depending on habitat, body size, and feeding habits (Roch *et al.* 2020, Jâms *et al.* 2020). MPs can be mistaken for food particles (*i.e.* due to similarities in size, shape, and/or colour) by visual predators such as planktivorous fish carrying out active particle feeding, or by suspension feeders, such as bivalves and sea cucumbers, carrying out particle capture, followed by sorting and then ingestion or direct digestion, depending on species (Ory *et al.* 2017, 2018, Ward *et al.* 2019, Roch *et al.* 2020). MPs can also be ingested indirectly by predators *via* trophic transfer following their ingestion by prey species (Nelms *et al.* 2018, Welden *et al.* 2018). They can also enter animals through respiration, either becoming tangled in respiratory organs or subsequently ingested, for example *via* the gills of fish or the respiratory trees of sea cucumbers (Koongolla *et al.* 2020, Mohsen *et al.* 2020, Sun *et al.* 2021).

Once ingested, most MPs are then likely excreted from the bodies of animals, with smaller particles excreted at the slowest rates (Jovanović 2017, Graham *et al.* 2019). These smaller particles (<130 µm) therefore have the potential to translocate from digestive tracts and into the circulatory systems and tissues of animals, where they may have an increased possibility to cause harm (Murano *et al.* 2020, da Costa Araújo and Malafaia 2021). Such transfer rates may be low. For example, Zeytin *et al.* (2020) experimentally incorporated 1-5-µm fluorescently-labelled microspheres into feed for the European sea bass (*Dicentrarchus labrax*) and found that 1 particle reached the fish fillet for every 18,000,000 ingested particles, which is equivalent to 0.00005% of particles transferring into muscle tissue. Kim *et al.* (2020) found that 10-300 µm fluorescent-labelled polyethylene microspheres did not transfer to the liver or muscle of rainbow trout (*Oncorhyncus mykiss*) after two weeks of dietary exposure to high concentrations of particles. There is, however, also evidence of larger particle sizes being present in the organs of animals, for example up to 438-µm MPs in fish livers, although it is unclear how such particles may have been transferred to these organs (Collard *et al.* 2017, Abbasi *et al.* 2018).

1.5 Ecotoxicology of microplastics

Once ingested or inhaled, MPs have the potential to cause harm to organisms *via* several pathways. A recent meta-analysis by Jacob *et al.* (2020) found that in fish, primary virgin MPs (*i.e.* fresh from the manufacturer) affected 32% of endpoints that had been studied, including significant effects on behavioural, sensory, and neuromuscular functions, metabolism, the alimentary and excretory system, the microbiome, and the immune system. The effects of MPs are highly variable across taxa, although smaller organisms such as larval fish and zooplankton may be more susceptible (Foley *et al.* 2018). In addition, the presence and extent of the effects of MPs on animals are highly dependent on the duration of exposure, concentration, shape, size,

and polymer type of the particles. Many laboratory toxicology studies tend to expose organisms to high concentrations of small (<100 µm) MPs, with only around 17% of experimental studies testing environmentally relevant concentrations (Bucci *et al.* 2020). To date, most MP studies have relied on visual pre-selection of MP particles prior to chemical validation *via* spectroscopy, meaning that these smaller MPs are poorly quantified in the environment, thereby creating a mismatch between field and laboratory experiments which makes it difficult to conduct ecological risk assessments.

Toxicity caused by MPs can result from physical interactions with the MP particles themselves, or *via* transfer of residual monomers or sorbed chemicals, including additives (*e.g.*, flame retardants, plasticizers, UV-stabilizers) and contaminants from the environment (*e.g.*, heavy metals, pharmaceuticals, persistent organic pollutants such as PCBs and DDT). However, laboratory and modeling studies suggest that exposure to sorbed hydrophobic contaminants transferred by MPs may currently be minimal compared to background levels of exposure, and thus not lead to increased accumulation in animal tissues (Koelmans *et al.* 2013, 2016, Herzke *et al.* 2016, Besseling *et al.* 2017, Diepens and Koelmans 2018). As such, it seems likely that the main ecotoxicological effects of MPs occurring in the marine environment will arise as a result of their concentration, size, shape, and polymeric composition. For example, according to a recent meta-analysis, studies investigating the toxicology of MPs were more likely to find an effect when they used fibres or smaller particles. (Bucci *et al.* 2020).

Preliminary ecological risk assessments suggest that only 0.17% of the global ocean's surface layer (0-5 m), and 1.5% of the surface layer of fresh waters, have MP concentrations high enough to cause harmful ecological effects (Koelmans *et al.* 2020, Everaert *et al.* 2020). However, concentrations in marine sediment in certain areas may have already reached toxic

levels (*i.e.*, high enough to cause effects to growth and/or reproduction), and more of the ocean is expected to be at risk with increasing MP release to the environment throughout the 21st century (Everaert *et al.* 2018). Furthermore, although some of these risk assessments use probabilistic assessments to account for the underestimation of smaller MPs in current studies, they rely primarily on data resulting from short-term exposure experiments that measure only a limited number of endpoints at the organismal or molecular level (*e.g.*, growth, reproduction, oxidative stress). Thus, ecological risk assessments are not yet able to consider the effects of chronic exposure to MPs or effects on species interactions. Some limited laboratory work has demonstrated that exposure to environmentally relevant concentrations of MPs over even a relatively short-term period (30 days) can cause changes in the upregulation of the expression of genes associated with immunity and stress and downregulation of those associated with long-term reproduction (Raap 2019). As such, chronic health effects of MPs should not be ruled out of ecological risk assessments.

1.6 Methods for studying microplastics

Methods for studying environmental concentration of MPs in seawater, sediment, and animals, can generally be broken down into steps consisting of (i) sample collection, (ii) sample purification, and (iii) particle identification (Stock *et al.* 2020). Sample collection involves collecting whole organisms, taking sediment cores or grabs, and taking either bulk water samples or filtering large volumes through at least one filter, and often a series of sieves or filters. To examine the sample for MPs, it must be first purified *via* the removal of inorganic content and non-synthetic materials. This is done *via* a digestion step, commonly using a strong base or enzymes to remove biogenic material, followed by a density separation step involving a high-density salt solution if sediment needs to be removed (Lusher *et al.* 2020). The sample is then

filtered. From there, particles are located and enumerated by manual or automated methods and then chemically identified. Due to the high potential for background contamination of samples due to particles settling from the air, contamination mitigation measures should always be undertaken and procedural blanks run alongside samples (Brander *et al.* 2020).

Manual selection of MPs generally involves light microscopy, judgement of whether a particle is potentially synthetic, and then removal of the particle using forceps - followed by chemical identification by Raman or FTIR spectroscopy. A chemical identification step has become widespread practice in recent years, but researchers did not always include this step in earlier studies, meaning that older studies might tend to over-report MP concentrations. Due to difficulties in visually identifying and extracting smaller particles, the manual selection method is most effective for >100-µm particles (Lusher *et al.* 2020, Primpke *et al.* 2020). Newer automated methods involve scanning and automatic chemical identification of either the entire filter, subsamples of it, or algorithmic particle detection and scanning processes (Primpke *et al.* 2020). FTIR spectroscopy is commonly used for automated particle identification and can identify particles as small as 10-20 µm. Despite being more logistically challenging, Raman spectroscopy has also been used and can theoretically identify particles as small as 1-5 µm (Primpke *et al.* 2020). Another novel method for identifying MPs involves thermal analysis using a pyrolytic step following by characterization of degradation products *via* Gas Chromatography Mass Spectrometry (GCMS) (Primpke *et al.* 2020). While the other methods allow for the reporting of MP concentrations by particle counts and characterization of particle size and shape, thermal methods are mostly destructive, mass-based and do not allow classification of particles, although they can account for particles down into the nano scale

(Primpke *et al.* 2020, Peñalver *et al.* 2020). As I was unable to employ automated or thermal methods, the results presented in this thesis are therefore most relevant to MPs >100 µm in size.

1.7 Objectives and structure of this thesis

This work aims to fill several key data gaps relating to MP occurrence in the marine environment, in seafood, and in coastal marine food webs, and the resulting implications for marine ecological communities and human food production. Chapter 2 combines field and literature evidence to consider whether current sampling methodologies are underestimating the presence of ingestible MPs in seawater. I compare the efficiency of two commonly used shore-based sampling methodologies (using different mesh sizes) for measuring MPs in seawater, in addition to exploring the relationship between mesh size and MP concentrations in 36 studies from the literature. Chapter 2 has been published in *Science of the Total Environment* (Covernton *et al.* 2019a). Chapter 3 investigates the impact of shellfish aquaculture on MP concentrations in bivalve shellfish and their local environment. It involves a large-scale transplant experiment across four areas important to shellfish aquaculture in British Columbia. This chapter has been published in *Aquaculture Environment Interactions* (Covernton *et al.* 2019b). Chapter 4 explores trophic transfer, bioaccumulation, and biomagnification of MPs in nearshore marine food webs in coastal British Columbia and has not been published at the time this thesis was submitted. Throughout the three "data chapters", I use the first-person pronoun "we", as the work was collaborative in nature. I have combined the references from all chapters into one reference section at the end of the thesis and figures have been re-numbered from the published versions to be concordant.

Chapter 2 - Size and shape matter: A preliminary analysis of microplastic sampling technique in seawater studies with implications for ecological risk assessment

Covernton, G. A., C. M. Pearce, H. J. Gurney-Smith, S. G. Chastain, P. S. Ross, J. F. Dower, and S. E. Dudas. 2019. Science of The Total Environment 667:124–132.

2.1 Introduction

Current methods for measuring seawater MP concentrations, both ship- and shore-based, come with a variety of advantages and limitations. These methods generally consist of either large-volume samples that are mass filtered or sieved in the field (*e.g.*, manta-trawls, neuston nets, and continuous intake on larger research vessels) or smaller-volume discrete samples (*e.g.* Niskin bottles and other containers) that are collected and then filtered in the field or laboratory (GESAMP 2015, Löder and Gerdts 2015, Miller *et al.* 2017, Courtene-Jones *et al.* 2017). Large-volume sampling methods like manta-trawls are often selected due to the reduced effort required to sort and count MPs that exceed the filter-pore or mesh size (commonly 300–350 µm) (Miller *et al.* 2017). Some recent studies, however, have suggested that the mesh sizes used in these sampling strategies allow smaller particles, as well as long fibres, to pass through the mesh due to their relatively small widths, thereby potentially underestimating microfibre concentrations by orders of magnitude (Kang *et al.* 2015, Barrows *et al.* 2017).

While studies using larger mesh sizes (300–350 µm) generally acknowledge that they are targeting the larger size fraction of MPs and neglecting the smaller sized particles, the implications of leaving the smaller size fraction out of most concentration estimates are generally not discussed. Studies of MPs ingested by marine invertebrates and fish often report that fibres and/or particles < 300 µm in diameter represent a large fraction of the particles found, if not the majority (Leslie *et al.* 2017, Wieczorek *et al.* 2018, Pellini *et al.* 2018, Phuong *et al.* 2018).

Failure to characterize a size fraction of MPs that is commonly consumed by marine animals means that consideration of long-term ingestion risk based on reported MP concentrations will be based on underestimates of MP concentrations occurring in the field. A further discrepancy arises when considering that most toxicology studies have investigated the effects of MP ingestion on animals by using particles less than 300 µm (often less than 100 µm) in diameter. As such, much of the available information on the physiological and ecological impacts of MPs is based on particle sizes that many seawater sampling studies are not quantifying. If the goal of microplastics research is to reach a point where ecological risk assessments can be conducted and appropriate countermeasures taken to limit the exposure of wildlife to 'safe' levels of MPs, then this is a serious issue. With an increasing number of microplastics studies being published and many stakeholders (*e.g.* non-governmental organizations, governments, citizen scientists, industry) interested in documenting and reducing MP contamination, it is therefore important to develop standardized sampling practices and create marine MP distribution data that are comparable among studies and regions, as well as useful for predicting and testing the effects of continued MP contamination on marine organisms, food webs, and the safety and security of seafood.

This chapter quantifies the effect of mesh size on estimated MP concentrations in seawater and the potential implications for relating these values to ecosystem health impacts. We compared the efficiency of two simple, commonly used, shore-based sampling methodologies and investigated the relationship between mesh size and MP concentrations reported in the literature. We conducted sampling at six sites in Baynes Sound, British Columbia (BC), Canada, an area that has many residential properties, shellfish aquaculture sites, and several marinas. Three of the sites were active, intertidal shellfish farms and three were un-farmed beaches. We

compared 1-L jar samples which were filtered to 8 µm in the laboratory with 10-L bucket samples which were sieved to 63 µm in the field and subsequently filtered to 8 µm in the laboratory. All samples were visually analysed for potential MPs using light microscopy and the known physical characteristics of MPs. In addition, mesh sizes, sample volumes, and seawater MP concentrations reported in 46 studies in the scientific literature (resulting in 62 data points) were analysed to determine the degree to which mesh size and sample volume influence MP concentration estimates.

2.2 Methods

2.2.1 Study area

Seawater samples were collected from six sites in Baynes Sound, Vancouver Island, BC (Fig. 1), the region with the highest density of shellfish aquaculture in the province. The Sound is also surrounded by many small communities and several marinas on both Vancouver Island and Denman Island. Three of the chosen sites were active intertidal shellfish farms, the other three being reference areas not used for shellfish aquaculture. The Mud Bay (MB) and Deep Bay (DB) farms grow Pacific oysters (*Crassostrea gigas*) and Manila clams (*Venerupis philippinarum*) with extensive use of polyethylene anti-predator netting and fencing in the intertidal. The Ships Point (SP) farm is used only for oyster culture and so lacked clam predator netting but had some polyethylene plastic fencing. Non-aquaculture sites ranged in distance from the nearest active shellfish aquaculture area (~60 m (SPREF), ~130 m (MBREF), and ~250 m (DBREF)).

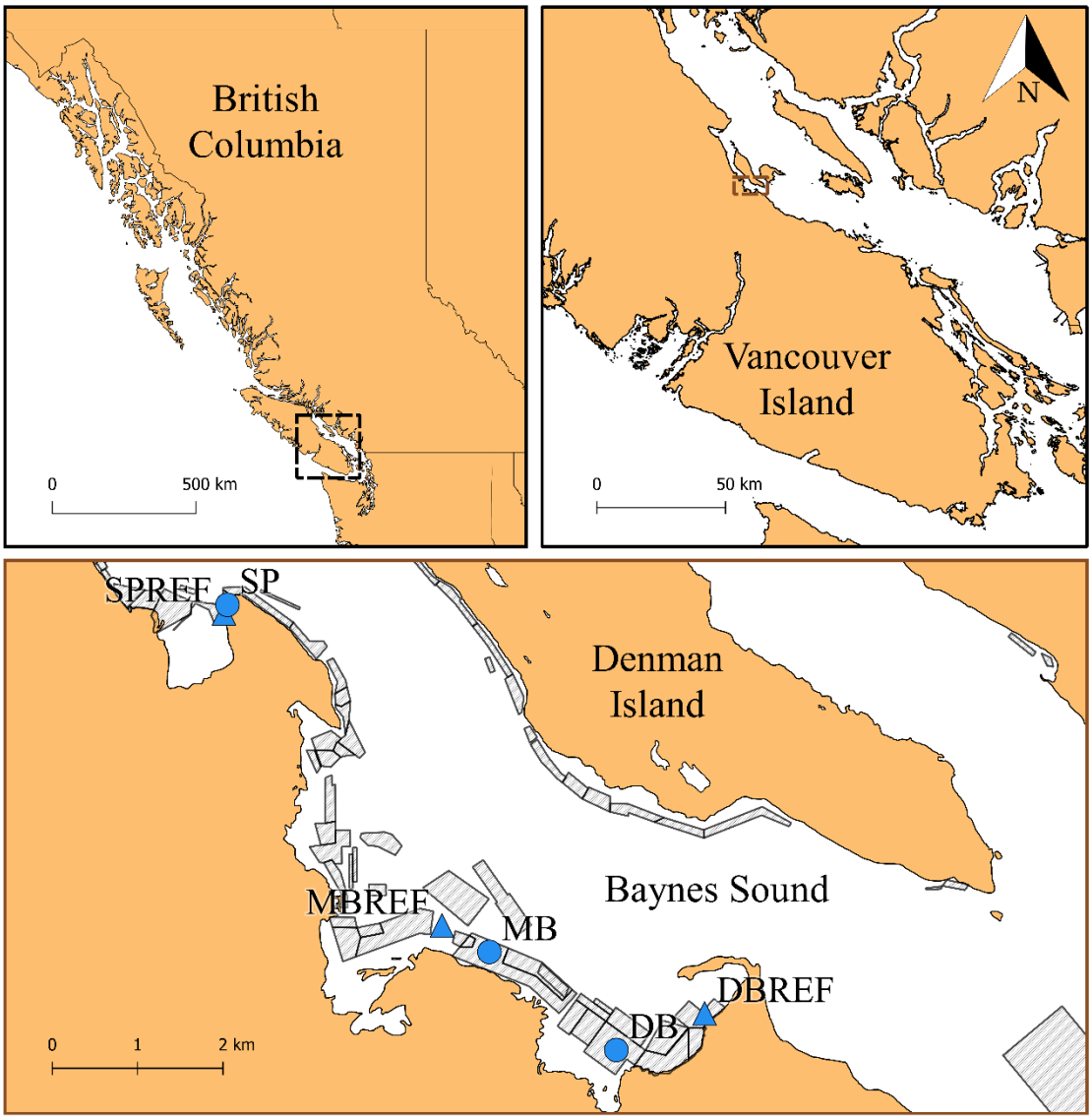

Figure 1: Map of seawater sampling collection sites in Baynes Sound, Vancouver Island, British Columbia, Canada. Shellfish aquaculture tenures are indicated by grey polygons. Circles and triangles indicate the sampling sites that were or were not, respectively, actively used for intertidal aquaculture at the time of the study. DBREF was previously farmed in 2014. Site abbreviations are: DB=Deep Bay, DBREF=Deep Bay Reference, MB=Mud Bay, MBREF=Mud Bay Reference, SP=Ships Point, and SPREF=Ships Point Reference.

2.2.2 Sample collection

To compare sampling methods, 1-L jar and 10-L bucket seawater samples were collected. These methods were selected as simple, commonly used, and cost-effective ways to collect shore-based water samples. Three replicate samples (for each method) were collected at each of the six sites during flood tide at the surface of ~1-m deep water by wading perpendicularly out from three flags placed in 20-m increments along a line parallel to the water's edge and collecting a representative sample for both methods at similar points. Jar samples were collected by first rinsing 1-L glass Mason jars with seawater and then quickly submerging them just below the surface. The lid was then tightly secured while holding the jar underwater. To avoid potentially contaminating the sample with particles from the lid's plastic lining, the lid was inverted so the all-metal surface was facing the sample. Bucket samples were collected by rinsing a 12-L stainless steel bucket with seawater and then pushing it straight down into the water, open side up, allowing it to fill with seawater until a line marking 10 L was reached. The bucket was then carried to shore and the water poured through a 63-µm stainless-steel sieve. We chose this mesh size because we hypothesized that it would exclude many fibres while capturing a plethora of small, non-fibrous MPs. The sieve was then rinsed into a 1-L glass Mason jar using an aluminium spray bottle holding distilled water, which had been vacuum filtered in the laboratory through a 1.6-µm Whatman GF/C filter paper. This jar was then capped as described above. All sample jars were taken to the laboratory and stored at -20°C until analysis.

2.2.3 Sample preparation

After thawing, the seawater was filtered through an 8-µm (nominal size) stainless steel woven mesh secured to the mouth of the Mason jar and the jar was inverted over a vacuum-filter assembly. Samples were then dried at 60°C for 48 hours or until a constant weight was

measured. To remove biological material, 100 mL of 10% potassium hydroxide (KOH) solution were added to each sample before covering with aluminum foil and incubating at 60°C for 24 hours. KOH is effective at removing biological material from samples (Foekema *et al.* 2013, Rochman *et al.* 2015) and a 24-hour incubation at 60°C has little effect on most plastic polymers (Dehaut *et al.* 2016).

After digestion, the samples were vacuum-filtered through a 47-mm diameter, 8-µm pore size polycarbonate (PCTE) membrane filter. Filter membranes were then placed in polystyrene PetriSlides for storage and later microscopic visualisation. The glass filter funnels were warmed before filtration, using de-ionised water at 60°C, to minimise precipitates forming from the digestate. All equipment that came in contact with the sample at any time was rinsed thoroughly with filtered de-ionised water before use. The KOH solution and all de-ionised water used were filtered through a 1.6-µm Whatman GF/C filter paper before use.

To reduce background contamination, protocols laid out by Woodall *et al.* (2015) were adapted, including use of a laminar flow hood to reduce contamination from air sources within the laboratory, workers wearing cotton coveralls and headscarves to prevent contamination from plastic-based clothing, and running three procedural blanks per day. Particles found in blanks were categorized in the same manner as those from environmental samples, and the average number from each set of three blanks was rounded up to the nearest integer and subtracted from the counts of each applicable size, colour, and shape category in the corresponding environmental sample. This method was used to prefer underestimation rather than overestimation, and to maintain positive-integer count data. All reported results were adjusted according to this method.

2.2.4 Visual identification

Potential MPs were visually identified using Olympus CX42 compound microscopes (Olympus, Tokyo, Japan). Visual analysis was conducted by placing the PetriSlides on the microscope stage, removing the cover, and manually scanning the whole sample at 100x magnification. To avoid sample contamination at this step, the microscope stage was enclosed in a clear plastic bag as outlined by Torre *et al.* (2016). Particle shapes (*e.g.,* fibres, fragments, spherules, films) and colour were noted. Potential microplastic fibres were distinguished from natural fibres according to rules determined through observation of known synthetic fibres and by referring to descriptions in previous studies (Hidalgo-Ruz *et al.* 2012). Fibres were identified as potential MPs if they lacked internal structure, including striations, and were an even width along their length. Particles were measured along their longest dimension, using Olympus cellSens software (Olympus, Tokyo, Japan), and assigned to four size categories: 10–99, 100–499, 500–999, and 1000–5000 µm. Although particles as small as 10 µm were counted, unless they were brightly coloured our visual ID could only reliably count particles as small as 100 µm along their longest dimension. Results are reported as mean ± standard deviation.

Fourier-transform Infrared (FTIR) spectroscopy was performed on a small subsample of fibres (29 of 259 total particles, 11.1%), but due to the small sample size the results are only provided in the supplementary material. Due to the high degree of uncertainty as to whether visually identified particles were plastic, or of a non- or semi-synthetic anthropogenic origin, particles are referred to as “potential microplastic particles” (PMPs). If visual identification error rates are assumed to be the same for both sample volumes, however, then the comparative ratio between the two mean concentrations generated by each method should be the same. Furthermore, as particle capture can be expected to vary as a factor of size and shape rather than

composition, *per se*, the exact chemical identity of the particles captured in this study are not as important as the geometric factors.

2.2.5 Seawater MP concentrations and mesh sizes reported in the literature

Using Web of Science© and the term 'microplastics' plus the terms: 'sea', 'seawater', or 'ocean', we reviewed the primary research literature from January 2004 to May 2018 for studies that reported MP concentrations in seawater. Those that did not report MP concentrations as mean values were excluded. We found forty-five studies that expressed mean volumetric concentrations of MPs in seawater, from which we noted the mesh sizes used for filtration. When studies collected samples using multiple methods with different mesh sizes (*e.g.*, two plankton nets with different mesh sizes) we considered each method separately, resulting in 62 data points (Table A1). When concentrations were only expressed as means at several sites or among years, the mean of means was used. In addition to mesh size and MP concentrations, the average sampling volume, the category of depth sampled, and the type of sampling method were also recorded (Table A1). Average sample volumes were taken directly from the literature or estimated based on reported towing parameters (*i.e.*, distance, time, dimensions of net opening) when consistent distances, or times, or speeds were used. Depths were defined as surface (sampling within only the top 1 m), epipelagic (0–200 m depth), bathypelagic (700–1000 m), and full water column (from the one study that sampled a large range of depths). Sampling methods were classified as discrete sampling (*i.e.*, jar or bottle, Niskin), net tow (*e.g.*, manta, neuston), dip net, pump (large volume, ship-based), and surface (sampling sea-surface microlayer).

2.2.6 Data analysis

All statistical analyses were carried out using the R software environment (R Core Team 2015). To determine the effect of sample size and site on PMP concentration reported from light

microscopy, we used a generalised linear model (GLM), specified with the glm function in base R, with site, sample type, and the interaction between site and sample type as factors. As these were count data, a Poisson-distributed error structure was assumed. Model fit was determined visually by assessing residuals *vs.* fitted plots for homogeneity of variance. We also conducted two separate Poisson GLMs for each sample type (*i.e.,* jar *vs.* bucket) to determine whether sample method may have affected the differences in PMP concentration estimates among sites. Comparisons among sites were conducted using Wald tests. The proportions of clear fibres, coloured fibres, and fragments/spherules, as well as of each size category, were compared between sampling methods using 2-sample Mann-Whitney U tests.

To test the effect of methodological factors on seawater MP concentration estimates in the literature, an initial linear mixed-effects model was specified using the lmer function in the lme4 package (Bates *et al.* 2015), with mesh size as a continuous predictor, sample method as a fixed effect, a term for the interaction between mesh size and sample method, and study identity (a unique value for each individual study) and sampling depth category as random effects. MP concentration was set as the response variable and transformed by taking the natural log (ln) to reduce heteroskedasticity. AICc (Akaike Information Criterion for small sample size) comparison determined that a better model fit was achieved by removing both random effects. Backwards selection *via* AICc comparison further determined that removing the interaction term improved model fit. The final model therefore included only mesh size and sample method as predictors.

Sample volume was only reported (or possible to estimate) in 30 studies (41 data points), so a separate analysis to determine the effect of volume on MP concentration estimates was performed using this reduced dataset. In this case, the initial linear mixed-effects model was

specified with mesh size, natural log-transformed sample volume, the interaction between mesh size and sample volume, and sample method as predictors, and with study identity and sampling depth as random effects. Backwards selection *via* AICc determined a better fit without the random effects, and so the final model included only mesh size, sample volume, and the interaction between the two terms as predictors.

2.3 Results

2.3.1. Experimental results

For all results, numbers have been adjusted according to previously mentioned blank corrections, and the counts represent potential microplastic particles (PMPs) only. The samples were processed in two runs, with the procedural blanks averaging 2.33 and 4.00 fibres of background contamination for each run. In addition, an average of 3.00 and 2.33 particles were identified as blue cotton fibres (coming from the coveralls) in the two runs. Non-fibre particles that could be classified as PMPs were not detected in the procedural blanks. Across all samples, a total of sixty-four blue fibres were visually identified as background contamination from the cotton coveralls and were excluded from the analysis. The number of blue cotton fibres encountered ranged from 0 to 8 per sample, with a mean of 1.78 ± 1.82 (n=36) per sample.

A Poisson GLM, with site and sample type as factors, revealed overall higher concentrations of PMPs in the 1-L (5.28 ± 4.17 particles/L, n=18) compared to the 10-L (0.91 ± 0.76 particles/L, n=18) samples (Fig. 2A, Table S2, p <0.01). At the site level, 1-L sample estimates of PMPs were 8.49 ± 6.79 times greater than the 10-L sample estimates, on average. The interaction between the two factors was also significant, however, indicating that the effect of sampling type varied by site, although interpretation of the degree of this interaction is limited

by the low sample size at each sample type and site combination and may simply reflect patchy distribution of particles.

There were also significant differences in PMP concentrations among sites (Fig. 2B, Table A2). Shellfish aquaculture farms did not consistently contain more MPs than non-aquaculture sites (Fig. 2B, Table A3. Separate GLMs conducted for 1-L and 10-L samples, however, demonstrated different significance patterns among the sites for the different sampling types (Fig. 2B, Table A3). Mean concentration estimates ranged from 1.00 to 10.33 particles/L for the 1-L samples and from 0.37 to 1.43 particles/L for the 10-L samples.

When both sample types were combined, fibres made up 87.64% of the 259 PMPs observed, with the rest (12.36%) being coloured fragments and one white spherule (the overall mean concentrations of fragments were not significantly different in the 1-L and 10-L samples, at 0.10 ± 0.38 and 0.16 ± 0.16 (n=18) particles/L, respectively). Most fibres were ~10 µm in diameter, although fibre width was not explicitly measured. Most fibres in the 10-L samples were clear in colour, but fibres in the 1-L samples were predominantly coloured (Fig. 3). Compared to the 1-L samples, the ratio of clear fibres to total PMPs in the 10-L samples was significantly higher (W=36, p<0.001), the proportion of blue fibres was not significantly different (W=169, p=0.11), the proportion of coloured fibres (excluding blue) was significantly lower (W=237.5, p<0.001), and the proportion of fragments and spherules was significantly higher (W=59, p=0.005) (Fig.3).

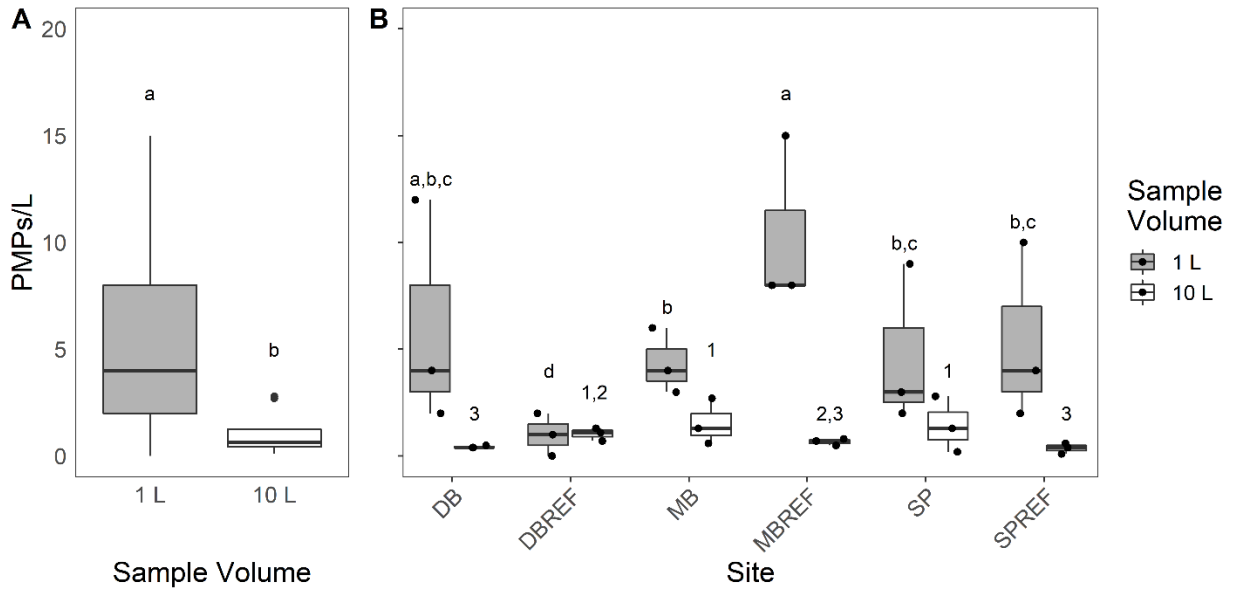

Figure 2: Boxplots of visual counts of the concentration of potential microplastic particles (PMPs)/L) in 36 seawater samples collected by two methods (1-L jar sample and 10-L filtered bucket sampling): (A) pooled among six sites (n=18) and (B) separated by site (n=3). Letters and numbers indicate significant differences among sites in the 1-L and 10-L samples, respectively, according to separate GLMs conducted on each sample type, with sites showing the same number/letter indicating a lack of significant difference ($p>0.05$) according to Wald tests. Box limits and whiskers show first and third quartiles, respectively, with outliers (in A more than 1.5 times the distance between the first and third quartiles away from the median) shown as points. In B, raw data are plotted on top of boxplots. Site abbreviations are: DB=Deep Bay, DBREF=Deep Bay Reference, MB=Mud Bay, MBREF=Mud Bay Reference, SP=Ships Point, and SPREF=Ships Point Reference.

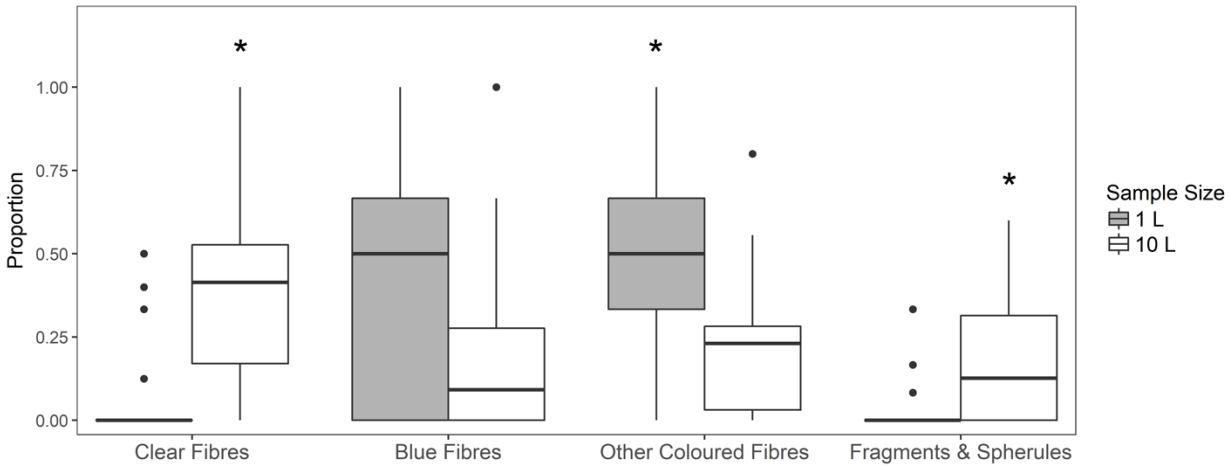

Figure 3: Boxplots of proportions of potential microplastic particle types in 36 samples, separated by sampling method (1-L jar sample and 10-L filtered bucket sampling). Asterisks indicate significant differences between methods as determined by two-sample Mann-Whitney U tests. Coloured fibres (aside from blue) are grouped together, as well as fragments and spherules. Box limits and whiskers show first and third quartiles, respectively, with outliers (more than 1.5 times the distance between the first and third quartiles away from the median) shown as points.

Of the PMPs identified, pooled across sites and sampling types, approximately 39% were between 100 and 499 µm in length, 33% were between 1000 and 5000 µm, 19% were between 500 to 999 µm, and 9 % were less than 100 µm (Fig. 4). The only significant difference between the two sampling methods in the proportion of particles by size was that significantly more 10–99 µm (W=1083, p=0.003) particles were detected in the 10-L samples than in the 1-L ones (Fig. 4). Those results were driven entirely by the detection of many small fragments in the 10-L samples at DBREF, MB, and SP, compared with very few fragment detections in the 1-L samples.

2.3.2 Seawater MP concentrations and mesh sizes reported in the literature

Seawater MP concentrations for each mesh size used in the 45 literature studies and our study resulted in 62 values ranging from 0.01 to 102,000 particles/m^3 (Table A1, Fig. 5). Forty-seven percent of the mesh sizes reported was in the 300–350 µm range and 73% used mesh bigger than 100 µm. Both mesh size and sampling method were significant predictors of MP concentration according to the first linear model, with an adjusted R^2 value of 0.60 ($F_{5, 56}$ = 17.62, p<0.001). The model fit showed a significant negative exponential influence of mesh size on reported MP concentration. It also suggested that towed samples estimated lower MP concentrations than all other methods, followed by pumps, dip nets, discrete samples, and sea-surface microlayer sampling in that order (Fig. 5A. In the second linear model, fit to the reduced dataset using mesh size, sample volume, and the interaction between the two factors, all terms were significant, with an adjusted R^2 value of 0.66 ($F_{3, 37}$ = 26.34, p<0.001, Table A4). Reported MP concentration decreased significantly with both increasing mesh size and increasing sample volume (Fig. 5A, B). While the effect of mesh size on MP concentration was exponential, the effect of volume was closer to linear.

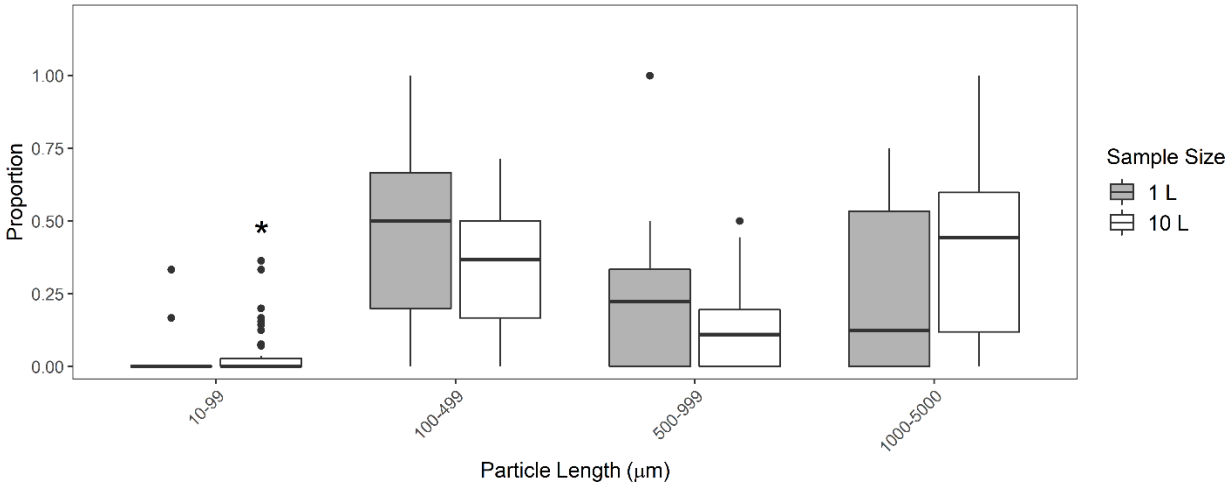

Figure 4: Proportions of potential microplastic particles in 36 samples in various size categories, separated by sampling method (1-L jar sample and 10-L filtered bucket sampling). Asterisk indicates a significant difference between methods as determined by a two-sample Mann-Whitney U test. Most particles found were greater than 100 µm in their longest dimension. Boxes and whiskers show first and third quartiles, respectively, with outliers (more than 1.5 times the distance between the first and third quartiles away from the median) plotted as points.

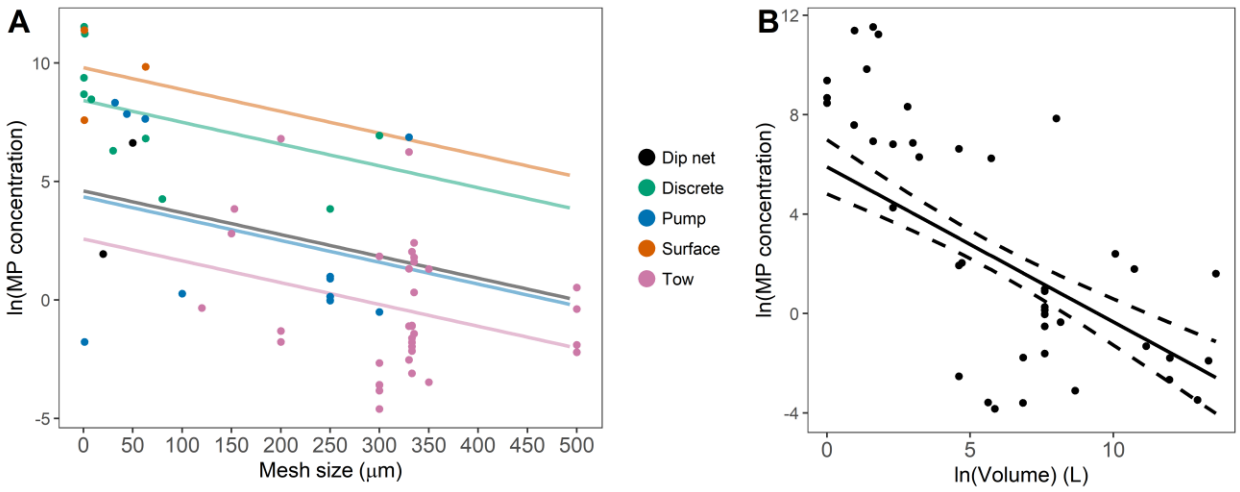

Figure 5: Microplastic particle (MP) concentrations (MPs/m^3) taken from 46 studies, including the present one, logarithmically transformed and plotted in relation to (A) the mesh size used to produce each concentration in each study, and (B) the volume of seawater sampled for those 30 studies that reported volume. The fitted lines in A represent a linear model fit with mesh size and sampling method as predictor variables ($R^2 = 0.65$, $p < 0.001$). The points and lines are coloured according to the category of sampling method, (dip nets are handheld nets, discrete samples include jars and bottles (including Niskin), pump samples are ship-based with intake line and electric pump, surface samples sample the sea-surface microlayer, and towed samples are nets (*e.g.*, manta and neuston trawls)). The fitted line in B represents a linear model fit with volume, mesh size, and the interaction between volume and mesh size as predictors. The model predictions and standard error (dashed lines) are fit using the average of mesh sizes reported (229.8 µm).

2.4 Discussion

Our 1-L jar samples estimated PMP concentrations that were approximately 8.5 times greater, on average, at the site level, or 5.8 times greater when samples were pooled, than estimates derived from the 10-L bucket samples (mean ± SD: 5.28 ± 4.17 and 0.91 ± 0.76 particles/L, respectively). Although we were not able to accurately measure the success rate of our visual identification of actual MPs, findings from our other work indicate that it was likely close to 13% (Covernton *et al.* 2019b). As such, the average concentration estimates would be changed to be 0.69 MPs/L and 0.12 MPs/L for the 1-L and 10-L samples, respectively. Although we were not able to distinguish between plastic and non-plastic anthropogenic particles, the consistently larger number of anthropogenic particles, especially fibres, sampled by the 1-L jars constitutes an important finding. Moreover, it is currently unknown as to what extent natural and semi-synthetic particles/fibres affect organismal health compared with synthetic ones, so the overall concentration of PMPs may be important to note. The 10-L samples contained more shapes and colours of particles compared with the 1-L samples (13 *vs*. 8 combinations of shape and colour). This result shows that retaining everything down to 8 µm provides higher, and potentially more accurate, estimates of microfibre concentrations in seawater samples (compared with 63 µm), although but the concomitant decrease in the volume of water sampled could reduce the ability to provide information on the diversity of particles present over the sampling area at large.

While filtering to 8 µm resulted in detection of significantly higher concentrations of microfibres compared to 63 µm, the two methods found similar concentrations of other PMPs, and 63-µm filtration resulted in a higher proportion of <100 µm particles being characterized than 8-µm filtration. These findings were likely due to the loss of fibres through the 63-µm mesh

(*i.e.*, since most fibres tend to be narrower than 63 µm), as some of them pass through during the filtering process (Barrows *et al.* 2017). Both of our sampling methods detected similar proportions of microfibres greater than one hundred µm in length, showing that the 63-µm mesh did not selectively retain longer fibres, but rather allowed some overall portion of total fibres to pass through. Some fibres are clearly retained by larger mesh sizes when they are caught horizontally in the mesh. There is also the possibility of filtration to capture fragments smaller than the mesh size when they adhere to the mesh itself and do not pass through the holes, as indicated by the presence of small fragments in the 10-L samples. It should be noted, however, that only particles larger than 100 µm were reliably detected using the compound microscope and visual microscopy. Smaller particles were detected if they were distinctive in shape or colouration, but any estimates of this size class using light microscopy are expected to produce biased results, so our findings for the <100-µm size category should be considered an underestimate. As noted by Song *et al.* (2015), visual identification methods tend to overestimate microplastic fibres and underestimate microplastic fragments. As such, it is hard to draw definitive conclusions about whether 8-µm or 65-µm mesh better samples small fragments. Regardless, the 8-µm filtration was clearly better at capturing fibres.

The two sampling methods both produced significant differences among sites, but the significant interaction between site and sampling method suggests that the size of the difference was not consistent. This shows the large amount of uncertainty associated with estimating MP concentrations in the field and the influence that sampling method can have, especially given the low sample sizes generally used in most studies. Although our sample sizes were also low (three samples per site), this is not unusual in microplastics research on seawater, where some studies have collected only a single sample per site (Setälä *et al.* 2016a, Zhang *et al.* 2017). This is a key

limitation for both the present study and most microplastics investigations, making it difficult to reach statistically-sound conclusions. Sample sizes are often low because of the significant amount of time, effort, and expense associated with processing and analysing environmental microplastics samples. As the spatial patchiness of MPs remains unknown, it would be impossible to definitively conclude whether the site differences we detected were due to variation among sites, stochastic variation within sites, or stochastic contamination of samples in the laboratory, thereby obscuring true patterns. Sampling method and mesh size must thus be chosen carefully, and MP concentrations estimated using different mesh sizes should be compared with caution. Future work should evaluate the optimal volume of seawater needed to accurately characterize the stochastic distribution of the various sizes and shapes of MPs in the environment.

Our analysis of forty-five previously published studies (46, including this one) suggests that mesh size, water volume size, and sampling method significantly influence estimates of MP concentrations in seawater. These relationships exist despite large variation in reported MP concentrations. The trend for MP concentrations to follow a negative, log-linear relationship with increasing mesh size suggests that larger mesh may be exponentially underestimating the MP concentrations available for ingestion by marine organisms. In addition, the linear decrease in reported concentrations with increasing sample volumes suggests that for researchers, reducing mesh size at the expense of sample volume will not be likely to underestimate MP concentrations. Although there was a significant interaction between mesh size and sample volume, the overall trend for reported MP concentrations to decrease with both increasing mesh size and sample volume remains clear. The fact that mesh size and sample volume were both

significant in the model supplies evidence of a strong and additive effect of both factors on reported MP concentration.

Surprisingly, discrete samples had consistently higher average MP concentration estimates than other methods, despite their small volumes. The lower estimates provided by ship-based pumping methods, which sample large volumes of water, but can use smaller mesh sizes, show that the higher mean MP concentrations provided by discrete samples may in some part be due to the increased variability associated with sampling smaller volumes of seawater. Reported concentrations increase exponentially, however, with decreasing mesh size across all sampling methodologies.

Overall, this indicates that sufficient replication of small-volume discrete samples should accurately estimate MP concentrations in seawater. For larger spatial scales, replication across space or large-volume pumped samples with small mesh sizes can be used. Our findings strongly indicate, however, that towed samples will consistently underestimate MP concentrations in seawater. Our model predicts that towed sampling methods using 300–350-µm mesh may be underestimating biologically important MP concentrations by one to four orders of magnitude (according to model predictions, factoring in standard error of the coefficients). Although it may seem intuitive that smaller mesh will capture more particles, we argue that this issue is sometimes mentioned, but rarely formally considered by studies that sample seawater for MPs, and that this has serious implications for the discussion of ecological risk. The negative correlation between sample volume and MP concentration, even when mesh size is controlled for, is a novel finding and shows that towed sampling devices may have issues extending beyond that of larger mesh that contribute to sampling bias (*e.g.*, MP distribution is patchy enough in the environment that large-scale sampling will underestimate some localized concentrations).

MPs less than 150 µm may be able to translocate into the tissues of humans (Wright and Kelly 2017) and thus may be the most toxicologically relevant size category for trophic transfer *via* seafood, as well as for marine mammals with similar physiology. An upper limit for toxicological interactions with marine fish and invertebrates has not been established, and a recent meta-analysis did not find a significant effect of particle size on feeding, growth, reproduction, or survival of fish and aquatic invertebrates (Foley *et al.* 2018). This study did not, however, take particle concentration into account, so this finding is difficult to interpret. Furthermore, most toxicology studies have only tested the effects of MPs <100-µm in diameter (Chae and An 2017) and many field studies found that MPs less than < 300-µm in diameter make up a large category of particles found in fish and aquatic invertebrates (Leslie *et al.* 2017, Pellini *et al.* 2018, Phuong *et al.* 2018). If most studies are underestimating the concentrations of these biologically important MPs by orders of magnitude, then the ingestion risk for humans and marine animals will be underestimated. If the goal of MP research is to understand their threat to marine ecosystems, then the sampling method must accurately estimate the concentrations of the most biologically relevant particles.

Microfibres are often more commonly encountered in the marine environment than other forms of MPs (Thompson *et al.* 2004, Claessens *et al.* 2011, Desforges *et al.* 2014). As such, replicated small-volume samples filtered in the laboratory, or high-volume pumped samples directly pressure-filtered over small mesh size, or through stacked sieves, may provide more accurate estimates of MP concentrations overall. Mesh size that samples are filtered through should be minimised as much as is feasible, ideally under 10 µm (the approximate width of many microfibres) to capture microfibres efficiently. Concerns over the reduced detection of rare particles in smaller volumes can be alleviated by increasing the total number of samples. Large-

volume samples using standard net towing methods may be useful for large-scale monitoring programs, provided that the mathematical relationship of mesh size to recovered particles is sufficiently well understood, which would allow back-calculation of the estimated number of smaller particles missed by net tows using coarser mesh. In the case where plankton trawls are conducted, jar or small-mesh dip net samples should also be carried out in replicate. While this may increase the cost and personnel time associated with MP sampling it is crucial to moving the field towards a point at which ecological risk assessments can be conducted. Consideration of sampling depth must also be made, as surface sampling has been shown to underestimate total buoyant MPs by as much as 30 times (Kooi *et al.* 2016). If future studies can characterize the key spatial scales of variability in MP concentrations, this will allow for further optimization of sampling procedures.

Our findings also have implications for laboratory ingestion studies, which must place biological impacts in the context of environmental MP concentrations and particle types. Although most research on MP ingestion impacts has been carried out using microbeads <100 µm in diameter, researchers have documented microfibre ingestion by a broad range of species (Rochman *et al.* 2015, Grigorakis *et al.* 2017, Lourenço *et al.* 2017) and have demonstrated some evidence of associated biological impacts (Au *et al.* 2015, Watts *et al.* 2015, Jemec *et al.* 2016). Accurately quantifying the concentrations of microfibres, as well as concentrations and types of MPs in general, is thus critical for planning relevant MP toxicology studies and for bridging the gap between laboratory and field studies of ecological risk.

Our findings show that the 1-L jar samples filtered through 8 µm yielded PMP concentrations averaging approximately 8.5 times higher, at the site level, than the 10-L bucket samples filtered through 63 µm. Neither sampling method detected consistent significant

differences in PMP concentration between shellfish farms and nearby non-aquaculture areas. Studies using larger mesh sizes, especially the commonly used 300–350-µm range, are almost certainly underestimating MP concentrations in seawater by orders of magnitude (using the definition of microplastics as particles between 1 and 5000 µm). MP concentration approximated a negative log-linear relationship with increasing mesh size in 46 studies (62 data points) that sampled seawater using a variety of methods. Our model predicted that 300–350-µm mesh will underestimate MP concentrations by approximately one to four orders of magnitude (according to model predictions, factoring in standard error of the coefficients) compared with discrete or pumped samples that can be filtered through much smaller mesh sizes (*e.g.,* less than 100 µm). There is also a concomitant, negative effect of sample volume on reported MP concentration, indicating that even net tows that sample large volumes of water report lower MP concentrations. Whether this is due to the patchiness of MP distribution, or some methodological factor, remains unclear. Underestimating biologically relevant MP (<150 µm) concentrations by orders of magnitude could have significant consequences for monitoring studies and future ecological risk assessments used to inform policy and management decisions. In addition, non-standardised methods make it difficult to interpret study comparisons. Researchers should carefully select a sampling method according to their research questions, but it seems clear that any attempt to assess the risk of MP ingestion to marine organisms and food webs must at least pair large-scale towing methods with filtration methods using mesh or filters less than 10 µm, to be able to retain narrow microfibres whose widths are commonly around that size. Standardised sampling practices that effectively sample the smaller size range of MPs will also allow for laboratory toxicology studies to better assess the physiological response of organisms following MP ingestion by using environmentally relevant concentrations of MPs that reflect the actual size of

particles found in seawater being evaluated, rather than estimates that may be orders of magnitude lower because they are derived from the biased sampling of larger particles from towed samples. Regional comparisons can still be conducted using towed nets but should not be taken as biologically relevant indications of MP concentrations. We suggest that when only plankton net trawls are used, authors can avoid misinterpretation by explicitly saying that they are not measuring the MPs that are commonly ingested by many marine fish and invertebrates.

Chapter 3: Microplastics in bivalves and their habitat in relation to shellfish aquaculture proximity in coastal British Columbia, Canada

Covernton, G., B. Collicutt, H. Gurney-Smith, C. Pearce, J. Dower, P. Ross, and S. Dudas. 2019. Aquaculture Environment Interactions 11:357–374.

3.1 Introduction

Fisheries and aquaculture industries represent potential sources of marine plastic pollution and pathways for MP contamination of seafoods, due to the extensive use of equipment made of synthetic materials (Lusher *et al.* 2017). In particular, shellfish aquaculture requires the use of ropes, rafts, floats, and trays that – due to low cost and durability – are usually composed of polystyrene, polypropylene, polyvinyl chloride, or high-density polyethylene (GESAMP 2016, Schoof and DeNike 2017). In some cases, cultured shellfish have been shown to contain higher MP concentrations than their wild counterparts (Mathalon and Hill 2014, Bendell 2015, Phuong *et al.* 2018) and it has been suggested that by using plastic infrastructure, shellfish aquaculture could be contaminating its own stock as well as the surrounding environment (Mathalon and Hill 2014, Castro *et al.* 2016). However, little is known about the extent to which shellfish aquaculture equipment contaminates the environment compared with other well-established sources, such as sewage effluent, urban runoff, and aerial dispersal (GESAMP 2016, Dris *et al.* 2016, Schoof and DeNike 2017).

The finding that MPs occur in shellfish has generated media attention and public concern about the potential health risks to humans of ingesting microplastics *via* shellfish consumption (Lusher *et al.* 2017). Figuring out the source of such MPs and attempting to reduce the contamination of shellfish, along with further understanding of their role as sources of MPs relative to other foods, will be important steps towards thoroughly understanding their safety and security as a food source, as well as promote trust among consumers that shellfish are safe to eat.

The impact of shellfish aquaculture on local MP accumulation in shellfish may be driven by a wide range of factors including geographic location, local oceanographic conditions, species, season, culture practices, and type/concentration of MPs. Accordingly, research is required to investigate these factors/considerations to determine aquaculture impacts on MP accumulation in shellfish.

The aims of this chapter were to compare MP concentrations in shellfish, water, and sediment from shellfish aquaculture sites to nearby non-aquaculture sites to determine the relationship with environmental variables (*i.e.*, sediment composition, amount of plastic at a site) and to investigate the source of MPs found in shellfish and their environment. We conducted a large-scale out-plant experiment, where shellfish (oysters and clams) individuals were collected from one site and transferred to aquaculture and non-aquaculture sites in six regions important for shellfish aquaculture in British Columbia (BC), Canada.

3.2 Methods

3.2.1 Study Area

The study was conducted in six regions in BC where shellfish aquaculture occurs: Discovery Islands, Okeover Inlet, Baynes Sound, Nanoose Bay, Ladysmith, and Clayoquot Sound (Fig. 6). Eleven shellfish aquaculture sites and ten non-aquaculture sites, with varying degrees of macroplastics present (*e.g.*, anti-predator nets, fences, floats, ropes, PVC pipes, and miscellaneous debris), were selected across these regions (see Table 1 for details). Non-aquaculture beaches were close enough to shellfish aquaculture sites to minimize differences in oceanography, sediment type, and species assemblages, resulting in locations ~60–530 m from active shellfish aquaculture sites (shortest over-water distance). The Joyce Point site in the

Discovery Islands lacked a suitable reference site within the distances used for the other beach pairs. All sites (shellfish aquaculture and non-aquaculture sites) were classified according to plastic levels using the following criteria: “high”: hundreds of square metres covered in plastic equipment and/or debris (*e.g.*, large-scale shellfish aquaculture operations that cultured clams and thus had more than two synthetic anti-predator nets deployed across the intertidal); “medium”: approximately ten or more square metres of visible plastic, typically when only one or two synthetic anti-predator nets or fences and/or several large synthetic debris items such as oyster trays were present; “low”: only scattered plastic items visible (*e.g.*, one or two ropes, a few scattered pieces of debris like car tires, buckets, or bottles); “none”: no plastic visible on site. These classifications were decided from photos taken by researchers in each cardinal direction at each point where any type of sampling occurred at every beach. See Fig. 6 and Table 1 for site locations and explanation of site abbreviations.

The Discovery Islands is a low-intensity, shellfish aquaculture region spread over hundreds of square kilometres and separated by several islands (Fig. 6). Okeover Inlet has a moderate density of shellfish aquaculture activity; higher than the Discovery Islands, but not as high as Baynes Sound. Baynes Sound has the highest density of shellfish aquaculture in BC, so all the reference sites – although being located in gaps between shellfish aquaculture sites – were still within close proximity to a high intensity of both intertidal and deep-water shellfish aquaculture. Nanoose Bay hosts several shellfish aquaculture operations, as well as recreational collection areas, but with a low degree of plastic use compared to Okeover Inlet and Baynes Sound. In Ladysmith, the aquaculture site was the only shellfish aquaculture operation in the immediate area, although Ladysmith Harbour, a large bay just south of the study area, is a highly active industrial area. The Meares Island aquaculture site in Clayoquot Sound on the west side of

Vancouver Island is not technically a harvest site and does not have any plastic infrastructure but is stocked with adult oysters from a nearby large deep-water operation that utilizes synthetic ropes and large, blue plastic drums as floats. Clayoquot Sound is home to both fish and shellfish aquaculture with an overall density similar to the Discovery Islands.

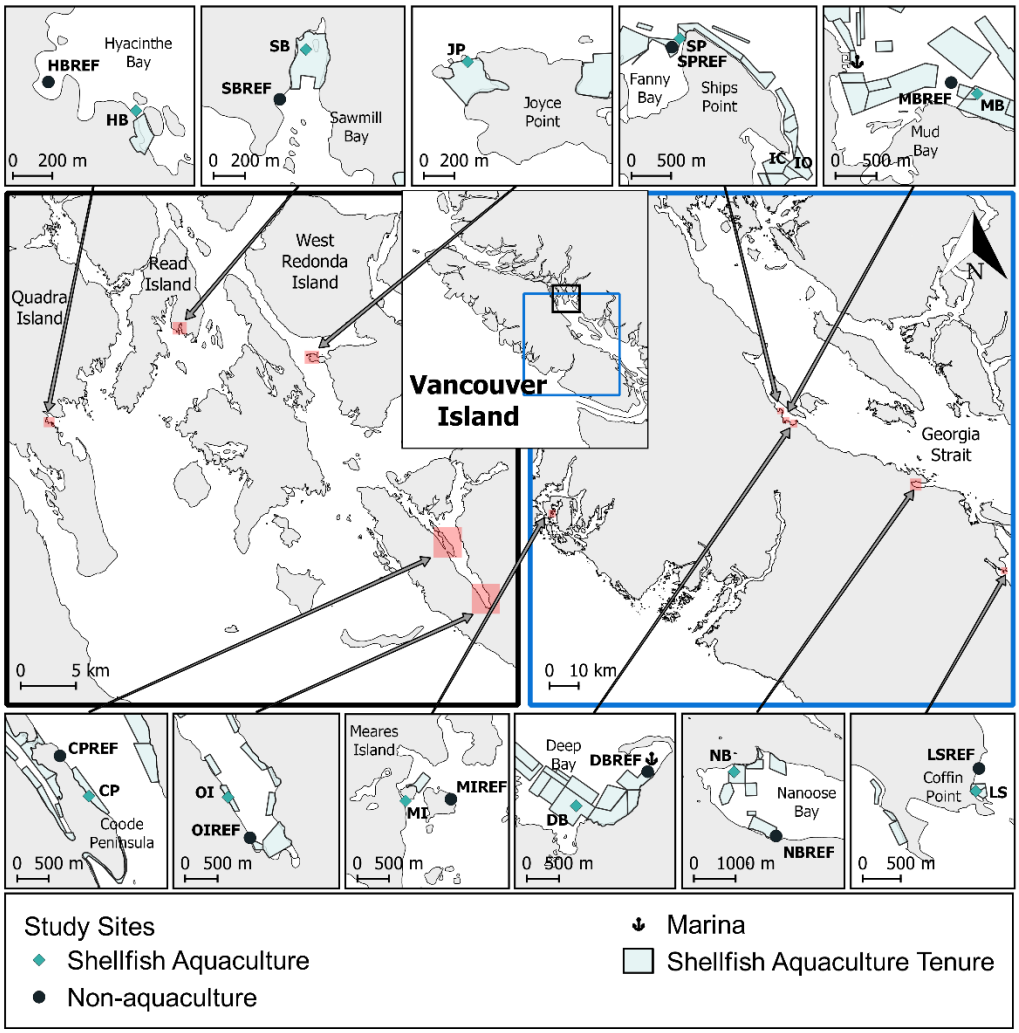

Figure 6: Map of study area showing the six regions key to the shellfish aquaculture industry in British Columbia where the study took place. Shellfish aquaculture tenures that have been leased from the government are shown but were not all necessarily in active use. Site of initial oyster and clam collection is indicated by IO and IC, respectively, both on the Ships Point panel. (1) Discovery Islands: HB=Hyacinthe Bay, HBREF=Hyacinthe Bay Reference, SB=Sawmill Bay, SBREF=Sawmill Bay Reference, JP=Joyce Point; (2) Okeover Inlet: CP=Coode Peninsula, CPREF=Coode Peninsula Reference, OI=Okeover Inlet, OIREF=Okeover Inlet Reference; (3) Clayoquot Sound: MI=Meares Island, MIREF=Meares Island Reference; (4) Baynes Sound: SP=Ships Point, SPREF=Ships Point Reference, MB=Mud Bay, MBREF=Mud Bay Reference, DB=Deep Bay, DBREF=Deep Bay Reference; (5) Nanoose Bay: NB=Nanoose Bay, NBREF=Nanoose Bay Reference; (6) Ladysmith: LS=Ladysmith, LSREF=Ladysmith Reference.

Table 1: Information on the 21 field sites, including region, species raised, site code used in this paper, sediment type (as determined from average grain-size class proportions from all sediment cores taken at each site and classified according to Wentworth (1922)), degree and types of plastic visible on site, and distance to nearest active shellfish aquaculture site.

Region	Species raised	Site code	Sediment type	Degree of plastic on site and type	Distance to nearest shellfish aquaculture site (m)
Discovery Islands	Clams and oysters	HB[A,B,C]	Gravelly sand	High: APN*	-
Discovery Islands	-	HBREF[A,B,C]	Gravelly sand	Low: some ropes and buckets	450
Discovery Islands	Clams and oysters	SB[A,B,C]	Gravelly sand	Medium: APN, a car tire	-
Discovery Islands	-	SBREF[B,C]	Sandy gravel	Low: one balloon ribbon	200
Discovery Islands	Oysters	JP[A]	Sandy gravel	Medium: some oyster nets and PVC tubes, floats close offshore	-
Okeover Inlet	Oysters	CP[B,C]	Gravelly sand	Medium: some APF**, oyster cages, and PVC tubing	-
Okeover Inlet	-	CPREF[A,B,C]	Gravelly sand	Low: a rope	240
Okeover Inlet	Oysters	OI[A,B,C]	Gravelly sand	Medium: APF, PVC tubing	-
Okeover Inlet	-	OIREF[A,B,C]	Sand	Low: some ropes	500
Nanoose Bay	Clams and oysters	NB[A,B]	***	High: APN and APF, PVC tubing, ropes, and floats	-
Nanoose Bay	-	NBREF[A]	***	None	330
Baynes Sound	Oysters	SP[A,B,C]	Gravelly sand	Medium: APF, some ropes and floats	-
Baynes Sound	-	SPREF[A,B,C]	Sand	Low: a boat anchored on the beach	60
Baynes Sound	Clams and oysters	MB[A,B,C]	Gravelly sand	High: APN and APF, some PVC tubing	-

Baynes Sound	-	MBREF[A,B,C]	Sandy gravel	None	130
Baynes Sound	Clams and oysters	DB[A,B,C]	Gravelly sand	High: APN and APF	-
Baynes Sound	-	DBREF[B,C]	Gravelly sand	Medium: Several washed up oyster trays and cages and some PVC tubes	250
Ladysmith	Oysters	LS[A,B]	Sand	Medium: Several oyster bags, some ropes and crates, and a car tire	-
Ladysmith	-	LSREF[B]	***	Low: a single rope	200
Clayoquot Sound	Stocked with oysters, not harvested	MI[A,B,C]	Gravelly sand with silt	Low: some oyster bags and ropes	240
Clayoquot Sound	-	MIREF[A,B,C]	Gravelly sand	None	530

* APN = anti-predator netting.
** APF = anti-predator fencing.
*** Sediment cores not taken.
[A]Indicates where clam samples were collected and analyzed.
[B]Indicates where oyster samples were collected and analyzed.
[C]Indicates where water samples were collected and analyzed.
HB=Hyacinthe Bay, HBREF=Hyacinthe Bay Reference, SB=Sawmill Bay, SBREF=Sawmill Bay Reference, JP=Joyce Point, CP=Coode Peninsula, CPREF=Coode Peninsula Reference, OI=Okeover Inlet, OIREF=Okeover Inlet Reference, NB=Nanoose Bay, NBREF=Nanoose Bay Reference, SP=Ships Point, SPREF=Ships Point Reference, MB=Mud Bay, MBREF=Mud Bay Reference, DB=Deep Bay, DBREF=Deep Bay Reference, LS=Ladysmith, LSREF=Ladysmith Reference, MI=Meares Island, MIREF=Meares Island Reference.

3.2.2 Bivalve Out-plants

A total of 1,110 Pacific oysters (*Crassostrea gigas*) ranging from 74 to 149 mm shell height (mean ± SD = 106.5 ± 13.6 mm) were collected on June 15, 2016 from an intertidal shellfish aquaculture site at Ships Point in Baynes Sound (Fig. 6). The oysters were labelled with a black permanent marker and the labels coated with a protective layer of cyanoacrylate glue. The oysters were stored in a flow-through seawater system for 3–9 days (unequal times across sites were due to the logistics of transporting oysters to 21 sites over a large geographic area) to facilitate survival during labelling and out-planting to all sites. To test for initial microplastic contamination, ten individuals were randomly collected after nine days and stored at -20°C until analysis (see below).

A total of 1,330 Manila clams (*Venerupis philippinarum*) ranging from 24 to 52 mm shell length (mean ± SD = 37.4 ± 39.9 mm) were collected on May 17, 2016 from an intertidal clam culture site at a different location at Ships Point (Fig. 6). A small area on the shell of each clam was sanded down using a rotary tool with sanding attachment (Dremel, Mount Prospect, Illinois, USA) and labelled as described above. The clams were then stored in a flow-through seawater system for 2–11 days until time of out-planting. Ten individuals were collected after 11 days and stored at -20°C until analysis for initial microplastic contamination (see below). Although this sampling (in the case of oysters as well) occurred at the end of the deployment period, a difference of several days in the flow-through system is small in comparison to the three months during which the clams were left at the study sites. These initial samples were taken to account for any MPs that had accumulated at the original site and that might therefore still be present at the end of the study.

The clams and oysters were out-planted May 22–29, 2016 and June 18–24, 2016, respectively. Clams were buried at a depth of roughly 2.5 cm at tidal heights of 1.6–2.2 m above mean lower low water while oysters were placed on the sediment at 0.9–1.9 m tidal heights, depending on the site. Twelve clams and ten oysters were deployed in 0.5 x 0.5-m quadrats, 10 m apart along each of two parallel transects (thus approximating similar tidal heights for each species within a site), totaling five quadrats per species per site and 60 clams and 50 oysters per site.

3.2.3 Sample Collection

All surviving bivalves that could be found were collected from August 22 to September 2, 2016. Because of a tendency to gape following freezing, clams were secured shut with natural rubber elastic bands and placed in sealed glass Mason jars for transport. Oysters were wrapped in burlap and sealed in clear-plastic freezer bags for transport. Particle identification later confirmed that the plastic freezer bags did not contaminate the sample. All bivalves were frozen at -20°C on the day of collection. For statistical purposes, shellfish samples were analyzed if survival was sufficient to allow for the analysis of ten individuals of a species at each site, resulting in oysters from 19 sites (insufficient survival at Joyce Point and the Nanoose Bay reference site) and clams from 17 sites (insufficient survival at Coode Peninsula and the reference sites for Sawmill Bay, Deep Bay, and Ladysmith) being examined for microplastics. In selecting individuals for analysis, and depending on which individuals had survived, bivalves from the first, third, and fifth quadrats along each transect were prioritized to capture site variability and efforts were made to analyze similar numbers of individuals from these quadrats. Any pseudo-replication was accounted for during statistical analysis by the use of hierarchical modeling.

Due to logistical constraints, sediment and water samples were collected and analyzed from only 16 of the 21 sites (excluding Joyce Point, Nanoose Bay, Ladysmith, and the reference sites from Nanoose Bay and Ladysmith), concurrent with shellfish sampling. Sediment cores were collected adjacent to the end and middle quadrats for each species, using 125-mL aluminum corers to a depth of 5.45 cm. This totaled six sediment samples per site, with the exception of both aquaculture and non-aquaculture sites for Sawmill Bay, and the Meares Island aquaculture site where only five samples were analyzed for each due to unavoidable sample loss during processing. Half of the samples were collected alongside oysters at 0.9–1.9 m and half of which were alongside clams at 1.6–2.2 m tidal heights.

Water samples were collected by wading to 0.5-m depth during flood tide in a line perpendicular to the shellfish transects at quadrats one, three, and five. At each sampling point, a 1-L sample was taken in a glass Mason jar, totaling three samples per site, although later sample loss resulted in only one sample from the aquaculture site at Okeover Inlet and two samples each from the aquaculture sites at Hyacinthe Bay and Sawmill Bay being analyzed.

Additional sediment samples for grain-size analysis were also collected, using a 5.08-cm diameter PVC corer to a depth of 10 cm, from the middle and both ends of the clam and oyster quadrats, resulting in three to five samples per site (limited in some cases by bedrock or large cobble). These samples were dried to constant weight, weighed, then separated into eight grain-size categories (<63, >63–124, >125–249, >250–500, >500–1000, >1000–2000, >2000–4750, and >4750 µm, adapted from Wentworth (1922)) using stacked sieves and a mechanical shaker. Each fraction was then weighed and the proportion by total sample weight was determined for each size fraction (Eleftheriou 2013). Beach slope was estimated at each site by running a

transect line perpendicular to the water's edge (~10–40 m, depending on site), then measuring the vertical displacement with a laser level and calculating the slope angle as arcsine(rise/run).

3.2.4 Sample Preparation

Shellfish were thawed at room temperature, their shell lengths/heights measured, and then all soft tissues removed from shells and dried at 60°C until constant weight. The dry tissues were weighed and then digested for 24 hours at 60°C in 10% potassium hydroxide (KOH) (40 mL for clams, 50 mL for oysters). KOH is effective at removing biological material from samples (Foekema *et al.* 2013, Rochman *et al.* 2015) and a 24-hour incubation at 60°C has little effect on most plastic polymers (Dehaut *et al.* 2016). Sediment samples were dried at 60°C until constant weight, weighed, and then subjected to overflow flotation using a fully saturated $CaCl_2$ solution (density ~ 1.4 g mL^{-1}). Due to the presence of high amounts of largely indigestible plant material, sediment samples were reduced in volume to 1/8 using a Folsom plankton splitter (resulting in a 15.6-mL sample) and then digested with 50 mL of 10% KOH at 60°C for 48 hours. Water was removed from the Mason jar samples by securing 8-µm (nominal size) woven, stainless-steel mesh to the mouth of the Mason jar using the metal ring and then inverting the jar over a vacuum filter assembly. Water samples were then dried at 60°C for 48 hours or until a constant weight was achieved. Next, 100 mL of 10% KOH solution were added to each sample, which was then covered with aluminum foil and incubated at 60°C for 24 hours.

Following the digestion, all samples were vacuum filtered through 47-mm diameter, 8-µm pore size polycarbonate (PCTE) membrane filters (Sterlitech, Kent, WA, USA). The glass filter funnels were warmed before filtration (using de-ionised water kept at 60°C) to minimise precipitates forming from the digestate. Filters were then placed in polystyrene PetriSlides (EMD Millipore, Burlington, MA, USA) for storage and later microscopic visualisation. All equipment

that touched the sample at any time was rinsed thoroughly with filtered de-ionised water. The KOH solution and all de-ionised water used were filtered through 1.6-µm Whatman GF/C filter paper before use.

To minimize background contamination, protocols laid out by Woodall *et al.* (2015) were adapted. All activity requiring sample exposure to ambient environmental conditions was conducted in a laminar flow hood to reduce contamination from air sources within the laboratory. Blue cotton coveralls and headscarves were worn at all times by laboratory workers to prevent contamination of the samples by synthetic clothing. Blue cotton fibres produced by the coveralls could be readily identified during visual microscopy due to their unique colour and structure. For each day of sample processing, three procedural blanks were also processed using identical laboratory methods.

3.2.5 Visual Identification

Visual analysis was conducted for all samples by placing the PetriSlides on a compound microscope stage, removing the cover, and manually scanning the entire sample at 100X magnification. To avoid sample contamination at this step, the microscope stage was enclosed in a clear plastic bag which was taped to the bench top and microscope at its edges, as outlined by Torre *et al.* (2016). MP shape (*e.g.*, fibres, fragments, spherules, films) and colour were noted. Potential microplastic fibres were distinguished from natural fibres according to criteria developed through observation of known synthetic fibres and descriptions from previous studies (Hidalgo-Ruz *et al.* 2012). Fibres were identified as suspected MPs if they lacked internal structure, including striations, and were an even width along their length. Each particle was measured along its longest dimension, using Olympus cellSens software (Olympus, Tokyo,

Japan), and assigned to one of six size categories according to the length of their largest dimension: 10–19, 20–49, 50–99, 100–499, 500–999, and 1000–5000 µm.

3.2.6 Spectroscopic Identification

A sub-sample of the suspected MPs extracted from shellfish and characterized by visual microscopy were identified using Fourier-transform infrared (FTIR) spectroscopy. To select the sub-sample of particles that would be analyzed, one each of the clam, oyster, and water samples from seven sites (the Deep Bay, Hyacinthe Bay, Mud Bay, and Okeover Inlet aquaculture sites, and the Hyacinthe Bay, Mud Bay, and Okeover Inlet reference sites) were selected randomly. A total of 44 suspected MPs (seven from oysters, nine from clams, 18 from water, and 10 from sediment samples, all of which were fibres) were analyzed. The particles were lifted from membranes using metal micro-forceps and placed on glass slides that had been coated with a thin layer of 20% dextrose solution for adhesion. Micro-ATR (attenuated total reflectance) FTIR spectroscopy was conducted on a Cary 660 FTIR spectrometer (Agilent Technologies Inc., Santa Clara, California, USA). The infrared signatures of samples taken from aquaculture equipment and plastic debris that were commonly found at the study sites were also examined. Particles were identified using comparisons with the Knowitall spectral library (Bio-Rad Laboratories Inc., Hercules, California, USA) of 250,000 entries. Spectral matches were confirmed using Quality Assurance/Quality Control as described in Ocean Wise laboratory Standard Operating Procedures.

3.2.7 Data Analysis

Particles found in blanks were categorized in the same manner as those from the environmental samples. The average number of particles from each set of three blanks (three sets per round of processing) was rounded up to the nearest integer and subtracted from the counts of each applicable size, colour, and shape category in the corresponding environmental sample (from the same round of processing). This method was used to ensure under- (as opposed to over-) estimation and to maintain a format of positive-integer count data. All corrected concentrations of suspected microplastics were then multiplied by a correction factor of 3/22 to account for the average amount of visual identification error as identified by FTIR spectroscopy (discussed below).

All statistical analyses were carried out using R (R Core Team 2015). Generalized linear mixed effect models (GLMMs) were run using the package glmmADMB (Fournier *et al.* 2012, Skaug *et al.* 2016). GLMMs are useful for capturing the variation within count data, which can only take the form of positive integers and, thus, cannot technically be normally distributed. Error structures approximating zero-inflated Poisson and Poisson distributions and random effects with random intercept and with or without random slope were compared for all GLMMs using second order Akaike Information Criterion (AICc) scores, specialized for small sample size, in the package MuMln (Barton 2018). The best-fitting model (lowest AICc) was selected on a case-by-case basis. In the GLMMs, 22/3 was used for all samples as an ‘offset’ term to account for the visual error rate. R uses ‘offset’ to specify linear predictor variables with a known coefficient of 1, rather than an estimated coefficient. In the case of the Poisson GLMMs used in this study, adding the natural log of these constants is mathematically equivalent to specifying each constant as the denominator for the MP count numbers in the model equation. However,

specifying the error factors in this way would fail to satisfy the assumption that Poisson-distributed data only take the form of positive integers. Therefore, the natural log of each constant was used to account for the fact that the other linear predictors are linked to the independent variable (MP count) by a log-link function.

Twenty-two GLMMS were specified according to Table 2. These models were first used to determine whether site location had an effect on MP concentrations in shellfish, seawater, and sediment samples. An offset term of ln(22/3 x dry-tissue weight) was specified for the shellfish models to account for the dry-tissue weight of each individual in addition to the visual identification error rate. Dry weight was used in the offset term rather than as a predictor variable since it did not correlate in any way with MP count for any species but was still useful as a measure of concentration to compare across individuals. For the oyster data, one outlying data point (an oyster from the Hyacinthe Bay reference site with an MP count of 18) was excluded from the analysis to reduce heterogeneity of variance (as visually assessed by residuals *vs.* fitted values plot). Next, the effect of region on MP concentrations in all sample types was tested. The same outlier was excluded for the oyster model and one outlier from the Discovery Islands was excluded from the water sample analysis to improve homogeneity of variance. To account for the fact that the non-aquaculture sites varied in distance from shellfish aquaculture sites, GLMMS were run with distance to nearest shellfish aquaculture site as a predictor for all sample types. Straight-line distance to the nearest shellfish aquaculture site was measured over water using shellfish tenure data from Fisheries and Oceans Canada, GPS coordinates of site locations, and the ruler tool in the computer program QGIS (QGIS Development Team 2018). One outlier was removed for the sediment model (one sample from the Sawmill Bay aquaculture site, again

assessed visually in a residuals *vs.* fitted plot). Two GLMMs were also run to determine whether the MP concentrations in seawater had an effect on MP concentrations in shellfish.

Table 2: Generalized linear mixed models (GLMMs) and the response and predictor variables, random effects and whether their slopes and intercepts were assumed to be random or fixed, 'offset' terms specified in R, and the assumed error structure. These models were used in the statistical analyses of variables relating to microplastic particle (MP) concentrations in clams, oysters, seawater, and sediment samples.

	Response Variable	**Predictor Variable(s)**	**Random effect(s)**	**Random effect(s) slope/intercept**	**'Offset' term(s)**	**Distribution**
A	MP count in clams	Site type (shellfish aquaculture/non-aquaculture)	Quadrat nested in site	Fixed slope/random intercept	Identification error; dry tissue weight	Zero-inflated Poisson
B	MP count in oysters	Site type (shellfish aquaculture/non-aquaculture)	Quadrat nested in site	Fixed slope/random intercept	Identification error; dry tissue weight	Zero-inflated Poisson
C	MP count in clams	Region	Quadrat nested in site	Fixed slope/random intercept	Identification error; dry tissue weight	Zero-inflated Poisson
D	MP count in oysters	Region	Quadrat nested in site	Fixed slope/random intercept	Identification error; dry tissue weight	Zero-inflated Poisson
E	MP count in clams	Distance to nearest shellfish aquaculture site	Quadrat nested in site	Fixed slope/random intercept	Identification error; dry tissue weight	Zero-inflated Poisson
F	MP count in oysters	Distance to nearest shellfish aquaculture site	Quadrat nested in site	Fixed slope/random intercept	Identification error; dry tissue weight	Zero-inflated Poisson
G	MP concentration in seawater (particles/L)	Site type (shellfish aquaculture/non-aquaculture)	Site	Fixed slope/random intercept	Identification error	Zero-inflated Poisson
H	MP concentration in seawater (particles/L)	Region	Site	Fixed slope/random intercept	Identification error	Poisson
I	MP concentration in seawater (particles/L)	Distance to nearest shellfish aquaculture site	Site	Fixed slope/random intercept	Identification error	Zero-inflated Poisson
J	MP count in sediment	Site type (shellfish aquaculture/non-aquaculture)	Site	Fixed slope/random intercept	Identification error	Zero-inflated Poisson

K	MP count in sediment	Region	Site	Fixed slope/random intercept	Identification error	Poisson
L	MP count in sediment	Distance to nearest shellfish aquaculture site	Site	Fixed slope/random intercept	Identification error	Zero-inflated Poisson
M	MP count in clams	MP concentration in seawater (particles/L)	Quadrat nested in site	Fixed slope/random intercept	Identification error; dry tissue weight	Poisson
N	MP count in oysters	MP concentration in seawater (particles/L)	Quadrat nested in site	Random slope/random intercept	Identification error; dry tissue weight	Poisson
O	MP count in clams	Beach slope (degrees); Grain size PC1; Grain size PC2	Quadrat nested in site	Fixed slope/random intercept	Identification error; dry tissue weight	Zero-inflated Poisson
P	MP count in oysters	Beach slope (degrees); Grain size PC1; Grain size PC2	Quadrat nested in site	Fixed slope/random intercept	Identification error; dry tissue weight	Zero-inflated Poisson
Q	MP concentration in seawater (particles/L)	Beach slope (degrees); Grain size PC1; Grain size PC2	Site	Fixed slope/random intercept	Identification error	Poisson
R	MP count in sediment	Beach slope (degrees); Grain size PC1; Grain size PC2	Site	Fixed slope/random intercept	Identification error	Poisson
S	MP count in clams	Amount of plastic on site	Quadrat nested in site	Fixed slope/random intercept	Identification error; dry tissue weight	Zero-inflated Poisson
T	MP count in sediment	Amount of plastic on site	Site	Fixed slope/random intercept	Identification error	Poisson
U	MP concentration in seawater (particles/L)	Amount of plastic on site	Site	Fixed slope/random intercept	Identification error	Poisson
V	MP count in oysters	Amount of plastic on site	Quadrat nested in site	Fixed slope/random intercept	Identification error; dry tissue weight	Zero-inflated Poisson

To approximate the sediment type at each site, an exploratory principal-components analysis (PCA) was conducted on the grain-size data using the prcomp function in R. PC1 and PC2, accounted for a combined 75.7% of the variance in multi-dimensional space for the grain-size categories and so were used as predictor variables in models that appropriately captured the variation in sediment type among beaches. Since grain size, beach slope, and the depositional nature of beaches are known to be correlated (Bascom 1951), separate GLMMs were run for each sample type to determine the effect of beach characteristics on MP concentration (with PC1, PC2, and beach slope used as continuous predictor variables). One outlier from the water samples was excluded from the analysis to improve homogeneity of variance (as visually assessed in a residuals *vs.* fitted plot).

To test for the impact of plastic presence at any given site on the number of MPs found in shellfish, sediment, and water samples, GLMMs were run with plastic category (high, medium, low, or none) as a predictor. One outlier was removed for the oyster dataset, as previously specified for the aquaculture *vs.* non-aquaculture models. For the water dataset, an outlier with an MP concentration of 18 was removed from the high plastic category to reduce heterogeneity of variance. To determine whether plastic category was significant, null models were compared with best-fit models using log-likelihood analysis of deviance tests.

3.2.8 Power Analysis

Power analyses using simulation were conducted separately on the clam and oyster data sets. All simulations were run using the package simr (Green and MacLeod 2016), which allows statistical power calculations for mixed-effects models through repeated simulation of a given model/experimental design, thereby enabling the user to calculate power curves to assess trade-offs between power and sample size. As the simr package requires models to be specified in

lme4 (Bates *et al.* 2015), the clam and oyster GLMMs (previously used to test for the difference between aquaculture and non-aquaculture sites) were modified to run in lme4 by removing any zero-inflated error structure and using regular Poisson error structures. For each model, new response data (MP count) were simulated 1,000 times and the specified model fit was statistically assessed with each iteration. The calculated power is the proportion of significant test results out of the 1,000 iterations at $\alpha = 0.05$. For the clam and oyster GLMMs, power curves were calculated to determine the statistical power of each test to detect significance. This was done using a reasonable effect size of -1 for non-aquaculture shellfish (*i.e.*, one less MP per individual in non-aquaculture shellfish than in aquaculture individuals), assuming the pre-existing data structure, but with varying sample size at each site and varying numbers of overall sites.

3.3 Results

3.3.1 Particle Numbers and Procedural Blanks

Procedural blanks had 0.50 ± 0.58 (clams), 0.37 ± 0.69 (oysters), 4 ± 2.65 (water), and 0.81 ± 1.36 (sediment) MPs (mean ± SD) per sample. A total of 253 (clam), 338 (oyster), 289 (water), and 295 (sediment) potential MPs were found. After accounting for contamination present in the blanks, total particle numbers in the clam, oyster, water, and sediment samples were adjusted to 212, 310, 203, and 254, respectively.

3.3.2 Particle Characteristics

In clams, 90.0% of the remaining suspected MPs (not yet accounting for whether they were plastic) were fibres, 4.4% were fragments, and 5.6% were spherules. In oysters, percentages were 90.5%, 2.4%, and 7.1%, respectively. Fibres in clams/oysters were

predominately clear (37.5%/55.1%), blue (29.5%/16.1%), black (13.5%/10.5%), or turquoise (6.5%/5.6%). The particles of all shapes were primarily 100–499 µm in size for both clams (52.8%) and oysters (49.0%) (Fig. 7). In seawater, 99.5% of particles were fibres, with blue (44.2%), pink (14.2%), turquoise (13.7%), black (12.2%), clear (6.6%), and red (6.1%) being the dominant colours and 1000–5000 µm (38.4%) and 100–499 µm (34.5%) being the dominant size fractions (Fig. 7). Fibres were also dominant in the sediment samples (99.2%) and were mostly clear (46.9%), blue (28.4%), or black (13.0%) and either 100–499 µm (36.6%), 1000–5000 µm (36.2%), or 500–999 µm (27.2%) in length, with no potential MPs <100 µm being detected (Fig. 7).

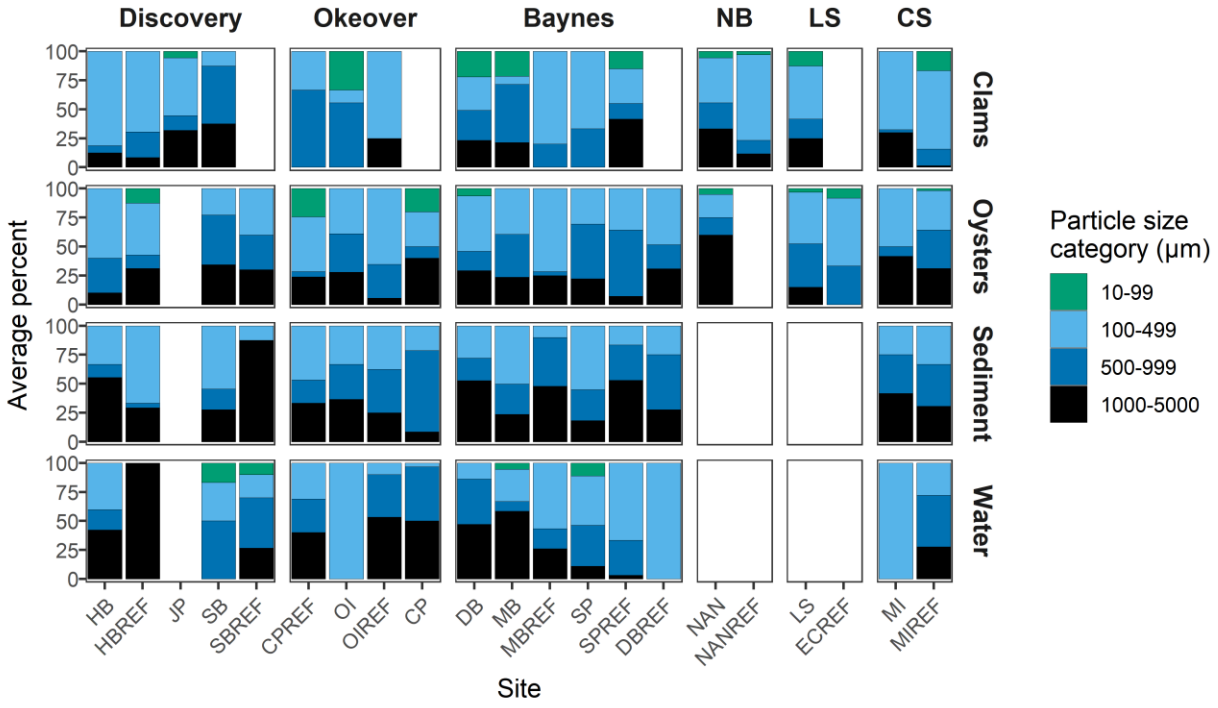

Figure 7: Average proportion of various potential microplastic particle sizes (longest dimension) of samples that contained these particles in Manila clams (Venerupis philippinarum), Pacific oysters (Crassostrea gigas), sediment samples, and seawater samples. Study region is indicated at the top, with NB standing for Nanoose Bay, LS for Ladysmith, and CS for Clayoquot Sound. HB=Hyacinthe Bay, HBREF=Hyacinthe Bay Reference, SB=Sawmill Bay, SBREF=Sawmill Bay Reference, JP=Joyce Point, CP=Coode Peninsula, CPREF=Coode Peninsula Reference, OI=Okeover Inlet, OIREF=Okeover Inlet Reference, NB=Nanoose Bay, NBREF=Nanoose Bay Reference, SP=Ships Point, SPREF=Ships Point Reference, MB=Mud Bay, MBREF=Mud Bay Reference, DB=Deep Bay, DBREF=Deep Bay Reference, LS=Ladysmith, LSREF=Ladysmith Reference, MI=Meares Island, MIREF=Meares Island Reference.

3.3.3 FTIR Analysis

Micro-FTIR analysis confirmed that only six of the 44 suspected microplastic fibres (*i.e.*, 13.6%) analysed were plastic (Fig. 8). Thus, as described in the methods section, a correction factor of 3/22 was applied to all reported suspected MP concentrations. In the four clam specimens analyzed, two polyester fibres were detected, along with seven non-plastic fibres. In the four oyster samples analyzed, one nylon fibre and one polyester fibre were detected, along with five cellulosic fibres, one of which was cotton. From the five water samples, one polyester fibre, one nylon-rayon blend fibre, and sixteen non-plastic fibres, including one cotton and one mineral fibre, were found. In the three sediment samples analyzed, all ten fibres were cellulosic. Analysis of some of the common plastic items at the study sites found that anti-predator nets from Mud Bay and Hyacinthe Bay were composed of polypropylene and an unknown polyolefin, and that anti-predator fences used at Mud Bay and Okeover Inlet consisted of polyethylene. Rope debris found on the two non-aquaculture sites at Okeover Inlet and Hyacinthe Bay was identified as polypropylene and nylon, while two plastic buckets buried in the intertidal at the Hyacinth Bay reference site were both polyethylene. These types of plastic, other than nylon, were not detected in the synthetic fibres found in clam, oyster, and water samples using FTIR.

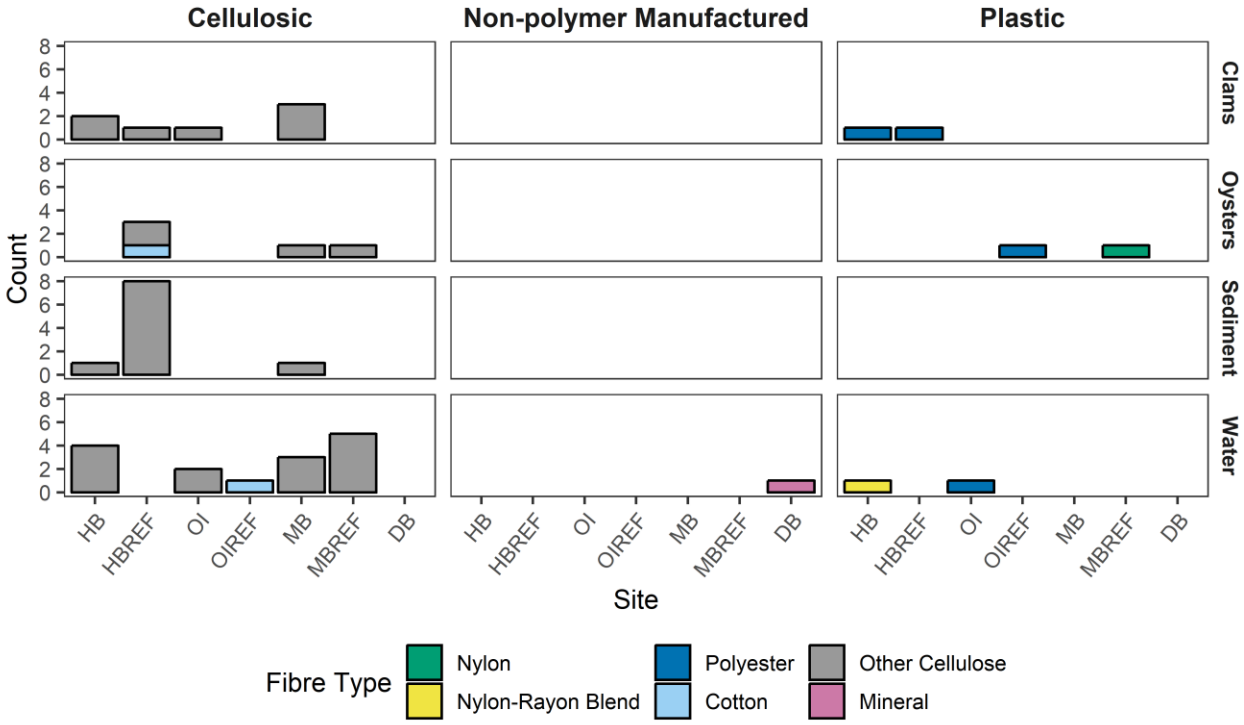

Figure 8: Fourier-transform infrared (FTIR) spectroscopy results for 44 putative microplastic particles confirming that six were plastic and composed of nylon, polyester, or a nylon-rayon blend. Material class is listed across the top and sample type across the right-hand side. Non-polymer manufactured materials include the one mineral fibre detected and cellulosic materials cover cotton and all other cellulose-based fibres, including natural (*e.g.*, naturally occurring plant fibres) and semi-synthetic (*i.e.*, rayon and viscose) that could not be reliably separated by FTIR spectroscopy. HB=Hyacinthe Bay, HBREF=Hyacinthe Bay Reference, OI=Okeover Inlet, OIREF=Okeover Inlet Reference, MB=Mud Bay, MBREF=Mud Bay Reference, DB=Deep Bay.

3.3.4 MP Occurrence

Of the shellfish analyzed for MP content, clams averaged 39.6 ± 3.5 (SD) mm in shell length and 0.8 ± 0.3 g in dry-tissue weight, while oysters averaged 108.8 ± 14.0 mm in shell height and 5.7 ± 2.4 g in dry-tissue weight. For the samples taken before outplant, clams contained 0.10 ± 0.10 MPs ind^{-1} or 0.16 ± 0.18 MPs g^{-1} dry tissue weight, after adjusting for contamination and identification error, and oysters contained 0.13 ± 0.16 MPs ind^{-1} or 0.02 ± 0.03 g^{-1} dry tissue weight. The clams collected from the outplant experiment had a range of ~0–2 MPs ind^{-1}, with an average of 0.16 ± 0.22 MPs ind^{-1} or 0.22 ± 0.31 MPs g^{-1} dry-tissue weight (Fig. 9). The oysters had a range of 0–3 MPs ind^{-1}, with an average of 0.22 ± 0.28 MPs ind^{-1} or 0.04 ± 0.06 MPs g^{-1} dry-tissue weight (Fig. 9). Shellfish outplanted on aquaculture sites did not contain significantly more MPs than those placed at non-aquaculture sites (clams: p=0.37, Table B1A; oysters: p=0.56, Table B1B). MP concentrations did not significantly differ among regions for either clams (p=0.06, Table B1C) or oysters (p=0.10, Table B1D). Distance to the nearest shellfish aquaculture site also had no significant effect on MP concentration in clams (p=0.66, Table B1E, Fig. 10) or oysters (p=0.37, Table B1F, Fig. 10).

The seawater samples had ~0–4 MPs L^{-1}, with a mean of 0.63 ± 0.68 MPs L^{-1} (Fig. 9), with no significant difference detected between shellfish aquaculture and non-aquaculture samples (p=0.65, Table B1G). Seawater MP concentrations differed significantly by region (p=0.04, Table B1H), with Baynes Sound and Okeover Inlet samples having more MPs than those from Discovery Islands and Clayoquot Sounds (0.72 ± 0.57 and 0.80 ± 0.69 *vs.* 0.52 ± 0.95 and 0.25 ± 0.23 MPs L^{-1}, mean ± SD, respectively). Distance to the nearest shellfish aquaculture site had no significant effect on seawater MP concentration (p=0.25, Table B1I, Fig. 10). No significant relationship was detected between MP concentrations in water samples and either

clam (p=0.78, Table B1J) or oyster samples (p=0.70, Table B1K) for sites where both shellfish and water samples were taken.

Sediment samples had ~0–3 MPs sample^{-1}, with a mean of 0.37 ± 0.43 MPs sample^{-1}. This is equivalent to an average of 23.84 ± 27.27 MPs L^{-1} or 23,840 MPs m^{-3} (Fig. 9). By dry weight, the average concentration was 19.97 ± 23.74 MPs kg^{-1}. No significant difference was detected in sediment MP concentrations between shellfish aquaculture and non-aquaculture samples (p=0.60, Table B1L). MP concentrations did not differ significantly among regions (p=0.08, Table B1M). Distance to nearest shellfish aquaculture site had no significant effect on sediment MP concentration (p=0.33, Table B1N, Fig. 10).

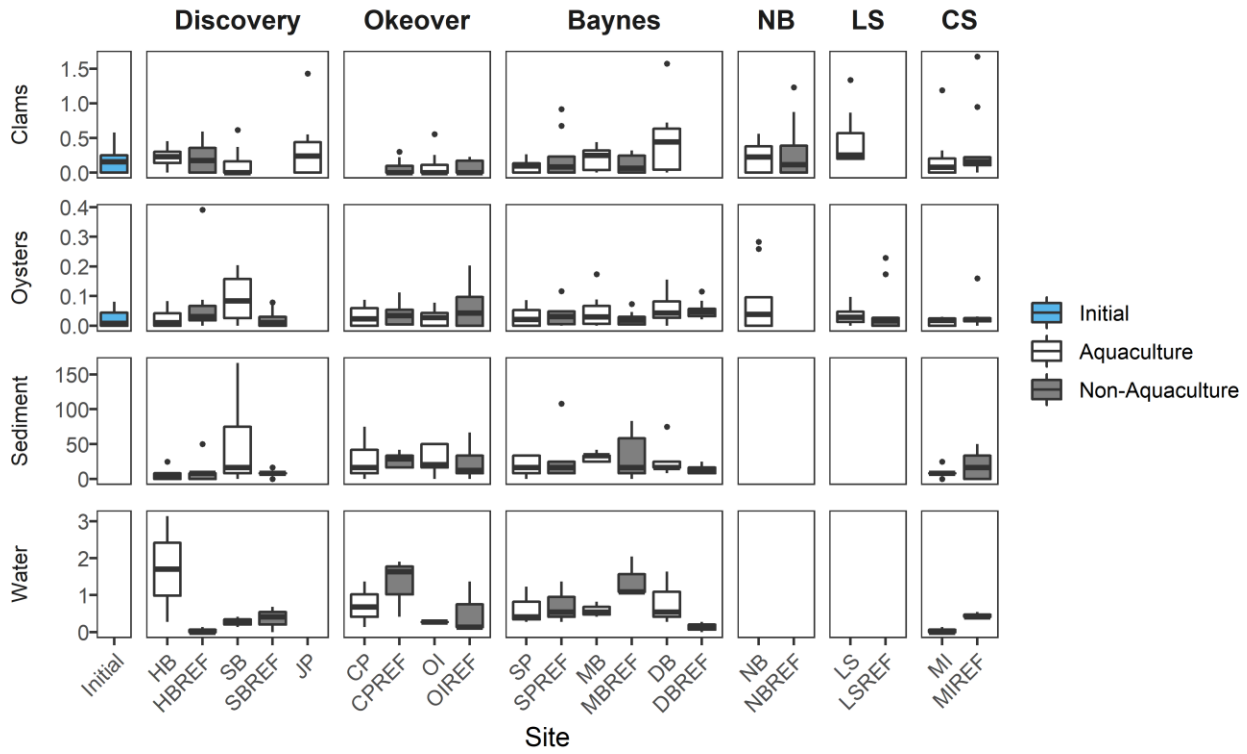

Figure 9: Boxplots of microplastic particle (MP) concentrations in Manila clams (Venerupis philippinarum, MP g^{-1} dry tissue weight, Pacific oysters (Crassostrea gigas, MP g^{-1} dry tissue weight), sediment samples (MP L^{-1}), and seawater samples (MP L^{-1}) taken at shellfish aquaculture and non-aquaculture sites. The 'initial' concentrations are oysters and clams that were sampled before they were outplanted to the various study sites. All concentrations are adjusted for identification error and for background contamination. Box limits and whiskers show first and third quartiles, respectively, with outliers (more than 1.5 times the distance between the first and third quartiles away from the median) shown as points. Study region is indicated at the top, with NB standing for Nanoose Bay, LS for Ladysmith, and CS for Clayoquot Sound. HB=Hyacinthe Bay, HBREF=Hyacinthe Bay Reference, SB=Sawmill Bay, SBREF=Sawmill Bay Reference, JP=Joyce Point, CP=Coode Peninsula, CPREF=Coode Peninsula Reference, OI=Okeover Inlet, OIREF=Okeover Inlet Reference, NB=Nanoose Bay, NBREF=Nanoose Bay Reference, SP=Ships Point, SPREF=Ships Point Reference, MB=Mud Bay, MBREF=Mud Bay Reference, DB=Deep Bay, DBREF=Deep Bay Reference, LS=Ladysmith, LSREF=Ladysmith Reference, MI=Meares Island, MIREF=Meares Island Reference.

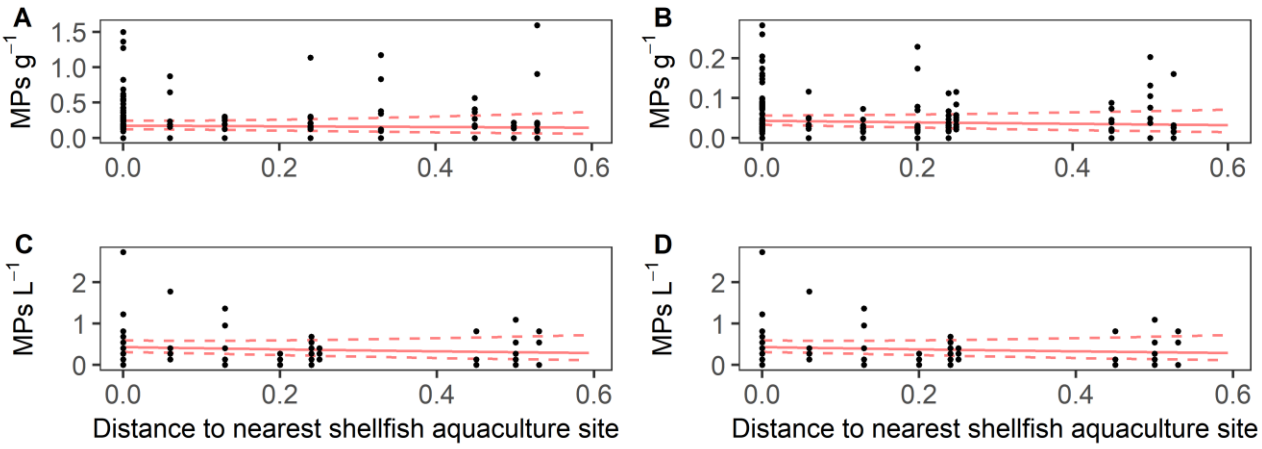

Figure 10: Microplastic particle (MP) concentrations in A) clams, B) oysters, C) water, and D) sediment, plotted against shortest overwater distance to nearest shellfish aquaculture site. Concentrations for oysters are in terms of dry tissue weight. All MP concentrations are adjusted for identification error and for background contamination. The solid red line indicates generalized linear mixed model (GLMM) fit, with random effects set to 0 and dry-tissue weight set to the average value for each of the shellfish species. The dashed red lines indicate the 95% confidence interval for the model fit. Distance to nearest shellfish aquaculture site did not significantly affect MP concentration in any of the models.

According to the loadings plot for the grain size PCA (Fig. 11), PC1 differentiates sediments having more gravel and coarse sand from those with fine sand and silt. PC2 mainly varied according to whether sediment was composed of more sand or gravel and did not vary much according to silt and fine sand composition. No significant effects of beach slope, PC1, or PC2 on MP concentration in clams were detected with the beach characteristics model (p=0.68, 0.23, 0.32, respectively, Table B1O). Similarly, beach slope and PC1 were not significant predictors of oyster MP concentration for the beach characteristics model (p=0.84, 0.83, respectively, Table B1P). PC2 did have a significant negative effect (p=0.01), however, suggesting that oysters on sandier beaches may have more MPs than those on gravel beaches. However, this effect size was extremely small, with only about 0.1 more MPs g^{-1} dry tissue weight, on average, predicted at sandier beaches. Beach slope, PC1, and PC2 showed no significant effect on MP concentration in the seawater samples (p=0.64, 0.28, 0.63, respectively, Table B1Q) or sediment samples (p=0.28, 0.10, 0.88, respectively, Table B1R).

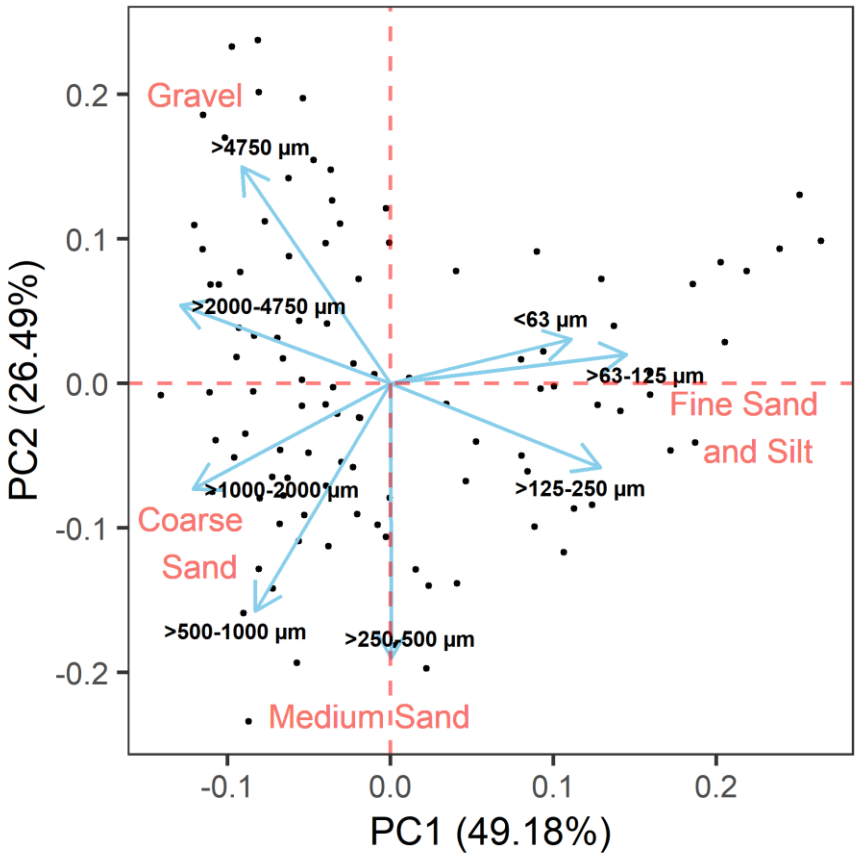

Figure 11: Plot of principle-component analysis results for eight size classes of sediment grain size across eighteen sites. PC1 and PC2 account for 75.7% of the variance with loadings plot showing which specific grain size classes (in µm) accounted for variation along each axis. Sediment size categories according to Wentworth (1922) are shown to demonstrate how the grain size data grouped in multi-dimensional space.

The amount of plastic found on a particular site did not significantly affect MP levels found in clams (p=0.34, Table B1S), sediment (p=0.13, Table B1T), or water samples (p=0.55, Table B1U), but did significantly affect MP levels in oysters (p<0.001, Table B1V). Beaches with no plastic on site had an average of 0.02 less MPs g^{-1} dry tissue weight in oysters than beaches with considerable amounts of plastic on site (0.05 *vs.* 0.03 g^{-1} dry tissue weight, on average, Fig. 12). Specifically, this is for the sites DB, MB, NB, and HB (high plastic) compared with MBREF and MIREF (no plastic). However, when considered in terms of individual, the mean number of MPs found in oysters on high *vs.* low plastic sites are identical (0.20 ind^{-1}). Differences according to weight occurred due to the oysters grown on non-aquaculture sites having higher dry tissue weights, on average. Comparisons between other levels of plastic impact (high-medium, high-low, medium-low, medium-none, low-none) were not significant (Table B1W).

3.3.5 Power Analysis

The power analysis showed that both the clam and oyster data sets were of sufficient power to detect one less particle per individual shellfish at a non-aquaculture *vs.* aquaculture site, given the experimental structure and sample sizes used. The clam analysis had a power of 96% to detect this effect size and would have surpassed a power of 90% with as few as four individuals per site. Further simulation suggests that given the current sample size of ten clams per site, as few as ten total sites (five of each type) would have been sufficient for 90% power to detect one less MP on average in non-aquaculture clams. The oyster analysis had a power of 93% and would have surpassed a power of 90% with as few as eight individuals per site. Further simulation suggests that given the current sample size of ten oysters per site, as few as 16 total

sites would have been sufficient for 90% power to detect one less MP on average in non-aquaculture oysters.

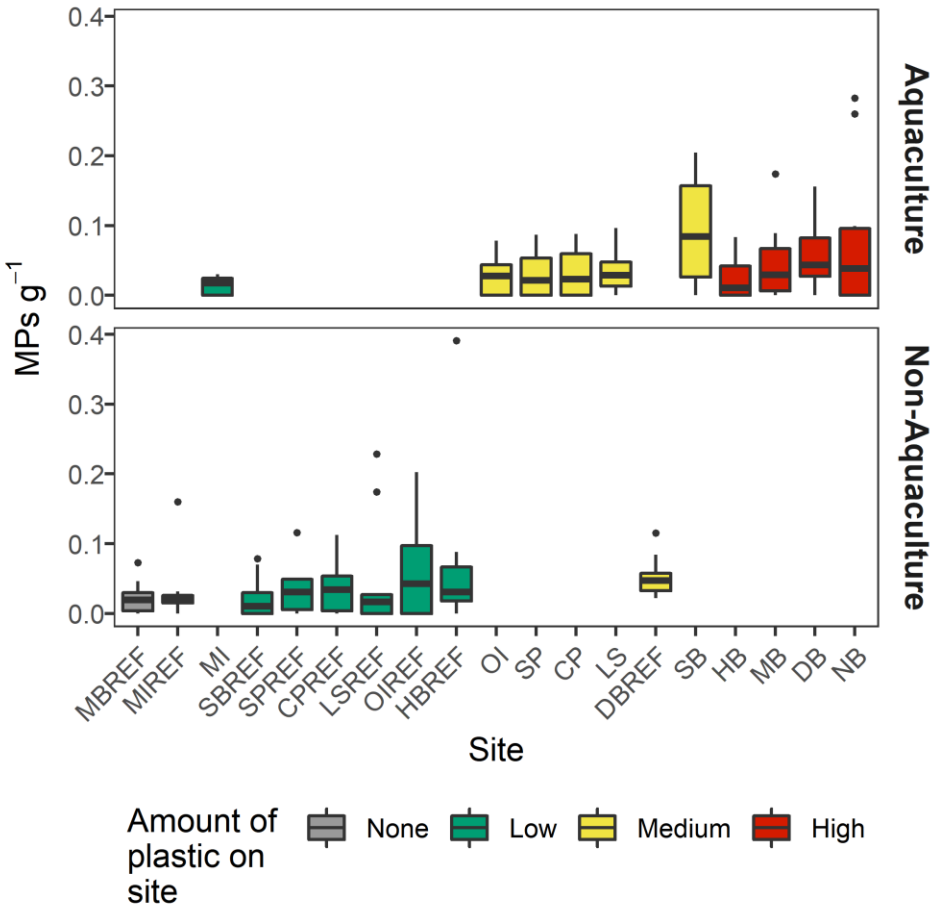

Figure 12: Boxplots of microplastic particle (MP) concentrations in Pacific oysters (Crassostrea gigas) at 19 study sites (aquaculture and non-aquaculture) according to amount of plastic equipment and debris on site. All concentrations are in terms of dry tissue weight and are adjusted for identification error and for background contamination. Box limits and whiskers show first and third quartiles, respectively, with outliers (more than 1.5 times the distance between the first and third quartiles away from the median) shown as points. MBREF=Mud Bay Reference, MIREF=Meares Island Reference, MI=Meares Island, SBREF=Sawmill Bay Reference, SPREF=Ships Point Reference, CPREF=Coode Peninsula Reference, LSREF=Ladysmith Reference, OIREF=Okeover Inlet Reference, HBREF=Hyacinthe Bay Reference, OI=Okeover Inlet, SP=Ships Point, CP=Coode Peninsula, LS=Ladysmith, DBREF=Deep Bay Reference, SB=Sawmill Bay, HB=Hyacinthe Bay, MB=Mud Bay, DB=Deep Bay, NB=Nanoose Bay.

3.4 Discussion

Our results show no significant difference in MP concentrations in shellfish or their habitat between shellfish aquaculture and non-aquaculture sites at a local scale (60–530 m) in coastal BC, suggesting that the observed MP concentrations may be related to other factors. Qualitative assessment of the amount of plastic on each site found a large variability of plastic use at shellfish aquaculture leases. Oysters from sites with 'high' plastic use, with hundreds of square metres of anti-predator netting, had significantly more MPs than oysters from non-aquaculture sites with no plastic debris. However, this effect size was small (0.05 *vs.* 0.03 MPs g^{-1} of tissue weight on average). Furthermore, when considered in terms of individual, the average MP concentrations were the same at high and no plastic sites (0.20 ind^{-1}). It can therefore be concluded that the difference in MP concentrations by body weight are driven by higher average tissue weight in the oysters grown at non-aquaculture sites (8.30 *vs.* 4.29 g dry tissue) where no macroplastics were present. Spectroscopic results illustrate that the sub-sampled particles identified as plastic were primarily polyester and nylon fibres and that none of the sampled nets were composed of either polymer. The high plastic sites were long, sloping, sandier beaches, which are preferred as shellfish aquaculture tenure locations. Sandier beaches were also linked with increased MP concentrations in oysters, however, again this is due to the difference in body size between shellfish aquaculture *vs.* non-aquaculture sites, as tissue weight was lower at the sandier beaches than the gravellier ones. These findings, along with a lack of correlation between distance to shellfish aquaculture site and MP concentrations, suggests that anthropogenic fibres found in shellfish and their environment in BC are likely not causally linked to shellfish aquaculture operations, but more likely related to textile fibre emissions, the most probable sources of which are sewage effluent and aerial dispersal (Carr 2017). The *in-situ* degradation of

nylon ropes, which could come from boating, fishing, and/or aquaculture activities, is also a potential source (Welden and Cowie 2017), but none of the materials that were analyzed from the studied shellfish aquaculture operations were actually nylon.

An earlier study in Baynes Sound (one of our study regions) found no difference between Manila clams on/off shellfish aquaculture sites (Davidson and Dudas 2016) and an Italian study found a similar result in mussels (Renzi *et al.* 2018). In some cases, cultured bivalves have been documented to contain significantly higher concentrations of MPs than wild shellfish (Mathalon and Hill 2014, Phuong *et al.* 2018, Ding *et al.* 2018), but this effect appears to be context dependant. In one case from China, cultured shellfish contained significantly fewer MPs than wild individuals when cultured in areas with a comparatively smaller human footprint (Li *et al.* 2016). Our findings indicate that MP concentrations in bivalves from non-aquaculture sites are similar to those in individuals on shellfish aquaculture sites, despite both site types being distributed across a range of densities of human activity. Our reference sites were only 60–530 m from the nearest shellfish aquaculture facility, which makes it difficult to conclusively rule out a contamination effect of shellfish aquaculture that extends beyond such a scale. However, we also did not detect any consistent regional patterns in MP concentrations that would suggest shellfish aquaculture as a source, considering that the density of their activity varied by region.

Previous work has suggested that Baynes Sound is extremely contaminated by small non-fibrous, spherical MPs with up to 25,000 MPs kg^{-1} of dry sediment (Kazmiruk *et al.* 2018), which is three orders of magnitude greater than our estimate of 19.97 MPs kg^{-1} dry sediment. We found that for the 21 sites examined (in Baynes Sound, Clayoquot Sound, Discovery Islands, southern Vancouver Island, and Okeover Inlet) there was a relatively homogenous distribution of MPs, which conflicts with Kazmiruk *et al.*'s (2018) suggestion that the high degree of

contamination in Baynes Sound is due to the high density of shellfish aquaculture in the region. Interestingly, Kazmiruk *et al.* (2018) reported most MPs counted to be less than 0.63 µm using automated photo-identification at 40X magnification (and no FTIR). Given that the lower limit for reliable visual identification of particles has been stated by some researchers as 100 µm in diameter (Dekiff *et al.* 2014, Lenz *et al.* 2015), the results of Kazmiruk *et al.* (2018) are unusual and unprecedented in the published literature.

Most polymers present in the subset of samples analysed using FTIR analyses did not match the composition of equipment used in local intertidal shellfish aquaculture, showing that other sources likely contributed to the MPs found in our samples. Given the limited size of the FTIR sub-sample, however, this does not necessarily rule out shellfish aquaculture as a source of any of the particles detected. A study in Xiangshan Bay, China found that approximately 56% and 37% of the MPs in seawater and sediment, respectively, were likely derived from local aquaculture activity showing that aquaculture can impact the environment with MPs (Chen *et al.* 2018). In that case, however, the 560-km^2 bay was covered by about one hundred km^2 of shellfish and finfish aquaculture activity, a far greater aquaculture coverage than presently occurs anywhere in BC. Thus, while shellfish aquaculture may have the potential to become a significant source of MPs in the environment under highly intensive culture conditions, there is no evidence from our study to suggest that this is currently the case in BC.

The lack of any consistent regional or site patterns in MP concentrations suggest large-scale mixing of MPs across our study area. Many of our sites were in the Strait of Georgia (SoG), which receives sewage effluent from the Greater Vancouver area as well as from many smaller municipalities along the east coast of Vancouver Island. SoG water is renewed by Pacific Ocean water over a period of several months to a year, depending on depth, and may thus cause

homogenization of MPs throughout the entire strait (Pawlowicz *et al.* 2007). Assuming a minimum sinking rate for fibres of 1 mm s^{-1} (calculated for 8-mm fibres by Bagaev *et al.*(2017)), a maximum flow rate of 1.5 m s^{-1} in the SoG (from www.oceannetworks.ca), and subtracting the lowest tidal height of our shellfish samples (0.92 m) from a normal tide range of 3.3 m (Thomson 1981) to assume a maximum depth of 2.38 m for the shellfish to filter feed, we can calculate a maximum sinking time for microfibres of 40 minutes and a maximum dispersal distance of 3.6 km. The particles found in this study, however, were much smaller than 8 mm and would thus be subject to micro-scale turbulence effects and low Reynolds number physics, both of which will likely decrease sinking rates, thereby increasing horizontal transport (Bach *et al.* 2012). Aggregation of MPs with each other and with biogenic particles (Michels *et al.* 2018) would further complicate the question of sinking rates. Kowalski *et al.* (2016) estimated sinking rates of 6–91 mm s^{-1} for 0.3–3.6-mm plastic pellets of various polymer types, but the fibres found in our study would again be expected to have slower sinking rates due to their higher aspect ratio. While MPs may be heterogeneous within the SoG to some extent (*e.g.*, near hot spots such as sewage outfalls), it is more likely that microfibres remain suspended in the water column over long distances, thereby leading to a more homogenous distribution. This possibility is supported by the ubiquitous presence of microplastics in the Arctic Ocean (Lusher *et al.* 2015) and in the deep sea (Woodall *et al.* 2014), regions which would not be expected to receive much direct contamination from anthropogenic sources. Other variables such as temperature (lower temperature, more dense seawater, slower sinking rates), salinity (higher salinity, greater density, slower sinking rates), and aerial transport may further influence the distribution of MPs in coastal BC, and further study of these processes is called for.

MP concentrations in our sediment samples were two orders of magnitude greater than those in our seawater samples, suggesting the eventual deposition and concentration of MPs in sediment. Other studies have also shown that sediment concentrations of MPs can be 1–4 orders of magnitude greater than in the overlying water (Woodall *et al.* 2014, Bagaev *et al.* 2017). Our estimates, however, should be taken with caution considering that the sediment samples were only ~15.6 mL in volume (after sub-sampling from 150-mL samples) and thus may not be representative of the environment at large. Counting just one extra MP particle in such small samples would lead to two orders of magnitude change in MP concentration per litre of sediment. As this is similar to the degree by which our sediment and water sample concentrations differed, overestimation of sediment concentration by sampling error cannot be ignored. Furthermore, the subsampled fibres from the sediment were all cellulosic, according to spectroscopy. Our visual error rates may have been much higher for sediment in that case, suggesting the presence of many non-plastic fibres in sediment and making it difficult to make any conclusions on MP deposition in our study areas.

The lack of any significant effect of water sample MP concentrations on shellfish or sediment concentrations suggests that the transfer of MPs from seawater to shellfish and sediment is driven at spatial or temporal scales not captured by the instantaneous water sampling used in this study. The particles found in both clams and oysters were both smaller in length than the dominant sizes of MPs found in seawater and sediment, indicating a preference for the capture and ingestion of smaller particles in accordance with the feeding strategies of bivalves (Ward and Shumway 2004). The phytoplankton commonly fed on by shellfish are often less than 100 µm in diameter, but high filtration efficiency has also been demonstrated for chain forming diatoms that can reach up to several hundred µm in length (Nakamura 2001). The low MP

concentrations in bivalves (*i.e.*, relative to the finding of 0–4 MPs L^{-1} of seawater), along with the predominance of smaller particles, indicates that bivalves may be able to selectively avoid certain MP particles, either by avoiding ingestion or by rejection into pseudofaeces (Defossez and Hawkins 1997), and that the smaller particles that are ingested do not accumulate to any major degree. Clams had an order of magnitude higher MP concentrations than oysters by tissue weight. This may show that clams are more at risk for potential health impacts of MP ingestion than oysters. Pacific oysters have pseudo-lamellibranch gills and can sort particles using both the gills and labial palps (Beninger *et al.* 2008), while clams have eu-lamellibranch gills, whereby selection function is lowered, which could explain why the clams concentrated MPs more than the oysters. We were not able to reliably measure MPs less than one hundred μm in diameter, however, so the absolute concentrations of this size class of particles in the sampled shellfish, and thus the potential for biological risk, remain unknown. Furthermore, this suggests that our concentration estimates for the smaller MPs should be considered conservative underestimates.

While the risk to human health from ingesting MPs *via* the consumption of shellfish has not yet been quantified, it will likely be low compared to other exposure pathways, given the low consumption of shellfish relative to other food items (in many cultures) and the magnitude of other exposure vectors. We found means of 0.22 ± 0.28 MPs ind^{-1} or 0.04 ± 0.06 MPs g^{-1} dry-tissue weight in Pacific oysters. Other studies have reported averages for the same species of 30 and 87 MPs g^{-1} dry weight from two locations on the Dutch coast (Leslie *et al.* 2017), 2.1 MPs $oyster^{-1}$ on the French Atlantic coast (Phuong *et al.* 2018), and 0.6 MPs $oyster^{-1}$ on the U.S. Pacific coast (Rochman *et al.* 2015). Our numbers are much lower than oysters sampled in Europe, but similar to those examined in the U.S. We found 0.16 ± 0.22 MPs ind^{-1} in Manila clams, while a previous study conducted in one of our experimental regions, Baynes Sound,

reported 11.3 and 8.4 MPs clam^{-1} on/off shellfish aquaculture sites (Davidson and Dudas 2016) and a study in China reported 5.7 MPs clam^{-1} (Li *et al.* 2015). The lower levels in the present study than in Davidson & Dudas (2016) are most likely due to no FTIR-adjustment in the latter. This is a frequent problem in microplastics research as the methodology is rapidly evolving, rendering it difficult to make comparisons with older studies or other regions using different experimental methods.

Statistics Canada (2018) reported that 1.58 kg of shellfish per person was available for consumption by Canadians in 2017 (does not adjust for losses such as waste and/or spoilage). Assuming that this amount of shellfish was actually consumed by the average Canadian, and that 50% consisted of Manila clams and 50% of Pacific oysters, with wet weight:dry weight ratios of 2 and 5 for Manila clams and Pacific oysters, respectively (Mo and Neilson 1994, Yang *et al.* 2010), our findings suggest that per capita Canadian consumption of MPs *via* shellfish could be as low as 87 particles per person per year. This is similar to an estimate of 123 particles per person per year in the U.K. generated by Catarino *et al.* (2018), who further noted that fibre exposure during evening meals could lead to consumption of 13,731–68,415 particles per person per year. It is therefore important to highlight that although MPs undoubtedly are found in shellfish, the risk of exposure to humans *via* their consumption can likely be considered negligible when compared with other sources of MP exposure.

Our findings suggest that shellfish aquaculture is not currently a major source of microplastics in BC waters. While this does not mean that shellfish aquaculture equipment is not releasing MPs into the environment from the plastic used in its operations, it does show that other sources of MPs (*e.g.*, textile emissions *via* sewage or aerial dispersal) may be dominating over any local signal from shellfish aquaculture. Significantly (albeit minimally) lower MP

concentrations by dry tissue weight in oysters grown on more gravelly beaches with no macroplastics present (*i.e.*, non-aquaculture sites) appear to be caused by greater tissue weight in these oysters, suggesting that the oysters did not ingest fewer MPs on the level of the individual. If precautionary best practices to minimize microplastic contamination are employed by shellfish farmers, such efforts would be best targeted towards removal of or alternatives for fibrous equipment like ropes and anti-predator nets which can photodegrade and potentially release substantial amounts of synthetic fibres into the environment.

Chapter 4: Microplastics >100 µm are not biomagnifying in coastal marine food webs of British Columbia, Canada

4.1 Introduction

Although numerous studies have documented the presence of MPs in the environment and in various animals, our understanding of the risks that MPs present to aquatic and terrestrial communities still is limited. From a toxicological standpoint, risk is proportionate to the product of hazard and exposure, where the former is the potential for harm and the latter is dependant on dose and time. Risks can also manifest on different time- and biological-scales of organization, including immediate effects to organisms and populations (*e.g.* changes in growth, reproduction, or mortality), as chronic shifts in behaviour and/or metabolism that shift energy budgets, species interactions, or *via* intergenerational effects (Fleeger *et al.* 2003, Muller *et al.* 2010, Skinner *et al.* 2011). Thus, as part of any ecosystem-level risk assessment for MPs, the routes and extent of exposure for different organisms (*e.g.*, relative exposure from diet *vs.* respiration and the contribution from different food sources) are important aspects to consider. As ingestion represents the main pathway by which MPs enter the bodies of animals (Pinheiro *et al.* 2020), understanding the trophic positions and feeding habits of animals will therefore be key to quantifying their exposure to MPs.

Within the field of ecotoxicology, bioaccumulation and biomagnification are two of the most important metrics for deciding ecological risk as they are key predictors of exposure. Bioaccumulation commonly refers to the relative rates that a contaminant enters and exits the body of an animal (Gobas *et al.* 1988). If excretion or chemical decomposition occurs faster than entry rates, no bioaccumulation occurs. This process is complex, however, since mass in/out does not account for the toxicities of varied sizes and shapes of MPs. For example, many bioaccumulating chemicals are lipophilic and are thus sequestered in the body and prevented

from being excreted. This process does not necessarily occur equally throughout the body and can be organ specific (Piscopo *et al.* 2016). Biomagnification occurs when a contaminant accumulates in the body of an animal and is then transferred to its predator. Predators will thus ingest higher contaminant concentrations in their food than their prey and an exponential magnification effect will occur along the food chain (Kelly *et al.* 2007).

Two commonly used metrics for bioaccumulation and biomagnification are the bioaccumulation factor and trophic magnification factor. The bioaccumulation factor can be calculated by taking the ratio of the concentration of a contaminant in an animal (commonly g kg^{-1}) to that in the surrounding water (commonly g L^{-1}) (Arnot and Gobas 2006). As MPs are often difficult to separate completely from all other materials, concentrations are more commonly expressed in terms of the number of particles rather than their mass *per se* (although this may overlook the fragmentation of ingested particles within animal bodies). The trophic magnification factor refers to the coefficient, or slope, of a regression between the log concentration of a contaminant in an organism and its trophic position (Borgå Katrine *et al.* 2011). Very few studies have examined these two metrics together for MPs or used them to compare exposure among animals feeding at different trophic levels. Quantifying and comparing these metrics within aquatic food webs can therefore figure out the role of individual and trophic dynamics of animals ingesting MPs and the relative degree to which animals with different feeding habits might be at risk.

Many studies have now reported entry of MPs into food webs and their trophic transfer (Santana *et al.* 2017, Carbery *et al.* 2018, Welden *et al.* 2018), including to higher trophic level predators such as grey seals (*Halichoerus grypus*) (Nelms *et al.* 2018). Most studies have investigated trophic transfer using laboratory experiments, however, and there is limited

evidence highlighting the degree to which accumulation, transfer, and biomagnification of MPs are occurring in and between trophic levels in the field. Some recent studies have suggested that factors other than trophic level may be more important for determining the ingestion and accumulation rates of MPs in marine animals (Gouin 2020, Walkinshaw *et al.* 2020, Miller *et al.* 2020, Covernton *et al.* 2021a). These include the ability to depurate MPs quickly, differences in feeding strategy and/or mechanism, degree of contamination of the local environment and even the stochastic probability of encountering an MP within a patchy local environment (Setälä *et al.* 2016b, Güven *et al.* 2017, Santana *et al.* 2017). For example, filter feeders and deposit feeders that primarily feed on pelagic *vs.* benthic phytoplankton would be feeding at the same trophic level but using different strategies and in different environments. This matter is further complicated by the fact that most studies focus only on the digestive tracts of animals and are methodologically limited to larger MPs (generally >100 µm). MPs may be able to translocate from digestive tracts into other animal tissues, although this is likely limited to smaller MPs <130 µm and predominately those under 10 µm in size (Zeytin *et al.* 2020, De Sales-Ribeiro *et al.* 2020, Kim *et al.* 2020, Covernton *et al.* 2021b). There is some evidence, however, that even larger MPs have the potential to translocate to the livers of marine fish, including 214 µm particles (mean size) in gilt-head seabream (*Sparus aurata*) and 124-438 µm particles in European anchovies (*Engraulis encrasicolus*) (Collard *et al.* 2017, Jovanović *et al.* 2018).

Although many studies have investigated the presence of MPs in individual species, few have documented the concentrations within multiple species of varying life-history and feeding strategies within the same food web. Furthermore, although some studies have estimated the trophic level at which different species are feeding, few have used quantitative food-web ecology methods to determine the trophic position of individual animals and to characterize their role

within a food web. These methods, including stable isotope analysis, are commonly employed by ecotoxicologists, however, to study the accumulation and biomagnification of other organic pollutants and heavy metals (*e.g.*, PCBs, mercury) in food webs. By pairing food-web analysis (Layman *et al.* 2012), typically by use of the stable-isotope tracers ^{13}C and ^{15}N, with contaminant analysis, bioaccumulation and trophic-magnification factors can be calculated. In the present study, we apply these methods to marine food webs in coastal British Columbia, Canada, to understand the trophic dynamics of MPs in the digestive tracts of animals, and livers of fish, feeding across multiple trophic levels. We also employ novel methods for classifying unknown particles *via* machine learning and for accounting for background contamination using Bayesian inference.

4.2 Methods

4.2.1 Study area

Samples were collected from three sites on southern Vancouver Island in British Columbia, Canada (Fig. 13). Elliot Beach, Coles Bay, and Victoria Harbour were selected as sites as they are representative urban and rural areas with low wave exposure and had similar species available that display some degree of residency. Elliot Beach is a rural public beach located at the mouth of a large inlet near the town of Ladysmith. The beach is a mix of exposed bedrock with cobble and sand. Nearby development is primarily private properties, although toward the head of the inlet, in Ladysmith Harbour, there are several marinas and a large industrial area where many log-booms are stored. A secondary sewage treatment plant serving the town of Ladysmith and surrounding area (~17,200 people) is found on the south side of the inlet, across from our sampling area. Coles Bay is a rural, sheltered bay within Saanich Inlet with

a wide sandy and cobble, gently sloping beach at its head and bedrock and boulders along its edges. There is a large, predominately subtidal, eel-grass meadow at the head of the bay. It is surrounded by private property and the Pauqachin First Nation reservation. Victoria Harbour is urban and surrounded by many active industrial sites, with the sampling site being found between a cruise-ship dock and a commuter helicopter pad, with a large breakwater to the south. The shoreline is highly modified, with little intertidal area, and consisting primarily of concrete walls or large boulders.

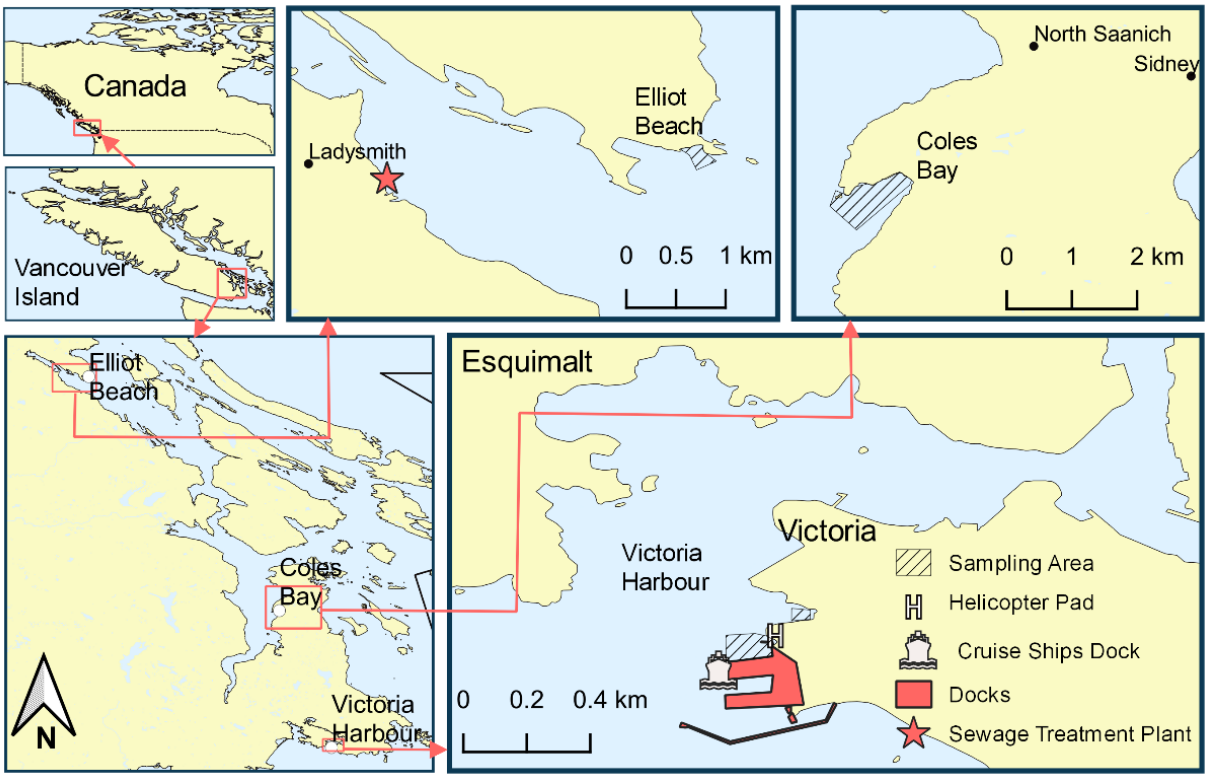

Figure 13: Study areas on Vancouver Island, British Columbia, Canada. The three panels on the right show the three sampling areas, while those on the left show their locations compared to one another and on Vancouver Island. Victoria Harbour is an industrial area and the large breakwater and docks, cruise ship docking area, and nearby commercial helipad are shown.

4.2.2 Approval for animal experiments

The Animal Care Committee at the University of Victoria approved all fish sample collection and euthanasia procedures according to Canadian Council on Animal Care standards (Protocol # 2018-011).

4.2.3 Water sample collection

Five 1-L jar samples and five plankton net surface tows were collected at each of the three sites on five separate days during summer low tides alongside other sample collection at the sites (July-August 2018). Both sample types were collected because large-volume tows can sample a larger spatial area but still underestimate MP concentrations (Covernton *et al.* 2019a). Furthermore, the bulk water samples would be representative of the MP concentrations present in all seston, while the plankton tows would be indicative of zooplankton and floating detritus. The jar samples were collected using 1-L glass mason jars that were dipped below the surface. The plankton tows were collected using a 150-µm mesh plankton net with a 0.53- m diameter opening. After collection, we used a garden pump sprayer filled with ambient seawater to rinse the material in the net into the cod end by spraying the outside of the net. The cod end was then rinsed into a 1-L glass mason jar using pre-filtered deionized water (see sample processing methods). At Coles Bay and Elliot Beach, samples from the shore were collected by wading to 1-m depth. The plankton nets were towed at the surface parallel to the water's edge for 5 minutes with the net held behind and to the side of the sampler to avoid collecting any disturbed sediments. GPS tracking was used to calculate distance travelled and estimate sample volumes based on the diameter of the circular net opening (~94-126 L). At Victoria Harbour, there was a steep drop off from the shore, so jar samples were collected off the edge of a small dock. The

plankton net was towed on the surface by swimming from a point on the dock to the edge of the cruise-ship dock (67 m, 67.5 L), while wearing a wetsuit and fins.

4.2.4 Animal sample collection

We collected species from pre-selected target species across a coastal shallow subtidal and intertidal food web at each site based on their presence at each site. Where possible, we pre-targeted species known to display some degree of site fidelity and that would be likely to have predator-prey interactions. Juvenile (<25 mm length) blue mussels (*Mytilus* spp.), likely a mix of *M. edulis, M. trossolus, M. galloprovincialis*, and their hybrids in coastal BC, were hand-picked from rocks in the upper intertidal. Juvenile Pacific littleneck clams (*Protothaca staminea*) and Manila clams (*Ruditapes philippinarum*) were dug from mid-intertidal sand. These small sizes were selected as being potential prey items of local crabs, flatfish, and shiner perch. Clams were secured shut using natural-rubber elastic bands to prevent gaping and all bivalve samples were frozen at -20ºC following collection. California sea cucumbers (*Apostichopus californicus*) and orange sea cucumbers (*Cucumaria miniata*) were collected from under lower intertidal rocks during low tide *via* wading or snorkelling. Sea cucumbers were then anaesthetized using dilute magnesium chloride (Lewbart and Mosley 2012), and their digestive tracts removed and frozen at -20ºC. Graceful rock crabs (*Metacarcinus gracilis*), Dungeness crabs (*Metacarcinus magister*), and red rock crabs (*Cancer productus*) were hand-collected in the shallows *via* wading during low tide, or from the subtidal *via* SCUBA. These were then euthanized with clove oil (>400 mg L^{-1}, according to University of Victoria standard operating procedures) and their stomachs were removed and frozen at -20ºC. Leather stars (*Dermasterias imbricata*) were picked from subtidal rocks during low tide, flash-frozen at -80ºC, and then later thawed and their stomachs (pyloric and cardiac) removed. Shiner surfperch (*Cymatogaster aggregata*), starry

flounders (*Platichthys stellatus*), and English sole (*Parophrys vetulus*) were caught using a beach seine, euthanized using clove oil (>400 mg L^{-1}), and then their digestive tracts and livers removed and frozen at -20ºC. SCUBA divers captured copper rockfish (*Sebastes caurinus*) and black rockfish (*Sebastes melanops*) *via* spearfishing, and then severed their gill arteries quickly with a dive knife. Their digestive tracts and livers were then removed and frozen at -20ºC. Various body measurements and weights were taken for all animals (Table 1). There was not an intertidal beach section available at Victoria Harbour, so we did not collect clams at this site. Surfperch were collected *via* beach seine from a boat ramp found around the corner from the cruise-ship docks at Victoria Harbour, but we were unable to collect enough flatfish (at least 10) at Victoria Harbour or Elliot Beach for MP analysis.

Table 3: Biometrics and sample size data for the animals collected from the three sampling sites. Shell length was measured for bivalves (longest dimension), carapace length for crabs (longest dimension across carapace), diameter for sea stars (distance between tips of two longest arms), total length of fish (measured from snout to tip of longest lobe of caudal fin). Sea cucumber length was not measured, as they can rapidly expand and contract at will. MPs = microplastics.

Site	Tissues analyzed for MPs	Species	Common name	Body measurement (mean) range (cm)	Wet body wet (mean) range (g)	Sample size
Coles Bay	Whole body	*Mytilus* spp.	Blue mussel	(1.9) 1.3-2.4 shell length	(0.8) 0.3-1.8	19
	Whole body	*Protothaca staminea*	Pacific littleneck clam	2.1 shell length	2.8	1
	Whole body	*Ruditapes philippinarum*	Manila clam	(2.0) 1.3-2.6 shell length	(2.1) 1.0-3.7	12
	Digestive tract	*Apostichopus californicus*	California sea cucumber	-	(14.3) 2.7-40.9	14
	Stomach	*Metacarcinus gracilis*	Graceful rock crab	(7.0) 6.1-8.1 carapace length	(57.5) 30.1-94.9	16
	Digestive tract & liver	*Cymatogaster aggregata*	Shiner surfperch	(8.5) 7.8-9.2 total length	(8.0) 5.6-9.6	16
	Digestive tract & liver	*Dermasterias imbricata*	Leather star	(12.4) 10.2-15.4 diameter	(60.5) 31.9-120.2	16
	Digestive tract & liver tract	*Parophrys vetulus*	English sole	(13.5) 11.6-15.6 total length	(26.8) 13.2-50.2	11
	Digestive tract & liver	*Platichthys stellatus*	Starry flounder	(16.0) 14.5-18.3 total length	(38.6) 20.6-66.7	4
	Digestive tract & liver	*Sebastes caurinus*	Copper rockfish	(14.9) 11.3-25.0 total length	(29.2) 21.2-243.2	10
Elliot Beach	Whole body	*Mytilus* spp.	Blue mussel	(1.6) 1.0-2.9 shell length	(0.4) 0.2-0.7	13
	Whole body	*Ruditapes philippinarum*	Manila clam	(1.7) 0.9-2.3 shell length	(1.6) 0.2-3.4	12

	Digestive tract	*Cucumeria miniata*	Orange sea cucumber	-	(22.9) 1.5-54.1	14
	Digestive tract	*Apostichopus californicus*	California sea cucumber	-	4.0	1
	Stomach	*Metacarcinus magister*	Dungeness crab	(8.1) 7.0-9.2 carapace length	(69.3) 45.1-116.5	16
	Digestive tract & liver	*Cymatogaster aggregata*	Shiner surfperch	(9.3) 8.1-10.0 total length	(10.0) 7.0-15.0	16
	Stomachs	*Dermasterias imbricata*	Leather star	(12.8) 10.2-15.6 diameter	(77.7) 37.1-123.7	15
	Digestive tract & liver	*Sebastes caurinus*	Copper rockfish	(21.7) 13.2-31.2 total length	(191.4) 55.8-572.1	18
	Digestive tract & liver	*Sebastes melanops*	Black rockfish	(20.7) 18.5-22.4 total length	(138.9) 110.4-169.4	3
Victoria Harbour	Whole body	*Mytilus* spp.	Blue mussel	(1.2) 0.9-1.6 cm shell length	(0.3) 0.1-0.5	14
	Digestive tract	*Cucumaria miniata*	Orange sea cucumber	-	(36.8) 3.3-96.7	16
	Digestive tract & liver	*Cymatogaster aggregata*	Shiner surfperch	(6.9) 6.1-7.8 total length	(4.7) 2.8-12.8	17
	Stomach	*Metacarcinus magister*	Dungeness crab	(8.3) 7.1-10.8 carapace length	(77.5) 54.8-149.1	12
	Stomach	*Cancer productus*	Red rock crab	(9.1) 8.0-9.9 carapace length	(86.4) 59.5-114.1	3
	Digestive tract & liver	*Sebastes caurinus*	Copper rockfish	(25.6) 19.2-31.2 total length	(294.0) 123.9-479.4	13
	Digestive tract & liver	*Sebastes melanops*	Black rockfish	(20.1) 16.5-22.3 total length	(123.2) 75.2-166.4	8

4.2.5 Stable isotope analysis

Stable isotope analysis was conducted for all animals that were analyzed for MP content. Tissue samples were collected from clam feet, the adductor muscles in mussels, sea cucumber buccal retractor muscles, sea star body walls (from an arm), crab muscle (from the merus of a cheliped), and fish muscle and livers (enough tissue to fill about 1/3–1/2 of a 1.5- mL microcentrifuge Eppendorf tube). Each sample was dried to constant weight at 40ºC (either in Eppendorf tubes or aluminum packets) and then placed in a 1.5-mL microcentrifuge Eppendorf tube if not already in one. Stainless-steel milling balls were then added to the tube and the sample ground at 30 Hz for at least 2 minutes, or until completely homogenized, using a MM400 mixer mill (Retsch, Haan, Germany). For each sample, ~0.5–1.5 mg of dried, homogenized tissue was then placed in a tin capsule and crimped shut. To remove inorganic carbon from the sea star ossicles and achieve more accurate $\delta^{13}C$, additional samples were placed in silver capsules and then acid fumigated by placing in a desiccator containing a beaker of 12-M HCl for 8 hours (Gale *et al.* 2013, Gianguzza *et al.* 2016).

The samples were analyzed for $\delta^{13}C$ and $\delta^{15}N$ at the UC Davis Stable Isotope Facility using a PDZ Europa ANCA-GSL elemental analyzer interfaced to a PDZ Europa 20-20 isotope ration mass spectrometer (Sercon Ltd., Cheshire, UK). The samples were combusted at 1000ºC in a reactor packed with chromium oxide and silvered copper oxide, and oxides removed in a reduction reactor (reduced copper at 650ºC). Helium was passed through a water trap (magnesium perchlorate and phosphorous pentoxide). The samples then had N_2 and CO_2 separated on a Carbosieve GC column (65ºC, 65 mL min^{-1}) before entering the isotope ratio mass spectrometer. Ten standards, composed of dogfish muscle tissue samples of consistent

isotopic values, were sent to the facility to be processed alongside the experimental samples for quantification of variance.

4.2.6 Microplastics quality assurance and control

To reduce sample contamination, laboratory workers wore yellow Tyvek© suits over their clothing during sample processing, pre-filtered all reagents through 1-µm glass-fibre filters, and conducted all work in an AirClean 600 laminar-flow hood (AirClean Systems, Creedmoor NC, USA). No particles from Tyvek© suits were found in any of the samples. A Blue Pure 211+ Air Purifier (Blueair, Inc., Chicago IL, USA) always filtered the laboratory air and surfaces were regularly wiped down with 70% ethanol. Three procedurals blanks, consisting of clean empty beakers subjected to the same procedures as the experimental samples, were tested alongside each sampling run. After filtration onto polycarbonate (PCTE) membrane filters (Sterlitech Corporation, Kent WA, USA) samples were stored in polystyrene PetriSlides (EMD Millipore, Oakville ON, Canada).

4.2.7 Water sample processing

The jar samples were directly filtered onto 1-µm polycarbonate membrane filters. The plankton-tow samples were filtered first through a 4.75-mm sieve and then rinsed back into the original sample jars. Square 8-µm nominal stainless-steel mesh was placed over the jar openings, secured using the rings from the mason jar lids, and then the jar inverted onto the mouth of a filter flask and vacuum filtered to remove all water. The jar and plankton-tow samples were then dried at 40ºC to constant weight. Once dry, the plant and algal tissues in the plankton tow samples were digested by adding 200 mL of 30% hydrogen peroxide (H_2O_2), sonicating for 5 minutes, and then incubating at 40ºC for 48 hours (Lusher *et al.* 2020). Samples were then rinsed with deionized water and filtered again through the stainless-steel mesh. To remove animal

tissues, 100 mL of 10% potassium hydroxide (KOH) were added to each sample, sonicated again for 5 minutes, and then incubated at 40ºC for 48 hours. The digestate was again rinsed and filtered to remove KOH and dried at 40ºC to constant weight. To remove sand, 100 mL of 52% sodium iodide (NaI), with a density of 1.6 g L^{-1}, was used to rinse each sample into a separatory funnel, with the funnel being left for at least 1 minute before releasing the bottom fraction and rinsing the supernatant through 250- and 150-µm sieves. The two sieved fractions were then separately filtered onto 8-µm polycarbonate membrane filters using a vacuum pump and a six-port filtration manifold. The filtered NaI solution was saved, adjusting the density back to 1.6 g L^{-1} with solid NaI, and then re-filtered to re-use the solution.

4.2.8 Animal sample processing

The bivalves were defrosted at room temperature, the outside of their shells rinsed, and then they were opened, and all the soft tissues removed from the shells. The tissues were then placed into small beakers covered with aluminum foil and dried at 40ºC to constant weight. The tissues were digested by adding 20 mL of 10% KOH to each sample and incubating at 40ºC for 5 days, and then filtered to one µm. After primary filtration and rinsing, any remaining fatty tissue was dissolved by adding 20 mL of sodium dodecyl sulphate (SDS) to the filter funnel, leaving for 5 minutes, and rinsing and filtering the sample several times. To remove sand, each membrane filter was placed within a clean beaker holding 30 mL of NaI solution, left for a minimum of 15 minutes, and then the filter removed and carefully rinsed of any adhered particulates using more NaI solution. Density separation was then conducted using the same procedure as for the plankton-tow samples, and then the samples were filtered to 1 µm.

Other animal samples were processed using similar methods as for the bivalves, with some modifications. The gastrointestinal tracts of sea cucumbers were digested using 30 mL of

KOH and the digestate sieved into <150- and ≥150-µm fractions prior to density separation, with <150-µm fractions filtered to 1 µm and ≥150-µm fractions to 8 µm. Crab stomachs were digested using 50 mL of KOH for 5 days and the digestate then sieved into <1-mm and ≥1-mm fractions. The smaller size fractions were filtered to one µm, as with the bivalve samples, while the larger size fractions were rinsed into a petri dish and dried at 40ºC prior to particle counting. Sea star stomachs were digested with 50 mL of KOH for 5 days and then split into <150- and ≥150-µm fractions and filtered, as with the bivalves. For flatfish, surfperch, and rockfish, gastrointestinal tracts (including pyloric caeca) and livers were processed separately, according to the same protocol as with sea star stomachs, although the latter were not size-fractioned. A density separation step (same as above) for the flatfish digestive tract samples was also added, but not for the crab, sea star, surfperch, and rockfish gut samples. For the latter, gastrointestinal tracts were cut open using scissors and the contents rinsed through a 4.75-mm sieve. The larger sieved fraction was all made up of partially digested animals, which were photographed and then digested and filtered separately from the filtrate and the rest of the stomach and intestines. The gut animal samples, and the remaining gastrointestinal tract samples, were sieved into ≥1-mm fractions in addition to <150- and ≥150-µm fractions.

4.2.9 Particle analysis

Visual analysis was conducted for all sample types, other than the ≥1-mm fraction for crabs and rockfish, by placing the PetriSlides on a compound microscope stage, removing the cover, and manually scanning the whole sample at 100X magnification. For the ≥1-mm fraction crab and rockfish samples, the petri dishes were viewed using a dissecting microscope. To avoid sample contamination during microscopy the microscope stage was enclosed in a clear plastic bag that was taped to the bench top and microscope at its edges, as outlined by Torre *et al.* (Torre

et al. 2016). During visual scanning, any potential MPs were identified, removed with forceps, and placed and labelled on double-sided sticky tape. Any un-naturally and/or brightly coloured particles were classified as potential MPs, as well as clear fibres that did not look natural (*i.e.*, lacked internal structure, including striations, and were an even width along their length). Shape (*e.g.*, fibres, fragments, spherules, films), colour, and length (longest dimension) of each potential MP particle were recorded.

Of 1,124 putative MP particles that were counted across all samples, 882 (78%) particles were extracted (without accidentally losing the particle during transfer) and analyzed using a micro-Raman spectrometer (HORIBA Raman Xplora Plus, HORIBA Ltd., Kyoto, Japan). Chemical identification *via* Raman spectroscopy was carried out using a 785-nm (range 50–2000 cm^{-1}) or 532-nm (range 50–4000 cm^{-1}) laser with a 100x long-working-distance microscope objective with a filter ranging from 0.1 to 100%; gratings of 600 or 1200 grooves mm^{-1}; 1–15 s acquisition time; 2, 4, 6, 8, or 10 accumulations; a confocal hole diameter of 100 or 300 mm; and a confocal slit width of 50 or 100 µm. When acquiring spectra, parameters were optimized, including adding delay time, to inhibit poor resolution, fluorescence, and particle burning. Spectra were compared to the SLoPP and SLoPP-E libraries (Munno *et al.* 2020), as well as to the BioRad KnowItAll Raman Spectral Library. Of these 882 particles, 779 (88% of analyzed, or 69% of total particles) were successfully identified and categorized as synthetic polymers (*e.g.*, polyester, nylon, polyurethane, acrylic), semi-synthetic (rayon), natural (*e.g.*, clear cellulosic fibres, minerals, salt), or natural anthropogenic (dyed cellulosic fibres, wool) particles. The remaining particles could not be classified due to poor spectra quality (*e.g.*, as a result of burning or fluorescence or a strong dye signature that could not confidently associated with a material type).

4.2.10 Data analysis

All analyses were carried out using R v4.0.3 (R Core Team 2020). Data on particle colour, shape, and material composition are presented using raw data that are not blank corrected (*i.e.*, as this was not done according to colour or polymer). For modeling purposes, the 345 particles of unknown identity had to be assigned to the synthetic or non-synthetic categories. To do this, we applied a random forest classification model using the Randomforest package (Liaw and Wiener 2002). The model was specified with particle type (synthetic, semi-synthetic, natural, or natural anthropogenic) as the response variable and expert user ID, sample type (*e.g.*, blanks, plankton tow, mussels), particle size, shape, colour, and length as predictor variables. User ID reflected the opinion of an expert (in this case GAC) as to whether a particle was likely natural or synthetic in composition, depending on factors including fibre structure and shape (based on hundreds of hours of visual and chemical analyses of potential MPs). The model was run over 250 trees with two variables allowed per split. After classification, we calculated total synthetic particle counts (MPs) for each sample, pooling across size fractions.

Bayesian, generalized, linear mixed-effects models (GLMMs) were used to explore several aspects of the data using JAGS (Plummer 2003), implemented *via* the R2jags (Su and Yajima 2020) package. Model fits were assessed using the DHARMa package (Hartig 2020), and the final models chosen because their simulated scaled-residuals plots did not suggest misspecification. Three Markov Chain Monte-Carlo (MCMC) chains were run for each model. When fitting models, the number of MCMC iterations were increased until $\hat{R}$ values, a standard convergence metric, for each estimated parameter reached 1.01 or lower. Hierarchical model structures were used for each GLMM, which accounted for uncertainty at several different levels.

In the lowest layer, we calculated the isotopic value for the baseline consumer, $\delta^{15}N_{base}$, at each site using the δ^{15}N values from mussels. Bivalves make excellent baseline references for isotopic modeling, as they are sedentary and consume a relatively consistent diet(Anderson and Cabana 2007). To build uncertainty into $\delta^{15}N_{base}$ a prior distribution of $\delta^{15}N_{base} \sim Gamma(\alpha, \beta)$ was specified, where mussel isotopic values from a site are assumed to be drawn from a gamma distribution with shape parameter α and rate parameter β. The gamma distribution has mean, $\mu = \frac{\alpha}{\beta}$, and variance, $\sigma^2 = \frac{\alpha}{\beta^2}$, which can be solved so that $\alpha = \frac{\mu^2}{\sigma^2}$ and $\beta = \frac{\mu}{\sigma^2}$. Thus, the prior distribution for $\delta^{15}N_{base}$ for each site can be specified using the mean, μ, and standard deviation, σ, of mussel δ^{15}N from each site.

In the second layer, the trophic position for an individual, TP_i, was approximated using a re-scaled estimate according to Hussey *et al.* (2014), which accounts for a linear change in the δ^{15}N trophic discrimination factor with increasing trophic level. They proposed the equation:

$$TP_i = \frac{\log(\delta^{15}N_{lim} - \delta^{15}N_{base}) - \log(\delta^{15}N_{lim} - \delta^{15}N_i)}{k} + 2$$

where $\delta^{15}N_{lim}$ is the saturating isotope limit as TP increases, $\delta^{15}N_{base}$ is the isotopic value of the baseline consumer (trophic level 2) in the food web, $\delta^{15}N_i$ is the isotope value of the sampled individual, and k is the rate at which $\delta^{15}N_{TP}$ approaches $\delta^{15}N_{lim}$. We used values of 0.315 for k and 21.926 for $\delta^{15}N_{lim}$ based on the results of their metanalysis. Uncertainty was also built into $\delta^{15}N_i$ using the prior $\delta^{15}N_{TP} \sim Normal(\delta^{15}N_{sample}, 0.052)$, where $\delta^{15}N_{sample}$ is the isotopic value of a sample, and 0.052 is the standard deviation of the dogfish muscle standards that were analyzed alongside the stable isotope tissue samples to quantify methodological variance.

To include uncertainty about observed particle counts in samples which have potentially been exposed to background contamination in the laboratory, we used a novel, probabilistic method which built a correction into the third layer of the hierarchical GLMMs. As count data that are not highly dispersed, observed particles counts are approximated well by the Poisson distribution. We assumed that observed particles $P_{observed}$ were Poisson distributed with mean $\lambda_{observed}$ and that the observed mean particle counts were equal to the true mean of the sample counts λ_{sample} plus the mean contamination entering a sample during processing, which was approximated by the mean MP count for the blank samples run alongside each sample. This can all be written as:

$$P_{observed} \sim Poisson(\lambda_{observed})$$

$$\lambda_{observed} = \lambda_{sample} + \lambda_{blanks}$$

$$\log(\lambda_{sample}) = L_j$$

with L_j being the linear equation for whichever model relating some predictor variables to the concentration of particles in the sample.

Several GLMMs were run on different portions of the data according to different linear equations. Each model had the previously described layers of uncertainty structure built in if the relevant variables were included in the model. To explore differences in seawater MP concentrations among sites, the linear equation $L_{seawater} = \alpha_{site}$ was applied with α_{site} the intercept term, according to site, with prior $\alpha_{site} \sim Normal(0, 1)$. To account for volume in the plankton tows, an offset term for sample volume V was added to the equation so that $L_{seawater} = \log(V) + \alpha_{site}$. For both models, the MCMC chains were run for 2,000 iterations with a burn-in of 500, without thinning, and then posterior predictive samples were generated for each site.

The relationship between trophic level and number of particles in the digestive tracts of animals (whole bodies for bivalves) was modeled according to $L_{digestive\ tracts} = \alpha_{species} + \beta_{TP}TP_i + \gamma_{site}$, with $\alpha_{species}$ a random intercept according to the sample species defined as $\alpha_{species} \sim Normal(0, \sigma_{species})$ with prior $\sigma_{species} \sim Exponential(1)$, β_{TP} a random slope for trophic position according to site with prior $\beta_{TP} \sim Normal(0, 1)$, and γ_{site} a fixed effect of site with prior $\gamma_{site} \sim Normal(0, 1)$. The MCMC chains were run over 7,000 iterations, with a burn-in of 500 and a thinning factor of 2. Individual-level bioaccumulation factors were calculated according to $BF = \frac{C_a}{C_w}$, where C_a is the MP concentration in the digestive tract of the animal, calculated by dividing the mean of the posterior for animal $\lambda_{observed}$ by the total wet body weight (kg) of the animal, and C_w is the mean of the posterior for seawater $\lambda_{observed}$ in particles L^{-1} from the jar samples at each site. We used the jar samples here, as the concentrations were much higher than the net tow sample estimates and likely more representative of true seawater concentrations (Covernton *et al.* 2019a). To quantify the effect of trophic level on digestive tract MP concentration in animals, posterior predictive simulations were generated from the model over 2000 randomized combination of all sites, species, and trophic position values ranging from one to six. Predictions were generated at the site level and combined across species. To quantify differences by species, posterior predictive simulations were also generated holding the estimate of trophic position for each species at its mean value and combining effects across site.

The relationship between trophic level and number of particles g^{-1} dry tissue in the fish livers was modeled according to $L_{livers} = \log(W_{sample}) + \alpha_{site} + \beta_{TP}TP_i$, with W_{sample} the dry weight of the sample, and the other terms and priors identical to the previous model. The MCMC chains were run over 5000 iterations, with a burn-in of 500 and no thinning. To quantify degree of biomagnification in fish livers, trophic magnification factors were calculated using the

posterior estimate for slope according to trophic position as $TMF = e^{\beta_{TP}}$. To quantify the effect of trophic level on fish liver MP concentrations, posterior predictive simulations were generated from the model with over 2000 randomized combination of all site and trophic-position values ranging from 1 to 4.5. Means and credibility intervals for the posterior estimates were generated at the site level.

To quantify trophic transfer in the rockfish digestive tracts data, the number of particles present in the partially digested material, in terms of particle g^{-1} dry weight according to site, was modeled using the linear equation $L_{transfer} = \log(W_{sample}) + \alpha_{species} + \gamma_{site}$ with the same priors as used above. The MCMC chains were run over 2000 iterations, with a burn-in of 500 and no thinning. To estimate the mean concentration of MPs expected to be transferred from ingested animals, posterior predictive samples were generated - combining the effects of all species and sites.

Assuming that the rockfish were all feeding prior to capture, comparing the difference in digestive tracts for individuals with full and empty stomachs should offer insight into whether most MPs are excreted alongside ingested food. We modeled this using the linear equation $L_{rockfish\ guts} = \gamma_{site} + \beta_{TP} + \beta_{TL} + \gamma_{site} + \gamma_{gut}$, where γ_{gut} is a fixed effect according to whether a rockfish had a full or empty gut, with prior $\gamma_{gut} \sim Normal(0, 1)$ and the other parameters and priors the same as previously mentioned. More MCMC iterations were needed than previous models due the smaller sample size and additional predictor variables, requiring 25,000 iterations, with a burn-in of 500 and a thinning factor of 5. Posterior predictive samples were generated across all combinations of species, site, empty or full stomachs, and 1000 values of trophic position and total length, ranging from the minimum to maximum values in the data

set. Overall predicted means and credibility intervals of posterior estimates were then calculated at the level of species and stomach fullness.

4.3 Results

4.3.1 Stable isotope analysis

Mussels and clams had similar $\delta^{13}C$ values, with most individuals from the other species more enriched in ^{13}C (Fig. 14). Sea stars were particularly enriched in ^{13}C compared to the other taxa. Similar $\delta^{15}N$ values occurred among individuals within a given species, other than for mussels, clams, sea cucumbers, and sea stars, which displayed large variation in $\delta^{15}N$. Two individual sea stars, one from Coles Bay and one from Elliot Beach, had $\delta^{15}N$ values higher than any other animal. The liver $\delta^{15}N$ values were less enriched, on average, than the muscle values for fish, so we used the average of the two, for each individual, in our modeling.

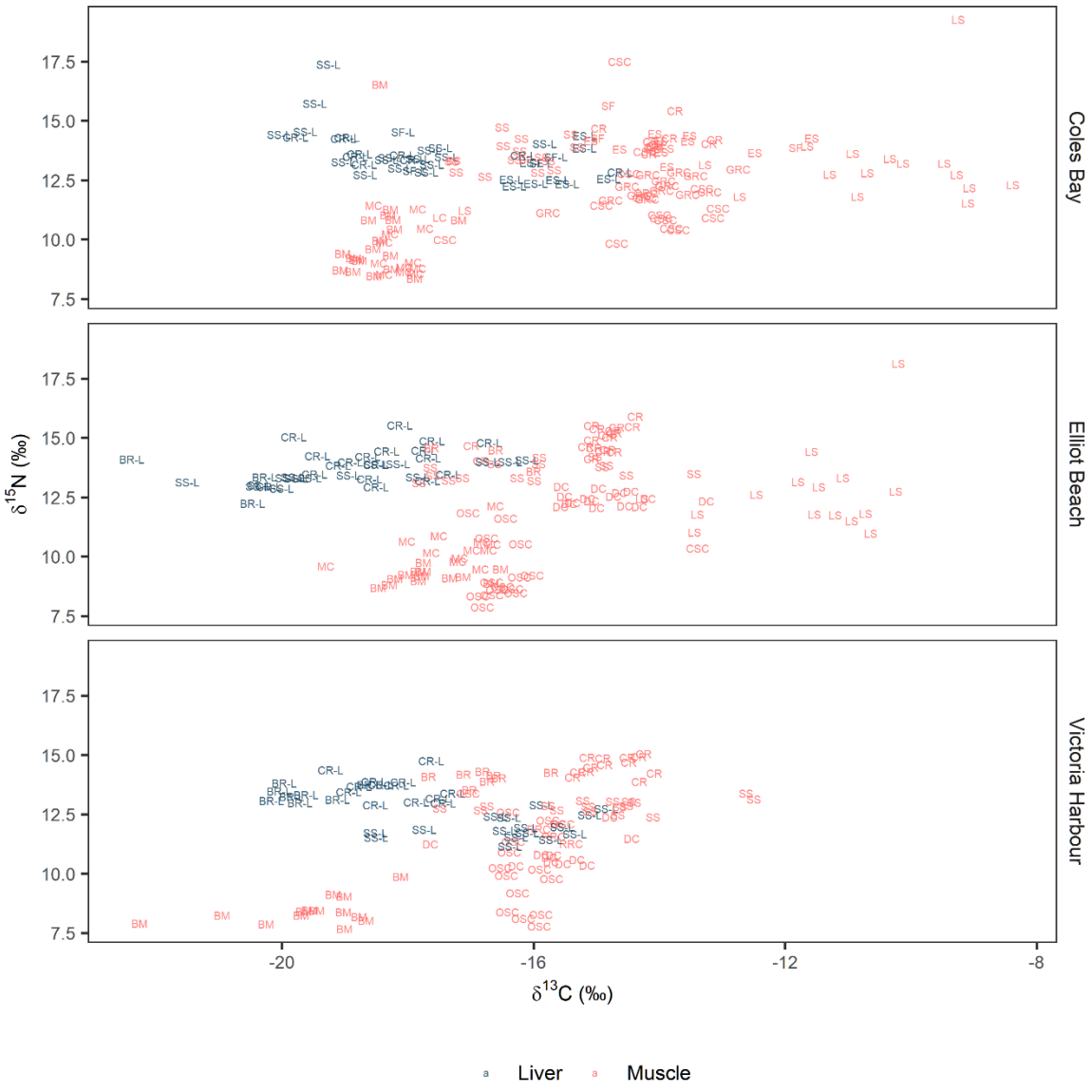

Figure 14: Stable carbon and nitrogen isotopic biplot for species collected at the three sample sites. Both liver and muscle samples were collected for the fish and tissue types are separated by colour. Species are labelled by abbreviated common names (BM = blue mussel, LC = littleneck clam, MC = Manila clam, OSC = orange sea cucumber, CSC = California sea cucumber, LS = leather star, RRC = red rock crab, GRC = graceful rock crab, DC = Dungeness crab, SS = shiner surfperch, ES = English sole, SF = starry flounder, CR = copper rockfish, BR = black rockfish).

4.3.2 Particle analyses

Of the 1124 potential MPs counted, 97.9% were fibres, 1.9% were fragments, and 0.2% were films (Fig. C1, C2). The most common particle colours were clear (26.9%), blue (24.0%), and black (22.0 %) (Fig. C1). For the 779 particles identifiable with Raman spectroscopy, 32.5% were classified as synthetic, 10.4% as natural, 54.0% as natural anthropogenic, and 3.1% as semi-synthetic (Fig. C2). Overall, polyester fibres were the most abundant type of MP found in the samples (80.2% of synthetic particles).

The random forest model displayed an overall accuracy of 74.2% (true positives) during fitting. According to a variable importance plot, the strongest predictors of particle type were user ID, particle colour, particle length, and sample type, with particle shape and site playing less of a role. According to a confusion matrix comparing predictions with the true data (Fig. C3), the model had difficultly classifying semi-synthetic fibres, likely because they were so rare. The model also sometimes classified synthetic particles as natural anthropogenic (22.9% of synthetic particles) and natural particles as synthetic (30.9% of natural particles).

4.3.3 Seawater concentrations

After classifying unknown particles, the uncorrected MP concentrations estimated by the plankton tows were 0.03 ± 0.02 particles L^{-1} (mean ± SD) for Coles Bay, 0.02 ± 0.01 particles L^{-1} for Elliot Beach, and 0.06 ± 0.03 particles L^{-1} for Victoria Harbour. Taking background contamination into account, the corrected GLMM estimated mean particle concentrations to be 0.02 (0.01–0.04, 95% credibility interval) particles L^{-1} for Coles Bay, 0.01 (0.01–0.03) for Elliot Beach, and 0.08 (0.06–0.12) for Victoria Harbour (Fig. 15a). The posterior for Victoria Harbour did not overlap with Coles Bay or Elliot Beach posteriors (which were similar to one another), indicating a statistically higher MP concentration at this site (Fig. C4). For the 1-L jar samples,

the uncorrected concentrations were 2.00 ± 2.92, 1.00 ± 1.22, and 2.40 ± 1.95 particles L^{-1} for Coles Bay, Elliot Beach, and Victoria Harbour, respectively. The model estimates were 1.54 (0.59–2.84), 0.74 (0.17–1.68), and 1.22 (0.30–2.52) particles L^{-1} for Coles Bay, Elliot Beach, and Victoria Harbour, respectively (Fig. 15b). The jar sample posteriors overlapped at all sites, suggesting no statistical difference (Fig. C5).

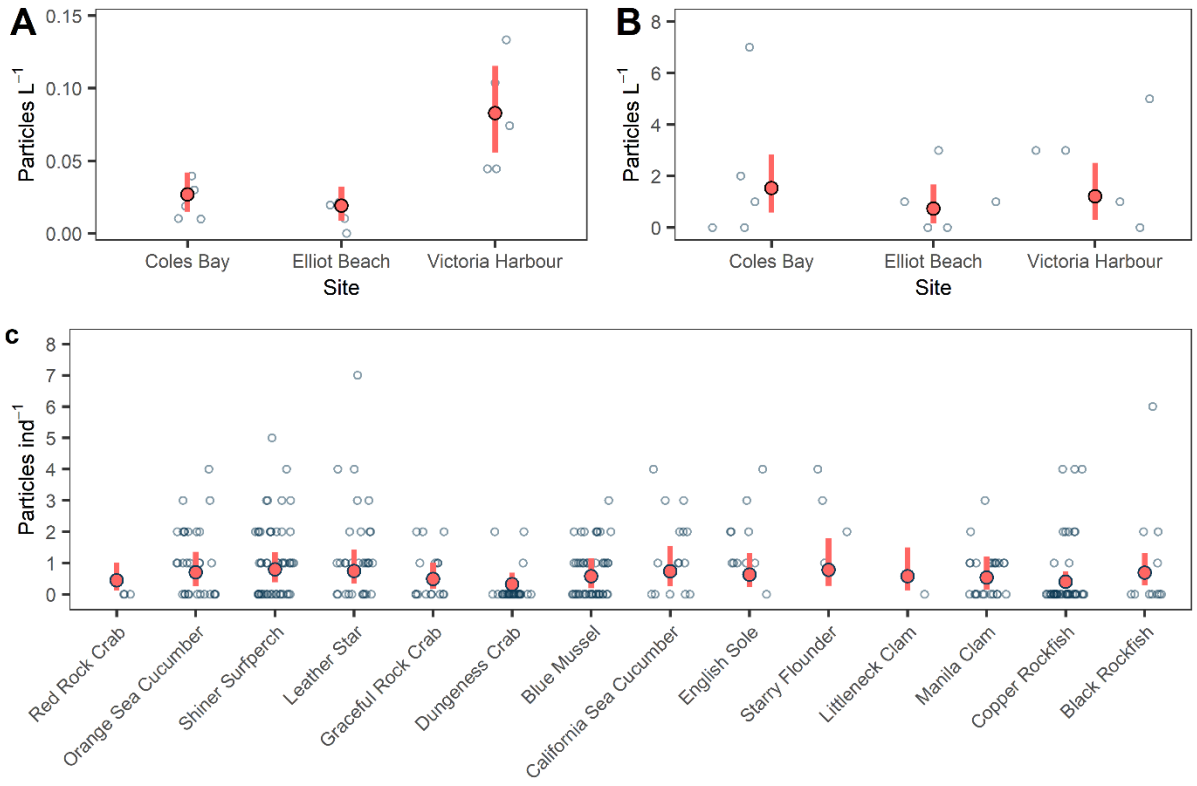

Figure 15: MP concentration from (a) plankton tow water samples, (b) jar water samples and (c) digestive tracts by species. The open circles are raw, uncorrected counts. The red circles and lines show mean posterior predictive mean concentrations and 95% credibility intervals for simulated model predictions, respectively. For the animals GLMM, the simulations were generated assuming the average trophic position for each species and the mean and credibility intervals calculated from joint MCMC posterior samples across the three sites.

4.3.4 Digestive tract concentrations and bioaccumulation factors

Uncorrected MP concentrations in animal digestive tracts ranged from 0 to 7 particles ind^{-1} with a mean of 0.89. The GLMM random intercept posteriors overlapped each other, suggesting no substantial differences among species, although there was some separation between Dungeness crabs (lower MP concentration) and shiner surfperch and leather stars (higher MP concentrations) (Fig. C6). Simulating from the model while holding trophic position at the average for each species resulted in overall lowest MP concentration for Dungeness crabs of 0.33 (0.11–0.69) particles ind^{-1} and overall highest concentrations for leather stars (0.74, 0.34–1.44), starry flounder (0.75, 0.26–1.73) particles ind^{-1}, and shiner surfperch (0.78, 0.37–1.33 particles ind^{-1}), respectively (Fig. 15c). There were differences by site, with animals from Victoria Harbour having 4.6 times higher MP concentrations than Elliot Beach (posterior mean of 1.43 vs. 0.31 MPs ind^{-1}), with the Coles Bay posterior being intermediate (0.74 MPs ind^{-1}) and overlapping the other sites (Fig. C6).

Expressing the mean of the fitted model posterior predictive MCMC samples in terms of the wet weight (ww) and dry weight (dw) of digestive tracts (whole bodies for bivalves) resulted in the highest overall mean concentration estimates for the California sea cucumbers, mussels, and shiner surfperch (Table 4). The lowest mean concentration estimates by tissue weight were for black and copper rockfish (Table 4). Individual bioaccumulation factors decreased exponentially with increasing trophic position (Fig. 16a). California sea cucumber bioaccumulation factors deviated from the overall trend and were higher than might otherwise be expected according to their trophic position (Fig. 16b).

Table 4: Trophic position and digestive tract microplastic concentration estimates for each species in terms of individual, wet weight, and dry weight of the digestive tract. Means of the posterior predictive samples for trophic position and true microplastics concentration were used to calculate means and ranges for individuals of each species at each site. Entries are arranged from lowest to highest mean trophic position.

Species	Site	Trophic Position		Particles ind^{-1}		Particles g^{-1} ww		Particles g^{-1} dw	
		Mean	Range	Mean	Range	Mean	Range	Mean	Range
Manila Clam	Coles Bay	1.83	1.56-2.34	0.69	0.67-0.72	1.06	0.57-1.89	9.05	3.82-27.13
Blue mussel	Coles Bay	1.99	1.53-4.45	0.76	0.73-0.92	4.07	0.7-9.15	105.4	0.83-1048.72
Littleneck clam	Coles Bay	2.19	-	0.79	-	1	-	9.57	-
California sea cucumber	Coles Bay	2.49	1.89-5.08	1.06	1.01-1.3	17.35	0.34-211.7	23.09	2.27-83.25
Graceful rock crab	Coles Bay	2.57	2.25-2.84	0.72	0.7-0.74	1.09	0.37-2.22	6.5	1.47-17.09
Leather Star	Coles Bay	2.99	2.28-6.72	1.22	1.14-1.74	0.91	0.18-6.45	5.33	1.31-30.42
English sole	Coles Bay	3.04	2.75-3.37	1.02	1-1.05	1.28	0.69-3.47	6.49	3.16-22.26
Shiner surfperch	Coles Bay	3.14	2.77-3.97	1.33	1.29-1.41	3.59	1.39-5.25	26.74	3.07-52.59
Starry flounder	Coles Bay	3.2	2.9-3.47	1.29	1.27-1.31	0.98	0.58-1.54	4.95	3.2-6.9
Copper rockfish	Coles Bay	3.21	3.02-3.61	0.72	0.7-0.73	0.35	0.04-0.73	1.44	0.27-3.87
Blue mussel	Elliot Beach	2	1.88-2.15	0.33	0.32-0.34	2.73	1.07-6.93	24.28	7.73-58.54
Orange sea cucumber	Elliot Beach	2.06	1.69-2.75	0.43	0.41-0.45	1.56	0.22-6.52	9.34	0.96-33.65
California sea cucumber	Elliot Beach	2.31	-	0.46	-	28.44	-	1,854.36	-
Manila clam	Elliot Beach	2.32	2.08-2.84	0.31	0.3-0.32	1.27	0.3-6.42	13.07	1.9-59.32
Dungeness crab	Elliot Beach	2.94	2.82-3.12	0.23	0.22-0.24	0.29	0.1-0.54	1.94	0.29-5.21
Leather star	Elliot Beach	3.11	2.49-5.86	0.55	0.5-0.76	0.13	0.05-0.26	0.89	0.32-2.34

Shiner surfperch	Elliot Beach	3.34	3.16-3.57	0.6	0.58-0.63	1.68	0.94-3.06	11.4	4.6-28.23
Black rockfish	Elliot Beach	3.41	3.11-3.65	0.54	0.53-0.57	0.12	0.09-0.14	0.6	0.49-0.75
Copper rockfish	Elliot Beach	3.72	3.32-4.17	0.33	0.31-0.35	0.05	0.01-0.09	0.34	0.04-1.24
Blue mussel	Victoria Harbour	2	1.82-2.35	0.81	0.74-0.85	14.36	5.67-28.51	407.92	55.22-4105.64
Orange sea cucumber	Victoria Harbour	2.47	1.84-3.45	0.94	0.74-1.1	0.66	0.07-2.39	4.82	0.84-13.95
Dungeness crab	Victoria Harbour	2.66	2.48-3.1	0.45	0.41-0.47	0.37	0.13-0.72	1.94	0.5-5.71
Red rock crab	Victoria Harbour	2.84	2.74-2.93	0.59	0.58-0.6	0.56	0.5-0.63	3.22	2.69-3.88
Shiner surfperch	Victoria Harbour	3.11	2.91-3.33	1.02	0.96-1.07	4.35	2.62-14.36	25.54	18.05-43.92
Black rockfish	Victoria Harbour	3.57	3.48-3.71	0.82	0.79-0.84	0.12	0.07-0.27	0.68	0.43-0.95
Copper rockfish	Victoria Harbour	3.72	3.49-4.07	0.47	0.44-0.5	0.05	0.02-0.08	0.35	0.15-0.89

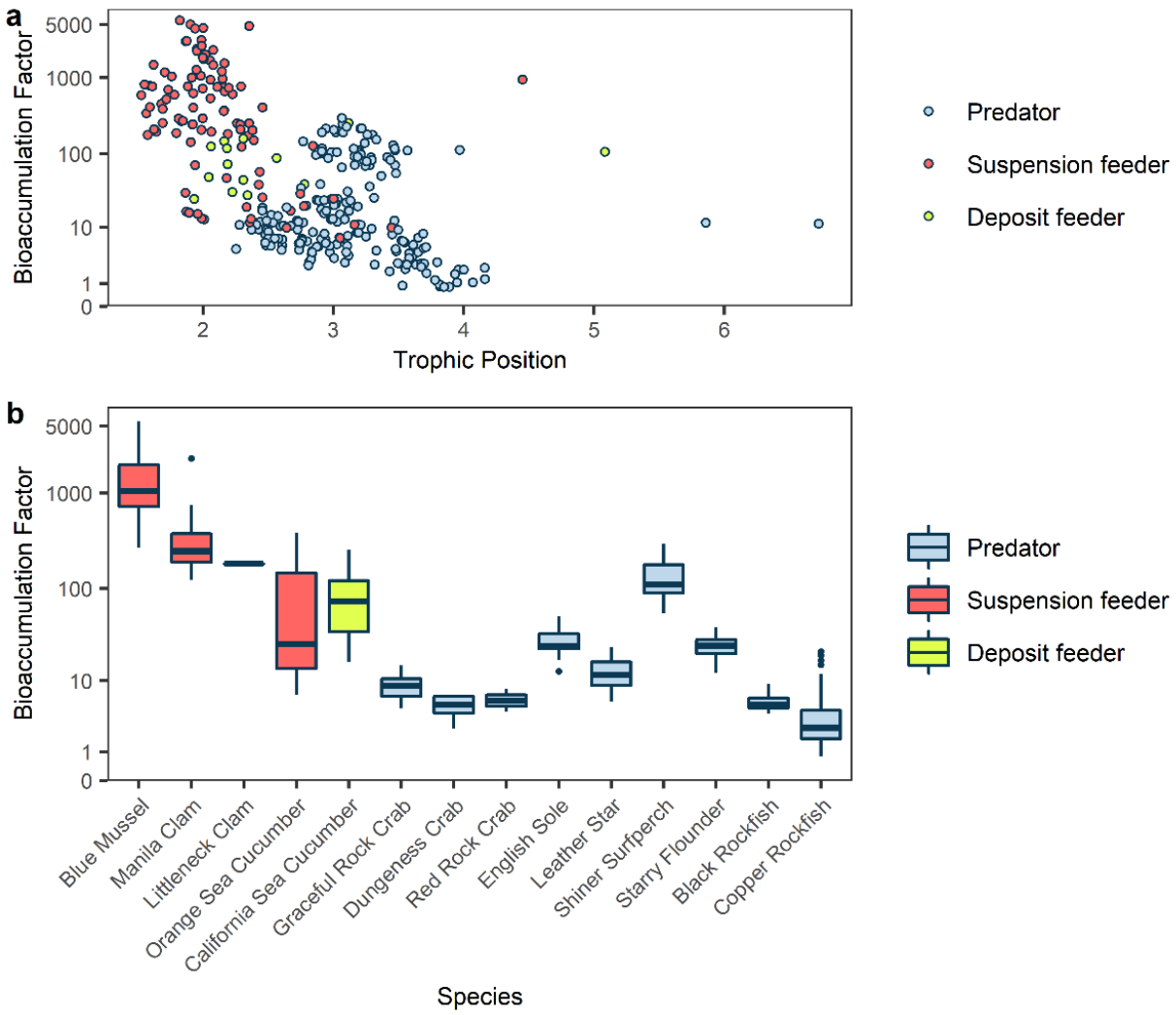

Figure 16: Individual bioaccumulation factors according to (a) trophic position and (b) the same data separated by species (arranged by increasing mean trophic position from left to right). The points and boxplots are coloured according to the feeding strategy of each species.

There was no correlation between trophic position and MP concentration for animal digestive tracts at either Coles Bay or Elliot Beach and a slightly negative slope for Victoria Harbour (Fig. C6, 17a). The digestive tract concentrations, pooled across species, were lowest for Elliot Beach and highest at Victoria Harbour, with Coles Bay intermediate, but the posteriors for all sites overlapped each other, and so any differences were not large (Fig. C6). Trophic position posterior estimates from the GLMM had a higher spread for Coles Bay, due to higher variance in baseline $\delta^{15}N$ values compared with other sites (Fig. C7). Coles Bay had the broadest range in trophic levels due to a single leather star with an estimated trophic position of 6.7, while Victoria Harbour had the lowest range in trophic levels (Table 2).

4.3.5 Fish liver concentrations and trophic magnification factor

Uncorrected MP concentrations in the fish livers ranged from 0 to 344.23 particles g^{-1} dry tissue, with a mean of 14.14, across species and sites, but after correcting for background contamination in the GLMM the estimates were much lower. Simulating from the model across trophic positions ranging from 2 to 4.5 produced mean posterior predictive values for mean MP concentrations ranging from 0.02 to 0.82 particles g^{-1} dw (Fig. 17b). The three sites did not differ according to model posteriors, but there was a negative correlation between trophic position and MP liver concentration (Fig. C8). However, the model simulation also shows that the difference was less than 1 particle g^{-1} across trophic levels and that most predicted mean values would be <1 particle g^{-1} (Fig. 17b). The trophic magnification factor – calculated using the posterior estimates for the slope of the relationship between trophic position and MP particles g^{-1} dry tissue weight, across all sites – was 0.54 (0.12–1.12).

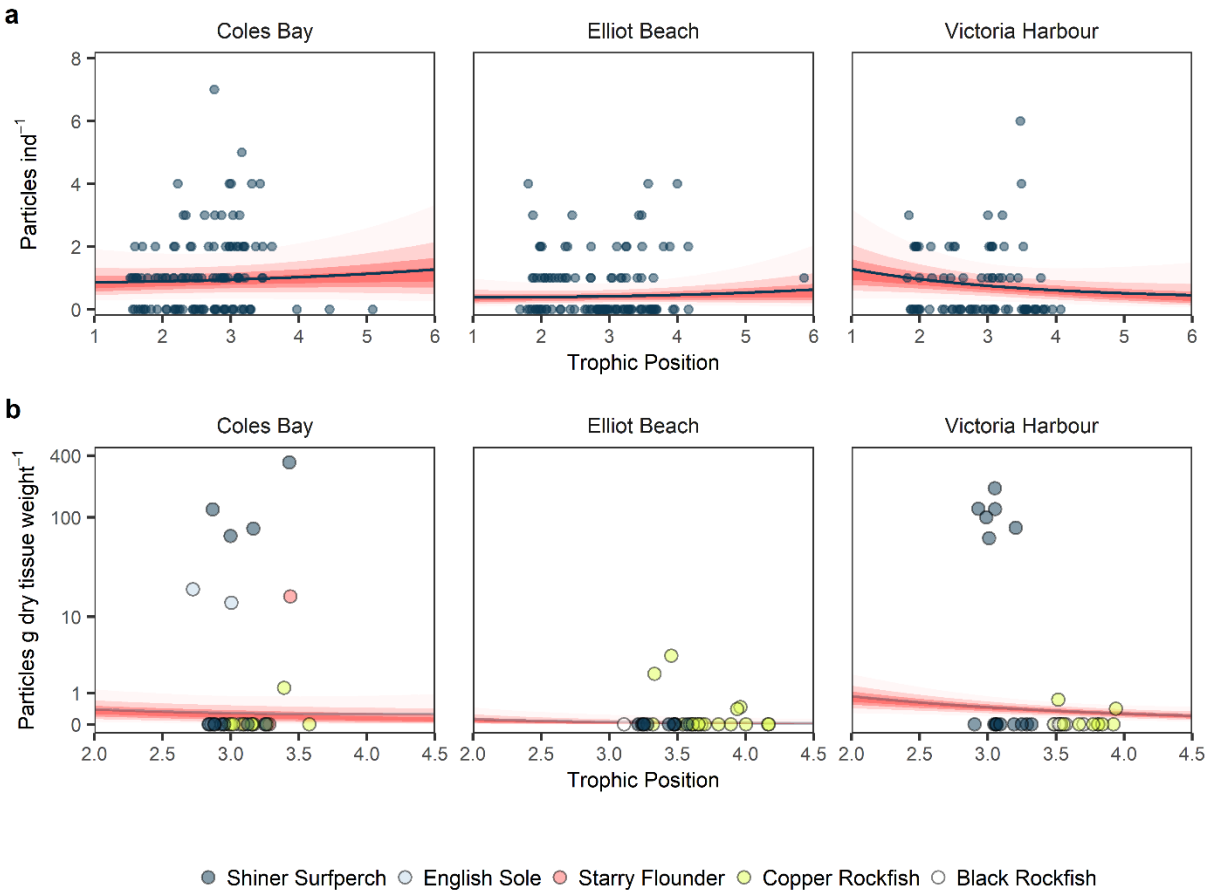

Figure 17: MP concentration at three sampling sites in relation to trophic position for (a) the digestive tracts of all sampled animals and (b) fish livers. The points represent raw, uncorrected data. In (b) they are coloured according to fish species. The lines show the mean of posterior predictive MCMC samples for Bayesian GLMMs. The increasingly light ribbons show 25, 50, 75, and 95% credibility intervals. In (a), the means and credibility intervals were calculated by combining posterior predictive samples across all levels of the species random effect.

4.3.6 Trophic transfer in rockfish

The ingested animals separated from the rockfish stomachs had an uncorrected mean MP concentration of 0.67 ± 0.92 particles sample^{-1} (pooled for each stomach). The GLMM estimate was a mean of 0.60 (0.19–1.3) particles per joint sample based on the combined site and species posteriors (Fig. 18A). There were no differences by rockfish species or by site (Fig. C9). According to the GLMM exploring differences between rockfish with empty and full stomachs, there were no substantial differences in model posteriors between species or by total length. However, trophic position was negatively correlated with rockfish digestive tract MP concentrations (posterior did not overlap with zero). Coles Bay rockfish had more MPs than Elliot Beach rockfish, and there was a strong effect of stomach fullness, with clear separation of model posteriors for empty versus full stomachs (Fig. C10). Digestive tracts from rockfish with full stomachs had an estimated mean MP concentration of 0.46 (0.03–1.98) and 0.69 (0.04–3.28) particles individual^{-1} for copper rockfish (*S. caurinus*) and black rockfish (*S. melanops*), respectively, compared with 0.06 (0.00–0.32) and 0.10 (0.00–0.53) particles individual^{-1} for the digestive tracts of rockfish with empty stomachs (Fig. 18B).

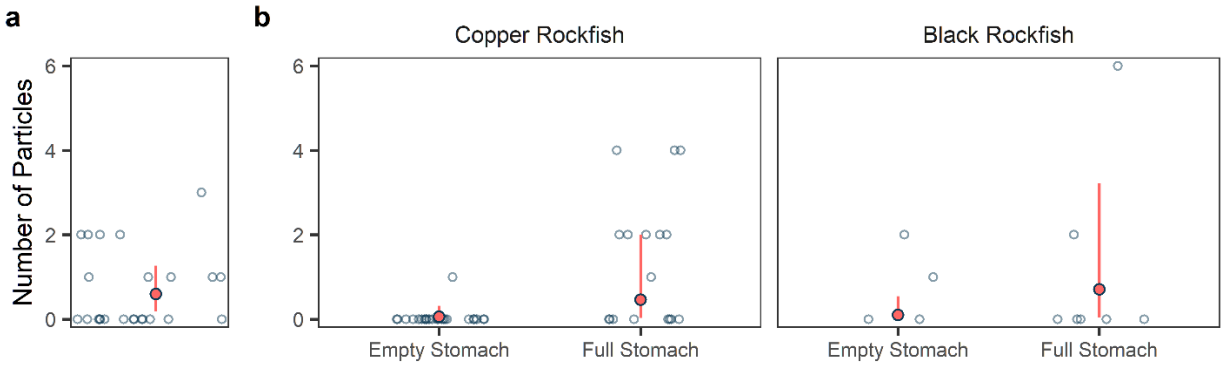

Figure 18: MP concentrations in (a) intact animals from all rockfish stomachs from all species and sites, and (b) in rockfish digestive tracts separated by species and stomach fullness. The open circles stand for raw, uncorrected data. The filled points show the mean of posterior predictive MCMC samples for Bayesian GLMMs and are horizontally jittered to improve visibility. The vertical lines show 95% credibility intervals.

4.4 Discussion

Animals spanning a range of trophic levels in three coastal marine food webs in British Columbia typically had low concentrations of MPs >100-µm in their digestive tracts (<1 particle ind^{-1} on average after accounting for background contamination), with no evidence of biomagnification. Bioaccumulation factors decreased with increasing trophic level. Unambiguous evidence of trophic transfer occurred in the rockfish stomachs, but low MP concentrations in the digestive tracts of individuals with empty stomachs compared with those containing ingested animals suggests that excretion of MPs is rapid, and that accumulation is primarily dependent on the MP ingestion rates relative to body size. MP concentrations in fish livers were also low (0.02–0.82 particles g dry tissue $weight^{-1}$ after accounting for background contamination), with a trophic magnification factor <1, suggesting trophic dilution (*i.e.*, rather than magnification).

4.4.1 Trophic position and feeding habits

The trophic position estimates matched well with literature descriptions of the feeding habits of the sampled species. Most of these species are known to display a high degree of site fidelity at the selected body sizes, the exceptions being the shiner surfperch and starry flounders (*i.e.*, no site fidelity), and the copper and black rockfish (intermediate fidelity and a high degree of vertical migration) (Gordon 1963, Day 1976, Diamond and Hankin 1985, Stone and O'Clair 2002, Hildenbrand *et al.* 2011, Hannah and Rankin 2011, Moser *et al.* 2013). It thus seems that the sampled animals occurred within the same food webs and that the stable-isotope analysis accurately captured the presumed trophic positions of studied individuals, although some caution in interpretation might be necessary. The leather stars could present an exception as their $\delta^{13}C$

values were more enriched than the other species, while the $\delta^{13}C$ values for the other species overlapped sufficiently to suggest that they relied on similar carbon sources.

Clams and mussels had similar trophic positions and can be assumed to be feeding primarily on phytoplankton and other planktonic particles. The sea cucumber species were slightly higher in trophic position, showing some consumption of animal material. Orange sea cucumbers live in crevices beneath rocks and boulders, from where they extend their buccal tentacles for suspension feeding. In contrast, California sea cucumbers live exposed on the substrate and sweep the surface with their feeding tentacles to collect particulate matter (Cameron and Fankboner 1984). The California sea cucumbers were more enriched in ^{13}C than the orange sea cucumbers, suggesting that that the orange sea cucumbers were feeding primarily on pelagic phytoplankton and zooplankton, while the California sea cucumbers were feeding on a mixture of deposited algal (or biofilm) and animal materials. Higher trophic position estimates for some California sea cucumber individuals (range of 1.89-5.08) likely reflect ingestion of decomposing animal material, including feces, from higher trophic level animals.

The size ranges of the crab species collected in this study are known to feed on a wide range of benthos including bivalves and other crustaceans, and sometimes juvenile fish and conspecifics (Stevens *et al.* 1982). This is supported by the estimated trophic positions which were slightly higher than those of the sea cucumbers, showing a greater contribution of animal material to the diet, but with some reliance on algal and plant material (especially for graceful rock crabs). Leather stars feed on a wide range of benthic species including sea anemones, sea cucumbers, hydroids, bryozoans, crab molts, and barnacles (Annett and Pierotti 1984). This is well reflected by the variable trophic position estimates for this species, suggesting a mix of algal/plant and animal dietary items. The high (> 5) trophic position estimates for two

individuals suggest that they might have been feeding on decomposing, high-trophic-level animals, or their feces. The separation between $\delta^{13}C$ values for the leather stars compared with the bivalves suggest they may have different base carbon sources, potentially more ^{13}C-enriched benthic producers for the former compared with more depleted primary producers for the latter (Christianen *et al.* 2017). The crab $\delta_{13}C$ values were intermediate between bivalves and leather stars, suggesting a mix of benthic and pelagic carbon sources.

Shiner surfperch feeds on benthic and pelagic pericarid crustaceans, polychaetes, and copepods, as well as algae, barnacles, and mussels (Gordon 1963, Barry and Cailliet 1981, Barry *et al.* 1996). Starry flounder feed primarily on benthic fauna, including bivalves, polychaetes, brittle stars, and small crabs (Orcutt 1950, Miller 1967, Jewett and Feder 1980). English sole also feeds primarily on benthic fauna, including polychaetes, amphipods, and bivalves (Kravitz and Pearcy 1976, Toole 1980, Barry *et al.* 1996). The trophic position estimates suggest that *P. vetulus* was feeding mainly on primary consumers, such as bivalves, while starry flounder and shiner surfperch had similar trophic positions and were also likely feeding on secondary consumers to some extent. Rockfish with full stomachs had ingested a mixture of *Petrolithes*, *Cancer*, and *Majoid* crabs, *Heptacarpus* and *Pandalus* shrimp, and various fishes, including sculpins. This matches well with their estimated trophic position of >3 for all individuals and suggests they were feeding on a mix of primary and secondary consumers. The fish $\delta_{13}C$ values were similar to those of the bivalves, indicating primary reliance on pelagic carbon sources.

4.4.2 Microplastic concentrations by species

The model estimates of MP digestive tract concentrations by species are within the range of those reported by other studies. The most extensive data exist for mussels, with one recent study finding averages of 0.20–0.94 particles g ww^{-1} (or 1.25–15.42 particles ind^{-1}) in wild

Mytilus spp. collected from Italy, Spain, the Netherlands, Germany, France, Croatia, Denmark, and Tunisia (Vinay Kumar *et al.* 2020). Our MP concentrations for mussels are higher in terms of wet weight, at 2.73-14.36 particles g ww^{-1}, but lower in terms of dry weight at 0.33-0.81 particles ind^{-1}. It should be noted that the mussels sampled in our study were small (0.9-2.9 cm in length), such that even a single MP in a mussel would result in a remarkably high wet weight concentration due to low body mass. Covernton *et al.* (2019b) found mean concentrations of 0.10 particles ind^{-1} and 0.16 particles g dw^{-1} for Manila clams as compared to means of 1.06-1.27 particles ind^{-1} and 9.05-13.07 particles g dw^{-1} in the present study. Mohsen *et al.* (2019) found that farmed sea cucumbers (*Apostichopus japonicus*) collected in China contained 0–30 MPs ind^{-1} in their digestive tracts compared with a lower range 1.69-5.08 MPs ind^{-1} observed here for Orange and California sea cucumbers, respectively. Xu *et al.* (2020) found MP concentrations in crabs collected from Hong Kong beaches that were significantly lower (mean 0.21 particles g^{-1} ww) in a predatory species (*Metopograpsus frontalis*) compared with two deposit feeding species (mean 2.84, 2.59 particles g^{-1} ww, *Austruca lacteal*, and *Macrophthalmus convexus*), although there were other species of both feeding types with intermediate concentrations. The crab species in our study are all predatory, which could explain the lower mean concentrations in comparison with the more contaminated Hong Kong crabs - 1.08, 0.32, and 0.54 particles g^{-1} ww for graceful rock, red rock, and Dungeness crabs, respectively, in addition to differences in environmental exposure. Rochman *et al.* (2015) reported a mean of 1.00 MP ind^{-1} in the digestive tracts of flatfish (*Citharichthys sordidus*), 0.30 particles ind^{-1} in yellowtail rockfish (*Sebastes flavidus*) and 0.00 particles ind^{-1} in vermillion rockfish (*Sebastes miniatus*) and copper rockfish (*S. caurinus*). Our mean concentration estimates for flatfish were 1.29 particles ind^{-1} (Starry flounder) and 0.92 particles ind^{-1} (English sole), and for rockfish were 0.54-0.82 particles ind^{-1}

(black rockfish) and 0.33-0.72 particles ind^{-1} (copper rockfish). However, as Rochman *et al.* (2015) did not consider particles <500 µm in size, this may account for our higher concentrations. As we were unable to locate comparative data on MP ingestion by shallow-water sea star species, our results likely represent the first estimates of MP ingestion by sea stars.

4.4.3 Bioaccumulation

Bioaccumulation factors for MPs in digestive tracts (calculated in terms of total body wet weight) decreased with trophic position, suggesting several orders of magnitude higher bioaccumulation for lower trophic-level than higher trophic-level animals. However, bioaccumulation is difficult to interpret in the context of transitory MPs in animal digestive tracts compared with its common usage for lipophilic chemical contaminants - which transit into and accumulate in the body fat of animals (Arnot and Gobas 2006). For example, Dawson *et al.* (2018) exposed Antarctic krill (*Eupausia superba*) to polyethylene MP spheres in their food for a period of 10 days followed by a 15-day depuration time, and found that MP concentrations remained constant in the krill bodies during the 10-day exposure before decreasing rapidly during depuration. They fed the krill for 4 hours per day on MP-contaminated food, followed by 20 hours with no food and sampled krill at days 1, 2, 4, 7, and 10, after allowing sampled individuals to feed on uncontaminated algae for an added 4 hours. MP concentrations in krill did not increase with time throughout their experiment, so the authors concluded that bioaccumulation was not occurring. However, the krill were unable to completely remove MPs before their next feeding period. As bioaccumulation is predicated on the idea that ingestion rates are higher than excretion rates this would suggest a low level of bioaccumulation rather than none. We therefore propose that bioaccumulation of MPs in digestive tracts should be considered the consistent presence of any MPs over time, in proportion to body size, rather than necessarily

an increase with time. As residence time of MPs in digestive tracts (and other tissues) will determine bioavailability of sorbed contaminants and residual monomers, and the exposure to these chemicals over time relative to body mass will determine toxicity (Watanabe *et al.* 1992), our measure of bioaccumulation is appropriate for considering potential toxicity of MPs to an animal.

Considering the earlier statement, our data imply at least an order of magnitude more bioaccumulation of MPs for suspension feeding bivalves and sea cucumbers relative to predatory species. Although the whole bodies of the bivalves were analyzed, the individuals were small (0.9-2.9 cm length, 0.1-1.8 g ww) and it is unlikely that the size range of particles analyzed would have been present in other organs. Suspension and deposit feeding sea cucumbers bioaccumulation factors were lower than the bivalves, but similar between species, despite different feeding habits. The bioaccumulation factors for predators, including crabs, sea stars, and fish, were at least an order of magnitude lower than bivalves and sea cucumbers for the crabs and rockfish. Flatfish and sea star bioaccumulation factors were in the same order of magnitude as the sea cucumbers and shiner surfperch had the highest numbers, nearly as high as those for the clams. Previous studies have shown that planktivorous fish may preferentially ingest MPs due to their similarity in size, shape, and sometimes colour, to typical prey items (Ory *et al.* 2017, 2018). This could explain why the flatfish and shiner surfperch in this study had high bioaccumulation factors, as these species all feed (to varying extent) on small animals of similar sizes to the observed MPs (*e.g.*, zooplankton, benthic worms). The isotopic enrichment values of the flatfish and surfperch further support this - suggesting pelagic carbon sources and feeding on secondary consumers (such as zooplankton). Shiner surfperch, which had especially high bioaccumulation factors, are a fast growing viviparous species that requires high weight-specific

food intake and which empties its digestive tract every ~8 hours (*i.e.* as compared to ~24 hours for rockfish) (Gordon 1963, Singer 1985). Frequent consumption of prey that resemble MPs could therefore explain why shiner surfperch had higher bioaccumulation factors than the other fish species in this study. Nonetheless, these higher bioaccumulation factors do not necessarily suggest that MPs are remaining in shiner surfperch digestive tracts for long periods of time, but rather that they are entering their bodies faster than (or at similar rates to) excretions rates and to a greater extent relative to their body mass than for the larger fish.

4.4.4 Trophic transfer and biomagnification

Our results showed that trophic transfer from prey to predator was occurring in the two rockfish species, with evidence of (i) MPs in the bodies of ingested prey, and (ii) higher MP concentrations in the digestive tracts of rockfish with full stomachs compared to those with empty stomachs. Copper rockfish have previously been shown to ingest 0.5 - 3.7% of their body mass in food daily (Murie 1995). Assuming these max/min food consumption percentages apply to copper and black rockfish and using the mean posterior for MP concentration in ingested animals by wet weight, we estimate a minimum intake of 0.03–0.12 particles day^{-1} and a maximum intake of 0.23–0.79 particles day^{-1} for the size range of rockfish that were sampled. These ranges suggest that, on average, an individual rockfish ingests less than one >100-µm MP every day *via* trophic transfer. Rockfish require ~9-12 hours to digest half of the food in a full stomach (Singer 1985), meaning that all food should be processed through the digestive tract within ~24 hours - allowing plenty of time for MPs to be excreted before the next meal. This could explain why MP concentrations for rockfish with empty stomachs were so low in this

study. Thus, accumulation of MPs is minimal in rockfish - further explaining why the models did not support the occurrence of biomagnification.

The digestive tracts of individual animals from all species had varying amounts of ingested food and debris, which is why we modeled digestive tract concentrations as particles ind^{-1} rather than particles g^{-1}. At the level of the individual, neither trophic magnification nor dilution was occurring. In fact, when viewed in terms of either digestive tract or body weight, trophic dilution would seem to be occurring, since larger animals had similar numbers of MPs to smaller animals. The similar slopes for the relationship of MP concentration with trophic position at each of the three sites, suggest that excretion occurs fast enough to prevent significant accumulation of MPs in digestive tracts. This lack of biomagnification in digestive tracts concurs with several recent reviews (Gouin 2020, Walkinshaw *et al.* 2020, Miller *et al.* 2020). Other studies have supplied evidence for the rapid excretion of MPs from digestive tracts – thereby limiting any biomagnification. Several studies using field-collected samples have also found no relationship between trophic level and MP concentrations in digestive tracts, gills, or muscle of various fish and invertebrate species (Güven *et al.* 2017, Welden *et al.* 2018, Bour *et al.* 2018, Akhbarizadeh *et al.* 2019, Filgueiras *et al.* 2020). A study by Zhang *et al.* (2019a) did find a significant, positive correlation between MP concentrations in gastrointestinal tracts and gills and trophic level across 11 fish and eight crustacean species collect from the East China Sea (although only on the order of a few more MPs between their highest and lowest sampled trophic levels). Welden *et al.* (2018) found that plaice (*Pleuronectes platessa*) collected from the Celtic Sea had ingested sand eels (*Ammodytes tobianus*) containing MPs, but there was no significant difference between prey and predator, suggesting a lack of MP retention.

Two studies have also employed stable isotopes analysis to measure MPs across trophic levels within food webs. Garcia *et al* (2021) investigated a food web within the Garonne river in the southwest of France. They found that although digestive tract concentrations of 700-5000-µm MPs did not increase with trophic position for freshwater fish they did increase for macroinvertebrates. However, they concluded that biomagnification was unlikely because ingestion of MPs appeared to be mostly direct and accidental rather than as a result of trophic transfer. Piarulli *et al.* (2020) examined benthic invertebrates from salt marsh sediments in three coastal lagoons on the northern Adriatic coast and found that only 4% of individuals contained MPs, and so were unable to establish a relationship with trophic position. However, it seems likely that such a low degree of contamination would preclude any biomagnification. Several laboratory studies have also demonstrated that, even under high MP exposure levels, excretion from the digestive tract is rapid and trophic dilution is the predominant outcome (Sun *et al.* 2017, Kim *et al.* 2018, Elizalde-Velázquez *et al.* 2020).

In study, we also showed that magnification of MPs in fish livers was not occurring, with a mean trophic magnification factor of 0.54 instead suggesting trophic dilution. Akhbarizadeh *et al* (2019) reported similar findings, calculating a trophic magnification factor of 0.72 in the gills and muscles of prawns (*Penaeus semisulcatus*), crabs (*Portunus armatus*), and fish (*Epinephelus coioides*, *Platycephalus indicus,* and *Liza klunzingeri*). It is possible that our lower size limit of 100 µm was not sufficient to accurately quantify MPs in fish livers, and that only smaller particles would be able to translocate to this organ. For example, according to Zitouni *et al.* (2020), the MPs found in muscle of the painted comber (*Serranus scriba*) were primarily 1.2–3 µm in size. Our estimated MP concentrations in the present study for fish livers were quite low (mean 0.10, range 0.00-1.29 particles g^{-1}) after background contamination was considered in the

GLMM. Multiplying the fitted values by liver sample dry weight results in a predicted "true" mean MP number of just 0.18 particles individual^{-1} which is ~4.5 times lower than the concentration in the fish digestive tracts (mean 0.79 particles ind^{-1}). Translocation of ingested MPs to fish livers has been proven in laboratory experiments - for example 1.4-1.6-µm spheres appeared in zebrafish (*Danio rerio*) livers after they were fed 1-5-µm spheres. Our result should thus be interpreted with caution, as the mechanism by which >100-µm MPs could translocate to fish livers is unclear (Kim *et al.* 2020).

4.4.5 Methodological considerations

We employed several new methods in the present work that will be useful for studying MPs in food webs and other contexts. We showed that stable isotope analysis was extremely useful for characterizing the feeding habits of animals and for studying the movement of MPs within food webs. Applying this method more broadly will enable researchers to better quantify the dynamics of MPs within specific food webs. This study also is the first application of a random forest model to classify unknown particles as synthetic or non-synthetic, using expert user input and particle characteristics and after training the model using spectroscopically verified particles. For studies still relying on visual and physical methods of identification of potential MPs it is often difficult to transfer and analyze 100% of the particles. Simply excluding these particles is problematic, so studies apply the proportion of analyzed particles that were MPs to correct the reported concentrations across all samples. However, this does not consider subtleties relating to particle size, shape, colour, or type of sample, as well as ignoring the ability of an experienced user to judge (or guess, to some degree) whether a particle might be plastic. Machine-learning classification models offer the potential to classify these unknown particles, while considering user input to allow a more detailed analysis. On our fitted data, the random

forest model correctly classified 73.9% of synthetic particles as synthetic and mis-classified 41.7% of semi-synthetic, 19.0% of natural anthropogenic, and 30.9% of natural particles as synthetic. Based on the model, 41.1% of unknown particles were classified as synthetic, in comparison to the 32.5% of spectroscopically- confirmed particles that were classified as synthetic.

Our use of Bayesian hierarchical models to incorporate uncertainty across levels of the analysis represents an approach that may be of broader use in the study of microplastics. To date, most researchers have accounted for background contamination of their samples using either simple deterministic blank subtraction (*i.e.*, whereby the mean MP content in blanks is subtracted from sample counts), or by ignoring counts that are above either the limit of detection or limit of qualification (Brander *et al.* 2020). The limit of detection is the mean MP count (or mass) from blanks (minimum of three replicates) plus two standard deviations. The limit of quantification is the limit of detection plus three standard de*via*tions from the mean of blanks (maximum 10 replicates). However, as MP concentrations in samples are often low, we argue that limits of detection and quantification would prevent any inferences for many systems and samples. The Bayesian approach applied here assumes that background contamination will follow a Poisson distribution, and allows for stochastic variation in blank subtraction (according to the type of sample) such that a distribution of possible "true" sample values is estimated. This approach will be of use for further MP research, which should compare the ability to make inferences around true MP sample numbers depending on the approach used to account for background contamination.

As in most other MP studies the main limitation for this study is the inability to reliably analyze particles <100 µm in size. Thus, our conclusions can only be applied to the larger MP

fractions. Smaller particles may be accumulating at higher concentrations, both in the digestive tracts and tissues of fish, and even possibly biomagnifying (Roch *et al.* 2020). While it seems likely that small micro- and nanoplastics will be excreted from digestive tracts along with larger MPs, the risk of translocation - and therefore accumulation - in other tissues is higher. Emerging technologies are beginning to allow for the analysis of smaller MPs. Automated Raman and FTIR spectroscopy have the potential to detect and classify particles down to 1–5 or 10–20 µm, respectively (Primpke *et al.* 2020). Thermal degradation methods followed by GCMS analysis of pyrolysis products, allow for even smaller particles to be quantified, although currently the output is only in terms of weight by polymer - particle counts are not yet possible. Further research combining methodologies like those employed here with some of these newer techniques will be essential for deciding whether smaller micro- and nanoplastics and associated chemicals are biomagnifying in food webs.

4.4.6 Conclusions

Our results suggest that smaller, lower-trophic-level animals may be at the greatest risk of any potential health effects caused by MP ingestion, given higher exposure rates relative to their body size - a finding supported by Walkinshaw *et al.* (2020) and Foley *et al.* (2018). Although we cannot completely rule out biomagnification of MPs under high-exposure scenarios or for MPs <100-µm, our findings from rockfish stomachs show that excretion appears to be fast enough to limit accumulation and to make magnification in digestive tracts unlikely, even under the above conditions. Preliminary risk assessments have proposed that under current MP exposure scenarios, few organisms are likely to experience any significant health effects in aquatic environments (Koelmans *et al.* 2020, Everaert *et al.* 2020). However, these assessments rely on acute exposure toxicity experiments and do not consider ingestion rates or the effects of

chronic exposure. Future ecological risk assessments will need to take these factors into consideration, which will include modeling the food-web dynamics of MPs. Our work provides a significant contribution to this effort by modeling the individual-level relationship between trophic position and digestive-tract MP concentrations among species spanning a range of feeding habits in coastal marine food webs, and by demonstrating and quantifying the relative importance of trophic transfer for MP ingestion by rockfish - relatively high trophic level long-lived species. We also present a novel method for accounting for background contamination *via* the use of Bayesian inference.

Chapter 5: General Conclusions and Synthesis

5.1 Current understanding suggests that microplastics may pose minimal risk to marine ecological communities, although sublethal and long-term effects need to be explored

Chapters 3 and 4 suggest that consumption of MPs >100 µm by animals in coastal marine food webs in British Columbia is low, of the order of 1-2 particles (or less) per digestive tract on average, and it is likely that this degree of ingestion presents a low acute risk to animal health. Ecological risk is often characterized using species sensitivity distributions and a derived predicted no-effect concentration (PNEC). Species sensitivity distributions are created by fitting a statistical distribution (commonly log-normal) to toxicity data collected from multiple species for the concentration of a particular chemical at which some threshold of toxicity is passed (*e.g.*, no effects limit). From there, the mean hazardous concentration for 5% of species is calculated and then divided by some assessment factor (usually determined by the regulatory body) to derive the PNEC (ECHA 2011). A variety of studies have generated PNEC values for MPs spanning four orders of magnitude. Zhang *et al.* (2019c) estimated a PNEC of 4.9 particles L^{-1} freshwater, Everaert *et al.* (2018) 6.7 particles L^{-1} seawater, Jung *et al.* (2021) a PNEC of 12 particles L^{-1} seawater, and Adam *et al.* (2021) 3,840 particles L^{-1} seawater. The maximum seawater MP concentrations reported in this thesis (1.95, 4, and 1.60 particles L^{-1} in Chapters 2, 3, and 4, respectively) were 3-2,400 lower than any of these PNECs. However, the PNECs from the mentioned studies were generated by combining data on the toxicity of fragments and fibres from a range of polymers and particles sizes and may therefore not reflect the particle type distribution in the areas sampled in this thesis.

One emerging approach to characterize the ecological risk of current environmental MP concentrations is to use probabilistic methods to interpolate the missing fractions of sizes,

shapes, and polymer shapes that are overlooked by specific studies. For example, Koelmans *et al.* (2020) corrected their species sensitivity distributions for polymer type and size (*i.e.*, such that under-reported size ranges were accounted for), while also only considering ingestible size ranges for each species, and calculated an effect threshold of 75.6 particles L^{-1} freshwater - above which biological harm could be expected to occur for an animal living in that environment. However, this method still does not account for differential concentration of MPs from the environment by distinct species, long-term effects of chronic particle exposure, toxicity associated with plastic biofilms, or higher degrees of weathering or sorbed contaminants. Seawater MP concentrations often do not correlate strongly with the number of MPs contained within an animal at any given time (Zhu *et al.* 2021), as their entry and residence time in animals depend on complex, interacting factors, including body size, feeding strategy, depuration times, rates of translocation to other tissues, and food-web relationships. As highlighted in Chapter 4, MP concentrations in smaller, suspension-feeding animals can be orders of magnitude higher than in large-bodied predators. Thus, although current exposure levels within British Columbian waters are below preliminary PNEC estimates, the potential for long-term toxicity and species-specific effects cannot be ruled out. Even subtle health effects for lower-trophic-level animals, such as decreased expression of reproduction-related genes in oysters (Raap 2019), have the potential to cause indirect effects on other species by shifting the resource landscape at the base of a food web - thereby creating energetic bottlenecks to higher trophic levels or by driving shifts in feeding habits and behaviours (Sherwood *et al.* 2002, Fleeger *et al.* 2003).

5.2 Microplastics likely present low risk to Canadian seafood consumers

The low concentrations of MPs found in the coastal marine species examined in this thesis, including some consumed by humans as seafood, suggest that the food safety risks from

British Columbian seafood are low and that MPs release from aquaculture plastic is not the main source of contamination. Cox *et al.* (2019) estimated a global average MP concentration in seafood of 1.48 particles g^{-1}, which translates to an average annual intake of approximately 15,000-20,000 particles $person^{-1}$ $year^{-1}$ based on the recommended American diet. This compares to an estimated consumption of 39,000-52,000 particles $person^{-1}$ $year^{-1}$ from all reviewed food sources, which account for just 15% of recommended caloric intake (Cox *et al.* 2019). In Chapter 4, I derive a lower-end estimate of MP consumption by Canadian shellfish consumers of 87 particles $person^{-1}$ $year^{-1}$. This number is much lower than the estimated annual consumption from all seafood for the average American, stated above, due to both the low concentrations of MPs in BC shellfish and the relatively low consumption of shellfish by the average Canadian. However, Canadians in communities that consume proportionately more shellfish will be expected to have higher exposures. The benefit of consuming seafood may outweigh any risks from ingesting MPs from this source, although further study is needed.

Few data exist for more commonly-consumed food groups such as dairy, red meat, poultry, grains, and fruits and vegetables – thereby making it difficult to compare the exposure rates of seafood with the rest of the average Canadian diet. Furthermore, fish tends to make up the most consumed form of seafood in Canada and generally excludes the digestive tract of the fish, where most MPs are found (Daniel *et al.* 2020). Although filling these data gaps on human dietary exposure of MPs is necessary, there are enough data available to characterize the extent to which a typical Canadian consumer might be exposed to larger (>100-µm) MPs. However, our current understanding of the health implications for humans from either short- or long-term exposure to MPs is still extremely limited, making it difficult to accurately characterize “risk”

from a public health standpoint. Researching these potential effects will therefore be critical to fully understanding the health risks of human exposure to MPs.

5.3 Fibres dominate the microplastics found in the marine environment of southern British Columbia

My results confirm that fibres make up the dominant form of >100-µm MPs in coastal marine environments of southern British Columbia. This agrees with several other recent studies in the region. For example, Collicutt *et al.* (2019) found a predominance of fibrous MPs in the digestive tracts of Chinook salmon (*Oncorhynchus tshawytscha*), in seawater, and in sediment samples collected from the east coast of Vancouver Island, in locations near the sampling sites used in the present work. The MP concentrations reported by Collicutt *et al.* (2019) were also similar to those in fish digestive tracts reported in Chapter 4, with an average of 1.2 MPs per digestive tract. MP fibres also dominated seawater and zooplankton samples collected from the offshore and coastal waters of British Columbia (Desforges *et al.* 2014, 2015). It is likely that the primary pathway by which these fibres enter the British Columbian marine environment is *via* sewage effluent following the release of fibres from textiles during clothes washing in domestic and industrial environments. Gies *et al.* (2018) carried out an analysis of MPs at a major sewage plant in Vancouver and found that, although 99% of MPs were retained in sludge, the plant was still estimated to release 30 billion MPs into the marine environment each year, the majority of which were fibres. Other work has suggested that fibres are the most prevalent form of MPs in seawater in many other parts of the world as well (Woodall *et al.* 2014, Lima *et al.* 2021).

5.4 The need to harmonize microplastics research methods and reporting

Significant differences in the collection, extraction, identification, and chemical analysis procedures used in different studies have led some researchers to call for standardization in the

MP field for nearly a decade (Hidalgo-Ruz *et al.* 2012). These calls take the form of desiring consistent methodologies to be used for the quantification of MPs in environmental samples. However, extracting and analysing the entire 1-5000-µm range of MPs is often cost prohibitive for many researchers, and different sample matrices require varying intensities of purification procedures that result in additional costs and methodological limitations to quantifying all types of MPs (Lusher *et al.* 2020). As such, it has been argued that a more practical approach is that of harmonization, by which studies are rigorous enough in their methodologies and transparent enough in reporting the details and limitations of these methodologies to at least enable inter-comparability (Provencher *et al.* 2020). For example, recent publications have suggested minimum reporting criteria that should be included in future MP publications (Dehaut *et al.* 2019).

As identified in Chapter 2, one key methodological factor for determining reported MP concentrations is the lowest size of particle that can be retained or identified in a study. Unfortunately, many studies report their lowest filter size, which is often small (about a few µm), but without naming a realistic value for the smallest particle size that they can detect. Unless a study is using an automated scanning spectroscopy method, it is unlikely that particles <100 µm can be reliably identified (Primpke *et al.* 2020). In Chapters 3 and 4, I explicitly state that our lowest size limit for reliably identifying MPs was 100 µm, and in Chapter 4 I only consider particles that were larger than this size. As researchers begin to interpolate missing MP fractions to better facilitate risk assessment, it is becoming increasingly important that researchers either set a realistic size cut-off (*i.e.*, below which they do not count MPs), or experimentally quantify the lowest size of particle that they can detect. Doing so will certainly help to address the underestimation problem that currently exists in the field.

5.5 The way forward: reconsidering traditional ecotoxicology in the face of a complex contaminant

An inescapable element of MPs research that becomes more evident with the exponentially increasing rate of publications in the field is that understanding the mechanisms and potential for these particles to cause ecological harm is exceedingly complex (Rochman *et al.* 2019). However, understanding whether such harm is occurring is essential for identifying and deciding the priority of MP mitigation policies relative to other environmental issues. As discussed in Chapter 4, advances in analytical technologies will eventually lead to more thorough characterization of the full size-complement of MPs, which will also allow for more environmentally relevant laboratory exposure scenarios to be conducted.

Nevertheless, the challenge remains of how to approach the toxicology of MPs as complex and highly variable mixtures occur in different environments. As discussed by Kramm *et al.* (2018), considering risk in the context of MPs may thus require a paradigm shift from traditional, single-organism, and chemical toxicity testing. This shift will not happen overnight, but will require disruptive environmental research and new perspectives that embrace the science of complex systems (Sedlak 2018, Khan 2018). As examined by de Souza Machado *et al.* (2019), novel contaminants such as MPs and endocrine disruptors require novel thinking and approaches, including the necessity for ecotoxicology to move beyond merely quantifying lethality, *per se*, to considering the resistance and resilience of entire biological systems – including food webs, communities, and ecosystems.

A “big data” approach that harnesses the power of modern computing platforms to enable the modeling of complicated systems might offer some solutions to the complexity problem presented by MPs and other novel contaminants. Similarly, a systems-biology approach, the

study of an organism as interacting networks, has the potential to better integrate the effects of multi-contaminant stressors (such as MPs) through the use of omics (genomics, proteomics, and metabolomics), by linking contaminants to the perturbations of "networks" within a single organism (Garcia-Reyero and Perkins 2011). Through understanding the mechanism by which individual components of a complex contaminant influence networks, the outcomes of combined contaminants can also be predicted. Dynamic energy budget theory can also be applied to model the effect of contaminants on individuals (Nisbet *et al.* 2000, Muller *et al.* 2010). By mathematically considering the balance of energy distribution between food intake, maintenance, growth, and reproduction, with the exchange of toxic chemicals in the environment, and how accumulated toxicants change the energetic budget, the effects on an organism's performance can be estimated. Such individual-level models can be scaled up using matrix- or agent-based models to predict long-term effects on population parameters from exposure to contaminants (Klok *et al.* 2007, Billoir *et al.* 2007, Muller *et al.* 2009, Johnston *et al.* 2014). If these population-level parameters are combined with modeling of complex species interactions, then predictions can be made about community-level responses (Prosnier *et al.* 2015). In this way, knowledge of sublethal effects on biological processes that have been found in the lab or field can be used to predict ecological outcomes at larger scales of biological organization. These approaches will obviously require a massive synthesis of knowledge and expertise. However, similar integrative approaches to complex systems are already appearing in other fields, for example the use of agent-based models in public health, may shed some light on how ecotoxicology can tackle the problem of chemical mixtures and chronic and sublethal contaminants.

Even with the approaches proposed above, fully understanding the complex interactions and effects of MPs in the environment will still take many years, while we continue to face exponentially increasing rates of plastic production and the seemingly insurmountable societal issue of how to limit their release to the environment (Borrelle *et al.* 2020). The strategy described above (*i.e.*, going from individual-, to population-level, and community-level responses using models) would seem to be a "bottom-up" approach. However, there is also the potential for a "top-down" approach to offer insight into the risk potential of MPs, and whether further precautionary actions are needed to limit their release to the environment. Such an approach would use community-level experiments exposing multiple, interacting species to environmentally relevant doses and mixtures of MPs and associated contaminants. The effects to community composition and food-web interactions could then considered. In this way, rather than having to infer emergent effects of MPs on biological communities and food webs, individual effects can be extrapolated from the "top down", based on the response of the communities.

Examples of this type of experimental approach already exist. For example, Green (2016) used mesocosms to demonstrate that exposure to polyethylene and polylactic acid MPs reduced species richness of benthic communities. A similar study, using the same MP types, found that benthic invertebrate assemblages were affected when European flat oysters (*Ostrea edulis*) were present, but not when blue mussels (*Mytilus edulis*) were (Green *et al.* 2017). While this "top-down" approach is not necessarily mechanistic, it still supplies strong evidence that action to reduce MP pollution of the environment is needed now. Regardless of the complexities associated with understanding MPs, there is already more than enough evidence suggesting that pollution of the environment with macroplastics is causing ecological harm (Bucci *et al.* 2020).

Since MP pollution stems from the production of plastics and mismanagement of plastic waste, global action to reduce the release of all sizes of plastics to the environment is needed now.

References

Abbasi, S., N. Soltani, B. Keshavarzi, F. Moore, A. Turner, and M. Hassanaghaei. 2018. Microplastics in different tissues of fish and prawn from the Musa Estuary, Persian Gulf. Chemosphere 205:80–87.

Adam, V., A. von Wyl, and B. Nowack. 2021. Probabilistic environmental risk assessment of microplastics in marine habitats. Aquatic Toxicology 230:105689.

Akhbarizadeh, R., F. Moore, and B. Keshavarzi. 2019. Investigating microplastics bioaccumulation and biomagnification in seafood from the Persian Gulf: a threat to human health? Food Additives & Contaminants: Part A 36:1696–1708.

Anderson, C., and G. Cabana. 2007. Estimating the trophic position of aquatic consumers in river food webs using stable nitrogen isotopes. Journal of the North American Benthological Society 26:273–285.

Andrady, A. L. 2011. Microplastics in the marine environment. Marine Pollution Bulletin 62:1596–1605.

Annett, C., and R. Pierotti. 1984. Foraging behavior and prey selection of the leather seastar *Dermasterias imbricata*. Marine Ecology Progress Series 14:197–206.

Arnot, J. A., and F. A. Gobas. 2006. A review of bioconcentration factor (BCF) and bioaccumulation factor (BAF) assessments for organic chemicals in aquatic organisms. Environmental Reviews 14:257–297.

Au, S. Y., T. F. Bruce, W. C. Bridges, and S. J. Klaine. 2015. Responses of *Hyalella azteca* to acute and chronic microplastic exposures. Environmental Toxicology and Chemistry 34:2564–2572.

Bach, L. T., U. Riebesell, S. Sett, S. Febiri, P. Rzepka, and K. G. Schulz. 2012. An approach for particle sinking velocity measurements in the 3–400 μm size range and considerations on the effect of temperature on sinking rates. Marine Biology 159:1853–1864.

Bagaev, A., A. Mizyuk, L. Khatmullina, I. Isachenko, and I. Chubarenko. 2017. Anthropogenic fibres in the Baltic Sea water column: Field data, laboratory and numerical testing of their motion. Science of The Total Environment 599–600:560–571.

Barrows, A. P. W., S. E. Cathey, and C. W. Petersen. 2018. Marine environment microfiber contamination: global patterns and the diversity of microparticle origins. Environmental Pollution 237:275–284.

Barrows, A. P. W., C. A. Neumann, M. L. Berger, and S. D. Shaw. 2017. Grab vs. neuston tow net: a microplastic sampling performance comparison and possible advances in the field. Analytical Methods 9:1446–1453.

Barry, J., and G. Cailliet. 1981. The utilization of shallow marsh habitats by commercially important fishes in Elkhorn Slough, California. Cal-Nevada Wildlife Transactions:38–47.

Barry, J. P., M. M. Yoklavich, G. M. Cailliet, D. A. Ambrose, and B. S. Antrim. 1996. Trophic ecology of the dominant fishes in Elkhorn Slough, California, 1974–1980. Estuaries 19:115–138.

Barton, K. 2018. MuMIn: Multi-Model Inference.

Bascom, W. N. 1951. The relationship between sand size and beach-face slope. Eos, Transactions American Geophysical Union 32:866–874.

Bates, D., M. Mächler, B. Bolker, and S. Walker. 2015. Fitting linear mixed-effects models using lme4. Journal of Statistical Software 67:1–48.

Bendell, L. I. 2015. Favored use of anti-predator netting (APN) applied for the farming of clams leads to little benefits to industry while increasing nearshore impacts and plastics pollution. Marine Pollution Bulletin 91:22–28.

Beninger, P. G., A. Valdizan, P. Decottignies, and B. Cognie. 2008. Impact of seston characteristics on qualitative particle selection sites and efficiencies in the pseudolamellibranch bivalve *Crassostrea gigas*. Journal of Experimental Marine Biology and Ecology 360:9–14.

Bergmann, M., S. Mützel, S. Primpke, M. B. Tekman, J. Trachsel, and G. Gerdts. 2019. White and wonderful? Microplastics prevail in snow from the Alps to the Arctic. Science Advances 5:eaax1157.

Besseling, E., E. M. Foekema, M. J. Van Den Heuvel-Greve, and A. A. Koelmans. 2017. The effect of microplastic on the uptake of chemicals by the lugworm *Arenicola marina* (L.) under environmentally relevant exposure conditions. Environmental Science & Technology 51:8795–8804.

Billoir, E., A. R. R. Péry, and S. Charles. 2007. Integrating the lethal and sublethal effects of toxic compounds into the population dynamics of *Daphnia magna*: A combination of the DEBtox and matrix population models. Ecological Modelling 203:204–214.

Borgå Katrine, Kidd Karen A, Muir Derek CG, Berglund Olof, Conder Jason M, Gobas Frank APC, Kucklick John, Malm Olaf, and Powell David E. 2011. Trophic magnification factors: considerations of ecology, ecosystems, and study design. Integrated Environmental Assessment and Management 8:64–84.

Borrelle, S. B., J. Ringma, K. L. Law, C. C. Monnahan, L. Lebreton, A. McGivern, E. Murphy, J. Jambeck, G. H. Leonard, M. A. Hilleary, M. Eriksen, H. P. Possingham, H. D. Frond, L. R. Gerber, B. Polidoro, A. Tahir, M. Bernard, N. Mallos, M. Barnes, and C. M. Rochman. 2020. Predicted growth in plastic waste exceeds efforts to mitigate plastic pollution. Science 369:1515–1518.

Bour, A., C. G. Avio, S. Gorbi, F. Regoli, and K. Hylland. 2018. Presence of microplastics in benthic and epibenthic organisms: Influence of habitat, feeding mode and trophic level. Environmental Pollution 243:1217–1225.

Brander, S. M., V. C. Renick, M. M. Foley, C. Steele, M. Woo, A. Lusher, S. Carr, P. Helm, C. Box, S. L. Cherniak, R. Andrews, and C. Rochman. 2020. Sampling and QA/QC: a guide for scientists investigating the occurrence of microplastics across matrices. Applied Spectroscopy 74:1099–1125.

Browne, M. A., P. Crump, S. J. Niven, E. Teuten, A. Tonkin, T. Galloway, and R. Thompson. 2011. Accumulation of microplastic on shorelines worldwide: sources and sinks. Environmental Science & Technology 45:9175–9179.

Bucci, K., M. Tulio, and C. Rochman. 2020. What is known and unknown about the effects of plastic pollution: a meta-analysis and systematic review. Ecological Applications 30:e02044.

Cameron, J. L., and P. V. Fankboner. 1984. Tentacle structure and feeding processes in life stages of the commercial sea cucumber *Parastichopus californicus* (Stimpson). Journal of Experimental Marine Biology and Ecology 81:193–209.

Carbery, M., W. O'Connor, and T. Palanisami. 2018. Trophic transfer of microplastics and mixed contaminants in the marine food web and implications for human health. Environment International 115:400–409.

Carl, V. C., M. Lieke, V. Brecht, V. Henk, and M. Tom. 2021. The biological plastic pump: evidence from a local case study using blue mussel and infaunal benthic communities. Environmental Pollution:115825.

Carr, S. A. 2017. Sources and dispersive modes of micro-fibers in the environment. Integrated Environmental Assessment and Management 13:466–469.

Castro, R. O., M. L. Silva, M. R. C. Marques, and F. V. de Araújo. 2016. Evaluation of microplastics in Jurujuba Cove, Niterói, RJ, Brazil, an area of mussels farming. Marine Pollution Bulletin 110:555–558.

Catarino, A. I., V. Macchia, W. G. Sanderson, R. C. Thompson, and T. B. Henry. 2018. Low levels of microplastics (MP) in wild mussels indicate that MP ingestion by humans is minimal compared to exposure via household fibres fallout during a meal. Environmental Pollution 237:675–684.

Chae, Y., and Y.-J. An. 2017. Effects of micro- and nanoplastics on aquatic ecosystems: Current research trends and perspectives. Marine Pollution Bulletin 124:624–632.

Chen, M., M. Jin, P. Tao, Z. Wang, W. Xie, X. Yu, and K. Wang. 2018. Assessment of microplastics derived from mariculture in Xiangshan Bay, China. Environmental Pollution 242:1146–1156.

Cheng, Y. L., J.-G. Kim, H.-B. Kim, J. H. Choi, Y. Fai Tsang, and K. Baek. 2021. Occurrence and removal of microplastics in wastewater treatment plants and drinking water purification facilities: A review. Chemical Engineering Journal 410:128381.

Christianen, M. J. A., J. J. Middelburg, S. J. Holthuijsen, J. Jouta, T. J. Compton, T. van der Heide, T. Piersma, J. S. S. Damsté, H. W. van der Veer, S. Schouten, and H. Olff. 2017. Benthic primary producers are key to sustain the Wadden Sea food web: stable carbon isotope analysis at landscape scale. Ecology 98:1498–1512.

Claessens, M., S. D. Meester, L. V. Landuyt, K. D. Clerck, and C. R. Janssen. 2011. Occurrence and distribution of microplastics in marine sediments along the Belgian coast. Marine Pollution Bulletin 62:2199–2204.

Collard, F., B. Gilbert, P. Compère, G. Eppe, K. Das, T. Jauniaux, and E. Parmentier. 2017. Microplastics in livers of European anchovies (*Engraulis encrasicolus*, L.). Environmental Pollution 229:1000–1005.

Collicutt, B., F. Juanes, and S. E. Dudas. 2019. Microplastics in juvenile Chinook salmon and their nearshore environments on the east coast of Vancouver Island. Environmental Pollution 244:135–142.

da Costa Araújo, A. P., and G. Malafaia. 2021. Microplastic ingestion induces behavioral disorders in mice: preliminary study on the trophic transfer effects via tadpoles and fish. Journal of Hazardous Materials 401:123263.

Courtene-Jones, W., B. Quinn, S. F. Gary, A. O. M. Mogg, and B. E. Narayanaswamy. 2017. Microplastic pollution identified in deep-sea water and ingested by benthic invertebrates in the Rockall Trough, North Atlantic Ocean. Environmental Pollution 231:271–280.

Covernton, G. A., H. L. Davies, K. D. Cox, R. El-Sabaawi, F. Juanes, S. E. Dudas, and J. F. Dower. 2021a. A Bayesian analysis of the factors determining microplastics ingestion in fishes. Journal of Hazardous Materials 413:125405.

Covernton, G. A., H. L. Davies, K. D. Cox, R. El-Sabaawi, F. Juanes, S. E. Dudas, and J. F. Dower. 2021b. A Bayesian analysis of the factors determining microplastics ingestion in fishes. Journal of Hazardous Materials 413:125405.

Covernton, G. A., C. M. Pearce, H. J. Gurney-Smith, S. G. Chastain, P. S. Ross, J. F. Dower, and S. E. Dudas. 2019a. Size and shape matter: a preliminary analysis of microplastic sampling technique in seawater studies with implications for ecological risk assessment. Science of The Total Environment 667:124–132.

Covernton, G., B. Collicutt, H. Gurney-Smith, C. Pearce, J. Dower, P. Ross, and S. Dudas. 2019b. Microplastics in bivalves and their habitat in relation to shellfish aquaculture proximity in coastal British Columbia, Canada. Aquaculture Environment Interactions 11:357–374.

Cox, K. D., G. A. Covernton, H. L. Davies, J. F. Dower, F. Juanes, and S. E. Dudas. 2019. Human consumption of microplastics. Environmental Science & Technology 53:7068–7074.

Crossman, J., R. R. Hurley, M. Futter, and L. Nizzetto. 2020. Transfer and transport of microplastics from biosolids to agricultural soils and the wider environment. Science of The Total Environment:138334.

Daniel, D. B., P. M. Ashraf, and S. N. Thomas. 2020. Microplastics in the edible and inedible tissues of pelagic fishes sold for human consumption in Kerala, India. Environmental Pollution 266:115365.

Davidson, K., and S. E. Dudas. 2016. Microplastic ingestion by wild and cultured Manila clams (*Venerupis philippinarum*). Archives of Environmental Contamination and Toxicology 71:147–156.

Dawson, A., W. Huston, S. Kawaguchi, C. King, R. Cropp, S. Wild, P. Eisenmann, K. Townsend, and S. Bengtson Nash. 2018. Uptake and depuration kinetics influence microplastic bioaccumulation and toxicity in Antarctic krill (*Euphausia superba*). Environmental Science & Technology 52:3195–3201.

Day, D. E. 1976. Homing behavior and population stratification in central Puget Sound English sole (*Parophrys vetulus*). Journal of the Fisheries Research Board of Canada 33:278–282.

De Sales-Ribeiro, C., Y. Brito-Casillas, A. Fernandez, and M. J. Caballero. 2020. An end to the controversy over the microscopic detection and effects of pristine microplastics in fish organs. Scientific Reports 10:12434.

Defossez, J.-M., and A. J. S. Hawkins. 1997. Selective feeding in shellfish: size-dependent rejection of large particles within pseudofaeces from *Mytilus edulis*. Marine Biology 129:139–147.

Dehaut, A., A.-L. Cassone, L. Frère, L. Hermabessiere, C. Himber, E. Rinnert, G. Rivière, C. Lambert, P. Soudant, A. Huvet, G. Duflos, and I. Paul-Pont. 2016. Microplastics in seafood: benchmark protocol for their extraction and characterization. Environmental Pollution 215:223–233.

Dehaut, A., L. Hermabessiere, and G. Duflos. 2019. Current frontiers and recommendations for the study of microplastics in seafood. TrAC Trends in Analytical Chemistry 116:346–359.

Dekiff, J. H., D. Remy, J. Klasmeier, and E. Fries. 2014. Occurrence and spatial distribution of microplastics in sediments from Norderney. Environmental Pollution 186:248–256.

Desforges, J.-P. W., M. Galbraith, N. Dangerfield, and P. S. Ross. 2014. Widespread distribution of microplastics in subsurface seawater in the NE Pacific Ocean. Marine Pollution Bulletin 79:94–99.

Desforges, J.-P. W., M. Galbraith, and P. S. Ross. 2015. Ingestion of microplastics by zooplankton in the northeast Pacific Ocean. Archives of Environmental Contamination and Toxicology 69:320–330.

Diamond, N., and D. G. Hankin. 1985. Movements of adult female Dungeness crabs (*Cancer magister*) In northern California based on tag recoveries. Canadian Journal of Fisheries and Aquatic Sciences 42:919–926.

Diepens, N. J., and A. A. Koelmans. 2018. Accumulation of plastic debris and associated contaminants in aquatic food webs. Environmental Science & Technology 52:8510–8520.

Ding, J.-F., J.-X. Li, C.-J. Sun, C.-F. He, F.-H. Jiang, F.-L. Gao, and L. Zheng. 2018. Separation and identification of microplastics in digestive system of bivalves. Chinese Journal of Analytical Chemistry 46:690–697.

Dris, R., J. Gasperi, M. Saad, C. Mirande, and B. Tassin. 2016. Synthetic fibers in atmospheric fallout: a source of microplastics in the environment? Marine Pollution Bulletin 104:290–293.

ECHA. 2011. Guidance on information requirements and chemical safety assessment Part B: hazard assessment. Page 68. European Chemicals Agency.

Eleftheriou, A. 2013. Methods for the study of marine benthos. John Wiley & Sons.

Elizalde-Velázquez, A., A. M. Carcano, J. Crago, M. J. Green, S. A. Shah, and J. E. Cañas-Carrell. 2020. Translocation, trophic transfer, accumulation and depuration of

polystyrene microplastics in *Daphnia magna* and *Pimephales promelas*. Environmental Pollution 259:113937.

Everaert, G., M. De Rijcke, B. Lonneville, C. R. Janssen, T. Backhaus, J. Mees, E. van Sebille, A. A. Koelmans, A. I. Catarino, and M. Vandegehuchte. 2020. Risks of floating microplastic in the global ocean. Environmental Pollution 267:115499.

Everaert, G., L. Van Cauwenberghe, M. De Rijcke, A. A. Koelmans, J. Mees, M. Vandegehuchte, and C. R. Janssen. 2018. Risk assessment of microplastics in the ocean: Modelling approach and first conclusions. Environmental Pollution 242:1930–1938.

Fazey, F. M. C., and P. G. Ryan. 2016. Biofouling on buoyant marine plastics: An experimental study into the effect of size on surface longevity. Environmental Pollution 210:354–360.

Filgueiras, A. V., I. Preciado, A. Cartón, and J. Gago. 2020. Microplastic ingestion by pelagic and benthic fish and diet composition: A case study in the NW Iberian shelf. Marine Pollution Bulletin 160:111623.

Fleeger, J. W., K. R. Carman, and R. M. Nisbet. 2003. Indirect effects of contaminants in aquatic ecosystems. Science of The Total Environment 317:207–233.

Foekema, E. M., C. De Gruijter, M. T. Mergia, J. A. van Franeker, A. J. Murk, and A. A. Koelmans. 2013. Plastic in North Sea fish. Environmental Science & Technology 47:8818–8824.

Foley, C. J., Z. S. Feiner, T. D. Malinich, and T. O. Höök. 2018. A meta-analysis of the effects of exposure to microplastics on fish and aquatic invertebrates. Science of The Total Environment 631–632:550–559.

Fournier, D. A., H. J. Skaug, J. Ancheta, J. Ianelli, A. Magnusson, M. N. Maunder, A. Nielsen, and J. Sibert. 2012. AD Model Builder: using automatic differentiation for statistical

inference of highly parameterized complex nonlinear models. Optim. Methods Softw. 27:233–249.

Gale, K. S. P., J.-F. Hamel, and A. Mercier. 2013. Trophic ecology of deep-sea *Asteroidea* (Echinodermata) from eastern Canada. Deep Sea Research Part I: Oceanographic Research Papers 80:25–36.

Garcia, F., A. R. de Carvalho, L. Riem-Galliano, L. Tudesque, M. Albignac, A. ter Halle, and J. Cucherousset. 2021. Stable isotope insights into microplastic contamination within freshwater food webs. Environmental Science & Technology 55:1024–1035.

Garcia-Reyero, N., and E. J. Perkins. 2011. Systems biology: leading the revolution in ecotoxicology. Environmental Toxicology and Chemistry 30:265–273.

GESAMP. 2015. Sources, fate and effects of microplastics in the marine environment: a global assessment. Page 96. IMO/FAO/UNESCO-IOC/UNIDO/WMO/IAEA/UN/UNEP/UNDP Joint Group of Experts on the Scientific Aspects of Marine Environmental Protection.

GESAMP. 2016. Sources, fate and effects of microplastics in the marine environment: part two of a global assessment. Page 220. IMO/FAO/UNESCO-IOC/UNIDO/WMO/IAEA/UN/ UNEP/UNDP Joint Group of Experts on the Scientific Aspects of Marine Environmental Protection.

GESAMP. 2019. Guidelines or the monitoring and assessment of plastic litter and microplastics in the ocean (Kershaw P.J., Turra A. and Galgani F. editors). Page 130. (IMO/FAO/UNESCO-IOC/UNIDO/WMO/IAEA/UN/UNEP/UNDP/ISA Joint Group of Experts on the Scientific Aspects of Marine Environmental Protection).

Gianguzza, P., F. Di Trapani, C. Bonaviri, D. Agnetta, S. Vizzini, and F. Badalamenti. 2016. Size-dependent predation of the mesopredator *Marthasterias glacialis* (L.) (*Asteroidea*). Marine Biology 163:65.

Gies, E. A., J. L. LeNoble, M. Noël, A. Etemadifar, F. Bishay, E. R. Hall, and P. S. Ross. 2018. Retention of microplastics in a major secondary wastewater treatment plant in Vancouver, Canada. Marine Pollution Bulletin 133:553–561.

Gobas, F. A. P. C., D. C. G. Muir, and D. Mackay. 1988. Dynamics of dietary bioaccumulation and faecal elimination of hydrophobic organic chemicals in fish. Chemosphere 17:943–962.

Gordon, C. D. 1963. Aspects of the life-history of Cymatogaster aggregata Gibbons. MSc Thesis, The University of British Columbia, British Columbia, Canada.

Gouin, T. 2020. Towards improved understanding of the ingestion and trophic transfer of microplastic particles – Critical review and implications for future research. Environmental Toxicology and Chemistry 39:1119–1137.

Government of Canada, F. and O. S. S. 2018. Consumption. http://www.dfo-mpo.gc.ca/stats/commercial/consumption-eng.htm.

Graham, P., L. Palazzo, G. Andrea de Lucia, T. C. Telfer, M. Baroli, and S. Carboni. 2019. Microplastics uptake and egestion dynamics in Pacific oysters, *Magallana gigas* (Thunberg, 1793), under controlled conditions. Environmental Pollution 252:742–748.

Green, D. S. 2016. Effects of microplastics on European flat oysters, *Ostrea edulis* and their associated benthic communities. Environmental Pollution 216:95–103.

Green, D. S., B. Boots, N. E. O'Connor, and R. Thompson. 2017. Microplastics affect the ecological functioning of an important biogenic habitat. Environmental Science & Technology 51:68–77.

Green, P., and C. J. MacLeod. 2016. SIMR: an R package for power analysis of generalized linear mixed models by simulation. Methods in Ecology and Evolution 7:493–498.

Grigorakis, S., S. A. Mason, and K. G. Drouillard. 2017. Determination of the gut retention of plastic microbeads and microfibers in goldfish (Carassius auratus). Chemosphere 169:233–238.

Güven, O., K. Gökdağ, B. Jovanović, and A. E. Kıdeyş. 2017. Microplastic litter composition of the Turkish territorial waters of the Mediterranean Sea, and its occurrence in the gastrointestinal tract of fish. Environmental Pollution 223:286–294.

Hale, R. C., M. E. Seeley, M. J. L. Guardia, L. Mai, and E. Y. Zeng. 2020. A global perspective on microplastics. J. Geophys. Res 125:e2018JC014719.

Hannah, R. W., and P. S. Rankin. 2011. Site fidelity and movement of eight species of Pacific rockfish at a high-relief rocky reef on the Oregon coast. North American Journal of Fisheries Management 31:483–494.

Harris, P. T. 2020. The fate of microplastic in marine sedimentary environments: A review and synthesis. Marine Pollution Bulletin 158:111398.

Hartig, F. 2020. DHARMa: residual diagnostics for hierarchical (multi-level/mixed) regression models.

Hartmann, N. B., T. Hüffer, R. C. Thompson, M. Hassellöv, A. Verschoor, A. E. Daugaard, S. Rist, T. Karlsson, N. Brennholt, M. Cole, M. P. Herrling, M. C. Hess, N. P. Ivleva, A. L. Lusher, and M. Wagner. 2019. Are we speaking the same language? Recommendations

for a definition and categorization framework for plastic debris. Environmental Science & Technology 53:1039–1047.

Herzke, D., T. Anker-Nilssen, T. H. Nøst, A. Götsch, S. Christensen-Dalsgaard, M. Langset, K. Fangel, and A. A. Koelmans. 2016. Negligible impact of ingested microplastics on tissue concentrations of persistent organic pollutants in northern fulmars off coastal Norway. Environmental Science & Technology 50:1924–1933.

Hidalgo-Ruz, V., L. Gutow, R. C. Thompson, and M. Thiel. 2012. Microplastics in the marine environment: a review of the methods used for identification and quantification. Environmental Science & Technology 46:3060–3075.

Hildenbrand, K., A. Gladics, and B. Eder. 2011. Crab tagging study: adult male Dungeness crab (*Metacarcinus magister*) movements near Reedsport, Oregon from a fisheries collaborative mark-recapture study. Pages 1–21. Oregon Wave Energy Trust, Portland, Oregon.

Hussey, N. E., M. A. MacNeil, B. C. McMeans, J. A. Olin, S. F. J. Dudley, G. Cliff, S. P. Wintner, S. T. Fennessy, and A. T. Fisk. 2014. Rescaling the trophic structure of marine food webs. Ecology Letters 17:239–250.

Jacob, H., M. Besson, P. W. Swarzenski, D. Lecchini, and M. Metian. 2020. Effects of virgin micro- and nanoplastics on fish: trends, meta-analysis, and perspectives. Environmental Science & Technology 54:4733–4745.

Jâms, I. B., F. M. Windsor, T. Poudevigne-Durance, S. J. Ormerod, and I. Durance. 2020. Estimating the size distribution of plastics ingested by animals. Nature Communications 11:1–7.

Jemec, A., P. Horvat, U. Kunej, M. Bele, and A. Kržan. 2016. Uptake and effects of microplastic textile fibers on freshwater crustacean *Daphnia magna*. Environmental Pollution 219:201–209.

Jewett, S. C., and H. M. Feder. 1980. Autumn food of adult starry flounders, *Platichthys stellatus*, from the northeastern Bering Sea and the southeastern Chukchi Sea1. ICES Journal of Marine Science 39:7–14.

Johnston, A. S. A., M. E. Hodson, P. Thorbek, T. Alvarez, and R. M. Sibly. 2014. An energy budget agent-based model of earthworm populations and its application to study the effects of pesticides. Ecological Modelling 280:5–17.

Jovanović, B. 2017. Ingestion of microplastics by fish and its potential consequences from a physical perspective. Integrated Environmental Assessment and Management 13:510–515.

Jovanović, B., K. Gökdağ, O. Güven, Y. Emre, E. M. Whitley, and A. E. Kideys. 2018. Virgin microplastics are not causing imminent harm to fish after dietary exposure. Marine Pollution Bulletin 130:123–131.

Jung, J.-W., J.-W. Park, S. Eo, J. Choi, Y. K. Song, Y. Cho, S. H. Hong, and W. J. Shim. 2021. Ecological risk assessment of microplastics in coastal, shelf, and deep sea waters with a consideration of environmentally relevant size and shape. Environmental Pollution 270:116217.

Kang, J.-H., O. Y. Kwon, K.-W. Lee, Y. K. Song, and W. J. Shim. 2015. Marine neustonic microplastics around the southeastern coast of Korea. Marine Pollution Bulletin 96:304–312.

Kazmiruk, T. N., V. D. Kazmiruk, and L. I. Bendell. 2018. Abundance and distribution of microplastics within surface sediments of a key shellfish growing region of Canada. PLOS ONE 13:e0196005.

Kelly, B. C., M. G. Ikonomou, J. D. Blair, A. E. Morin, and F. A. P. C. Gobas. 2007. Food web-specific biomagnification of persistent organic pollutants. Science 317:236–239.

Khan, F. R. 2018. Ecotoxicology in the Anthropocene: are we listening to nature's scream? Environmental Science & Technology 52:10227–10229.

Kim, J., D. G. Poirier, P. A. Helm, M. Bayoumi, and C. M. Rochman. 2020. No evidence of spherical microplastics (10–300 μm) translocation in adult rainbow trout (*Oncorhynchus mykiss*) after a two-week dietary exposure. PLOS ONE 15:e0239128.

Kim, S. W., D. Kim, Y. Chae, and Y.-J. An. 2018. Dietary uptake, biodistribution, and depuration of microplastics in the freshwater diving beetle *Cybister japonicus*: Effects on predacious behavior. Environmental Pollution 242:839–844.

Klok, C., M. Holmstrup, and C. Damgaard. 2007. Extending a combined dynamic energy budget matrix population model with a Bayesian approach to assess variation in the intrinsic rate of population increase. An example in the earthworm *Dendrobaena octaedra*. Environmental Toxicology and Chemistry 26:2383–2388.

Koelmans, A. A., A. Bakir, G. A. Burton, and C. R. Janssen. 2016. Microplastic as a vector for chemicals in the aquatic environment. Critical review and model-supported re-interpretation of empirical studies. Environmental Science & Technology 50:3315–3326.

Koelmans, A. A., E. Besseling, A. Wegner, and E. M. Foekema. 2013. Plastic as a carrier of POPs to aquatic organisms: a model analysis. Environmental Science & Technology 47:7812–7820.

Koelmans, A. A., M. Kooi, K. L. Law, and E. van Sebille. 2017. All is not lost: deriving a top-down mass budget of plastic at sea. Environmental Research Letters 12:114028.

Koelmans, A. A., P. E. Redondo Hasselerharm, N. H. Mohamed Nor, and M. Kooi. 2020. Solving the non-alignment of methods and approaches used in microplastic research in order to consistently characterize risk. Environmental Science & Technology 54:12307–12315.

Kooi, M., J. Reisser, B. Slat, F. F. Ferrari, M. S. Schmid, S. Cunsolo, R. Brambini, K. Noble, L.-A. Sirks, T. E. W. Linders, R. I. Schoeneich-Argent, and A. A. Koelmans. 2016. The effect of particle properties on the depth profile of buoyant plastics in the ocean. Scientific Reports 6:33882.

Koongolla, J. B., L. Lin, Y.-F. Pan, C.-P. Yang, D.-R. Sun, S. Liu, X.-R. Xu, D. Maharana, J.-S. Huang, and H.-X. Li. 2020. Occurrence of microplastics in gastrointestinal tracts and gills of fish from Beibu Gulf, South China Sea. Environmental Pollution 258:113734.

Kowalski, N., A. M. Reichardt, and J. J. Waniek. 2016. Sinking rates of microplastics and potential implications of their alteration by physical, biological, and chemical factors. Marine Pollution Bulletin 109:310–319.

Kramm, J., C. Völker, and M. Wagner. 2018. Superficial or substantial: why care about microplastics in the Anthropocene? Environmental Science & Technology 52:3336–3337.

Kravitz, M., and W. Pearcy. 1976. Food of five species of cooccuring flatfishes on Oregon's continental shelf. Fishery Bulletin 74:984–980.

Kvale, K., A. E. F. Prowe, C.-T. Chien, A. Landolfi, and A. Oschlies. 2020. The global biological microplastic particle sink. Scientific Reports 10:16670.

Layman, C. A., M. S. Araujo, R. Boucek, C. M. Hammerschlag-Peyer, E. Harrison, Z. R. Jud, P. Matich, A. E. Rosenblatt, J. J. Vaudo, L. A. Yeager, D. M. Post, and S. Bearhop. 2012. Applying stable isotopes to examine food-web structure: an overview of analytical tools. Biological Reviews 87:545–562.

Lee, H., M. Ju, and Y. Kim. 2020. Estimation of emission of tire wear particles (TWPs) in Korea. Waste Management 108:154–159.

Lenz, R., K. Enders, C. A. Stedmon, D. M. A. Mackenzie, and T. G. Nielsen. 2015. A critical assessment of visual identification of marine microplastic using Raman spectroscopy for analysis improvement. Marine Pollution Bulletin 100:82–91.

Leslie, H. A., S. H. Brandsma, M. J. M. van Velzen, and A. D. Vethaak. 2017. Microplastics en route: Field measurements in the Dutch river delta and Amsterdam canals, wastewater treatment plants, North Sea sediments and biota. Environment International 101:133–142.

Lewbart, G. A., and C. Mosley. 2012. Clinical anesthesia and analgesia in invertebrates. Journal of Exotic Pet Medicine 21:59–70.

Li, J., X. Qu, L. Su, W. Zhang, D. Yang, P. Kolandhasamy, D. Li, and H. Shi. 2016. Microplastics in mussels along the coastal waters of China. Environmental Pollution 214:177–184.

Li, J., D. Yang, L. Li, K. Jabeen, and H. Shi. 2015. Microplastics in commercial bivalves from China. Environmental Pollution 207:190–195.

Liaw, A., and M. Wiener. 2002. Classification and regression by randomForest 2:6.

Lima, A. R. A., G. V. B. Ferreira, A. P. W. Barrows, K. S. Christiansen, G. Treinish, and M. C. Toshack. 2021. Global patterns for the spatial distribution of floating microfibers: Arctic Ocean as a potential accumulation zone. Journal of Hazardous Materials 403:123796.

Liu, J., Y. Yang, J. Ding, B. Zhu, and W. Gao. 2019. Microfibers: a preliminary discussion on their definition and sources. Environmental Science and Pollution Research 26:29497–29501.

Löder, M. G. J., and G. Gerdts. 2015. Methodology used for the detection and identification of microplastics—a critical appraisal. Pages 201–227 *in* M. Bergmann, L. Gutow, and M. Klages, editors. Marine Anthropogenic Litter. Springer International Publishing.

Lourenço, P. M., C. Serra-Gonçalves, J. L. Ferreira, T. Catry, and J. P. Granadeiro. 2017. Plastic and other microfibers in sediments, macroinvertebrates and shorebirds from three intertidal wetlands of southern Europe and west Africa. Environmental Pollution 231:123–133.

Lusher, A. L., P. C. H. Hollman, and J. J. Mendoza-Hill. 2017. Microplastics in fisheries and aquaculture: status of knowledge on their occurrence and implications for aquatic organisms and food safety. FAO Fisheries and Aquaculture Technical Paper, Food and Agriculture Organization of the United Nations, Rome, Italy.

Lusher, A. L., V. Tirelli, I. O'Connor, and R. Officer. 2015. Microplastics in Arctic polar waters: the first reported values of particles in surface and sub-surface samples. Scientific Reports 5:14947.

Lusher, A., K. Munno, L. Hermabessiere, and S. Carr. 2020. Isolation and extraction of microplastics from environmental samples: an evaluation of practical approaches and recommendations for further harmonisation. Applied Spectroscopy 74:1049–1065.

Mathalon, A., and P. Hill. 2014. Microplastic fibers in the intertidal ecosystem surrounding Halifax Harbor, Nova Scotia. Marine Pollution Bulletin 81:69–79.

Michels, J., A. Stippkugel, M. Lenz, K. Wirtz, and A. Engel. 2018. Rapid aggregation of biofilm-covered microplastics with marine biogenic particles. Proc. R. Soc. B 285:20181203.

Miller, B. S. 1967. Stomach contents of adult starry flounder and sand sole in East Sound Orcas Island Washington. Journal of the Fisheries Research Board of Canada 24:2515–2526.

Miller, M. E., M. Hamann, and F. J. Kroon. 2020. Bioaccumulation and biomagnification of microplastics in marine organisms: A review and meta-analysis of current data. PLOS ONE 15:e0240792.

Miller, M. E., F. J. Kroon, and C. A. Motti. 2017. Recovering microplastics from marine samples: A review of current practices. Marine Pollution Bulletin 123:6–18.

Mo, C., and B. Neilson. 1994. Standardization of oyster soft tissue dry weight measurements. Water Research 28:243–246.

Mohsen, M., Q. Wang, L. Zhang, L. Sun, C. Lin, and H. Yang. 2019. Microplastic ingestion by the farmed sea cucumber *Apostichopus japonicus* in China. Environmental Pollution 245:1071–1078.

Mohsen, M., L. Zhang, L. Sun, C. Lin, Q. Wang, and H. Yang. 2020. Microplastic fibers transfer from the water to the internal fluid of the sea cucumber *Apostichopus japonicus*. Environmental Pollution 257:113606.

Moser, M. L., M. S. Myers, J. E. West, S. M. O'Neill, and B. J. Burke. 2013. English sole spawning migration and evidence for feeding site fidelity in Puget Sound, U.S.A., with implications for contaminant exposure. Northwest Science 87:317–325.

Muller, E. B., R. M. Nisbet, and H. A. Berkley. 2010. Sublethal toxicant effects with dynamic energy budget theory: model formulation. Ecotoxicology 19:48–60.

Muller, E. B., C. W. Osenberg, R. J. Schmitt, S. J. Holbrook, and R. M. Nisbet. 2009. Sublethal toxicant effects with dynamic energy budget theory: application to mussel outplants. Ecotoxicology 19:38.

Munno, K., H. De Frond, B. O'Donnell, and C. M. Rochman. 2020. Increasing the accessibility for characterizing microplastics: introducing new application-based and spectral libraries of plastic particles (SLoPP and SLoPP-E). Analytical Chemistry 92:2443–2451.

Murano, C., C. Agnisola, D. Caramiello, I. Castellano, R. Casotti, I. Corsi, and A. Palumbo. 2020. How sea urchins face microplastics: uptake, tissue distribution and immune system response. Environmental Pollution 264:114685.

Murie, D. J. 1995. Comparative feeding ecology of two sympatric rockfish congeners, *Sebastes caurinus* (copper rockfish) and *S. maliger* (quillback rockfish). Marine Biology 124:341–353.

Nakamura, Y. 2001. Filtration rates of the Manila clam, *Ruditapes philippinarum*: dependence on prey items including bacteria and picocyanobacteria. Journal of Experimental Marine Biology and Ecology 266:181–192.

Napper, I. E., B. F. R. Davies, H. Clifford, S. Elvin, H. J. Koldewey, P. A. Mayewski, K. R. Miner, M. Potocki, A. C. Elmore, A. P. Gajurel, and R. C. Thompson. 2020. Reaching new heights in plastic pollution—preliminary findings of microplastics on Mount Everest. One Earth 3:621–630.

Nelms, S. E., T. S. Galloway, B. J. Godley, D. S. Jarvis, and P. K. Lindeque. 2018. Investigating microplastic trophic transfer in marine top predators. Environmental Pollution 238:999–1007.

Nisbet, R. M., E. B. Muller, K. Lika, and S. a. L. M. Kooijman. 2000. From molecules to ecosystems through dynamic energy budget models. Journal of Animal Ecology 69:913–926.

Orcutt, H. G. 1950. The life history of the starry flounder, *Platichthys stellatus* (Pallas). State of California Department of Natural Resources Division of Fish and Game Bureau of Marine Fishes, Sacramento, California.

Ory, N. C., C. Gallardo, M. Lenz, and M. Thiel. 2018. Capture, swallowing, and egestion of microplastics by a planktivorous juvenile fish. Environmental Pollution 240:566–573.

Ory, N. C., P. Sobral, J. L. Ferreira, and M. Thiel. 2017. Amberstripe scad *Decapterus muroadsi* (*Carangidae*) fish ingest blue microplastics resembling their copepod prey along the coast of Rapa Nui (Easter Island) in the South Pacific subtropical gyre. Science of The Total Environment 586:430–437.

Pabortsava, K., and R. S. Lampitt. 2020. High concentrations of plastic hidden beneath the surface of the Atlantic Ocean. Nature Communications 11:4073.

Pawlowicz, R., O. Riche, and M. Halverson. 2007. The circulation and residence time of the strait of Georgia using a simple mixing-box approach. Atmosphere-Ocean 45:173–193.

Pellini, G., A. Gomiero, T. Fortibuoni, C. Ferrà, F. Grati, N. Tassetti, P. Polidori, G. Fabi, and G. Scarcella. 2018. Characterization of microplastic litter in the gastrointestinal tract of *Solea solea* from the Adriatic Sea. Environmental Pollution 234:943–952.

Peñalver, R., N. Arroyo-Manzanares, I. López-García, and M. Hernández-Córdoba. 2020. An overview of microplastics characterization by thermal analysis. Chemosphere 242:125170.

Phuong, N. N., L. Poirier, Q. T. Pham, F. Lagarde, and A. Zalouk-Vergnoux. 2018. Factors influencing the microplastic contamination of bivalves from the French Atlantic coast: Location, season and/or mode of life? Marine Pollution Bulletin 129:664–674.

Piarulli, S., B. Vanhove, P. Comandini, S. Scapinello, T. Moens, H. Vrielinck, G. Sciutto, S. Prati, R. Mazzeo, A. M. Booth, C. Van Colen, and L. Airoldi. 2020. Do different habits affect microplastics contents in organisms? A trait-based analysis on salt marsh species. Marine Pollution Bulletin 153:110983.

Pinheiro, L. M., J. A. Ivar do Sul, and M. F. Costa. 2020. Uptake and ingestion are the main pathways for microplastics to enter marine benthos: A review. Food Webs 24:e00150.

Piscopo, M., M. Ricciardiello, G. Palumbo, and J. Troisi. 2016. Selectivity of metal bioaccumulation and its relationship with glutathione S-transferase levels in gonadal and gill tissues of *Mytilus galloprovincialis* exposed to Ni (II), Cu (II) and Cd (II). Rendiconti Lincei 27:737–748.

Plummer, M. 2003. JAGS: A program for analysis of Bayesian graphical models using Gibbs sampling.

Primpke, S., S. H. Christiansen, W. Cowger, H. De Frond, A. Deshpande, M. Fischer, E. Holland, M. Meyns, B. A. O'Donnell, B. Ossmann, M. Pittroff, G. Sarau, B. M. Scholz-Böttcher, and K. Wiggin. 2020. Critical assessment of analytical methods for the harmonized and cost efficient analysis of microplastics. Applied Spectroscopy 74:1012–1047.

Prosnier, L., M. Loreau, and F. D. Hulot. 2015. Modeling the direct and indirect effects of copper on phytoplankton–zooplankton interactions. Aquatic Toxicology 162:73–81.

Provencher, J. F., G. A. Covernton, R. C. Moore, D. A. Horn, J. L. Conkle, and A. L. Lusher. 2020. Proceed with caution: the need to raise the publication bar for microplastics research. Science of The Total Environment 748:141426.

QGIS Development Team. 2018. QGIS Geographic Information System. Open Source Geospatial Foundation.

R Core Team. 2015. R: A language and environment for statistical computing. R Foundation for Statistical Computing, Vienna, Austria.

R Core Team. 2020. R: a language and environment for statistical computing. R Foundation for Statistical Computing, Vienna, Austria.

Raap, M. 2019. Anthropogenic modifications and their impacts on shellfish physiology. MSc Thesis, University of Victoria, Victoria.

Renzi, M., C. Guerranti, and A. Blašković. 2018. Microplastic contents from maricultured and natural mussels. Marine Pollution Bulletin 131:248–251.

Roch, S., C. Friedrich, and A. Brinker. 2020. Uptake routes of microplastics in fishes: practical and theoretical approaches to test existing theories. Scientific Reports 10:1–12.

Rochman, C. M., C. Brookson, J. Bikker, N. Djuric, A. Earn, K. Bucci, S. Athey, A. Huntington, H. McIlwraith, K. Munno, H. D. Frond, A. Kolomijeca, L. Erdle, J. Grbic, M. Bayoumi, S. B. Borrelle, T. Wu, S. Santoro, L. M. Werbowski, X. Zhu, R. K. Giles, B. M. Hamilton, C. Thaysen, A. Kaura, N. Klasios, L. Ead, J. Kim, C. Sherlock, A. Ho, and C. Hung. 2019. Rethinking microplastics as a diverse contaminant suite. Environmental Toxicology and Chemistry 38:703–711.

Rochman, C. M., A. Tahir, S. L. Williams, D. V. Baxa, R. Lam, J. T. Miller, F.-C. Teh, S. Werorilangi, and S. J. Teh. 2015. Anthropogenic debris in seafood: plastic debris and

fibers from textiles in fish and bivalves sold for human consumption. Scientific Reports 5:14340.

Ryberg, M. W., M. Z. Hauschild, F. Wang, S. Averous-Monnery, and A. Laurent. 2019. Global environmental losses of plastics across their value chains. Resources, Conservation and Recycling 151:104459.

Santana, M. F. M., F. T. Moreira, and A. Turra. 2017. Trophic transference of microplastics under a low exposure scenario: insights on the likelihood of particle cascading along marine food-webs. Marine Pollution Bulletin 121:154–159.

Schoof, R. A., and J. DeNike. 2017. Microplastics in the context of regulation of commercial shellfish aquaculture operations. Integrated Environmental Assessment and Management 13:522–527.

Sedlak, D. L. 2018. Disruptive environmental research. Environmental Science & Technology 52:8059–8060.

Setälä, O., K. Magnusson, M. Lehtiniemi, and F. Norén. 2016a. Distribution and abundance of surface water microlitter in the Baltic Sea: A comparison of two sampling methods. Marine Pollution Bulletin 110:177–183.

Setälä, O., J. Norkko, and M. Lehtiniemi. 2016b. Feeding type affects microplastic ingestion in a coastal invertebrate community. Marine Pollution Bulletin 102:95–101.

Sherwood, G. D., J. Kovecses, A. Hontela, and J. B. Rasmussen. 2002. Simplified food webs lead to energetic bottlenecks in polluted lakes. Canadian Journal of Fisheries and Aquatic Sciences 59:1–5.

Singer, M. M. 1985. Food habits of juvenile rockfishes (*Sebastes*) in a central California kelp forest. Fishery Bulletin 83:531–542.

Singh, R. P., S. Mishra, and A. P. Das. 2020. Synthetic microfibers: pollution toxicity and remediation. Chemosphere 257:127199.

Skaug, H., D. Fournier, B. Bolker, A. Magnusson, and A. Nielsen. 2016. Generalized linear mixed models using "AD Model Builder."

Skinner, M. K., M. Manikkam, and C. Guerrero-Bosagna. 2011. Epigenetic transgenerational actions of endocrine disruptors. Reproductive Toxicology (Elmsford, N.Y.) 31:337–343.

Song, Y. K., S. H. Hong, M. Jang, G. M. Han, M. Rani, J. Lee, and W. J. Shim. 2015. A comparison of microscopic and spectroscopic identification methods for analysis of microplastics in environmental samples. Marine Pollution Bulletin 93:202–209.

de Souza Machado, A. A., C. M. Wood, and W. Kloas. 2019. Novel concepts for novel entities: updating ecotoxicology for a sustainable Anthropocene. Environmental Science & Technology 53:4680–4682.

Stevens, B. G., D. A. Armstrong, and R. Cusimano. 1982. Feeding habits of the Dungeness crab *Cancer magister* as determined by the index of relative importance. Marine Biology 72:135–145.

Stock, F., V. K. B. Narayana, C. Scherer, M. G. J. Löder, N. Brennholt, C. Laforsch, and G. Reifferscheid. 2020. Pitfalls and limitations in microplastic analyses. Pages 1–30 *in* F. Stock, G. Reifferscheid, N. Brennholt, and E. Kostianaia, editors. Plastics in the Aquatic Environment - Part I: Current Status and Challenges. Springer Nature Switzerland AG, Berlin, Heidelberg.

Stone, R. P., and C. E. O'Clair. 2002. Behavior of female Dungeness crabs, *Cancer magister*, in a glacial southeast Alaska estuary: homing, brooding-site fidelity, seasonal movements, and habitat use. Journal of Crustacean Biology 22:481–492.

Su, Y.-S., and M. Yajima. 2020. R2jags: using R to run “JAGS.”

Sun, D., J. Wang, S. Xie, H. Tang, C. Zhang, G. Xu, J. Zou, and A. Zhou. 2021. Characterization and spatial distribution of microplastics in two wild captured economic freshwater fish from north and west rivers of Guangdong province. Ecotoxicology and Environmental Safety 207:111555.

Sun, X., Q. Li, M. Zhu, J. Liang, S. Zheng, and Y. Zhao. 2017. Ingestion of microplastics by natural zooplankton groups in the northern South China Sea. Marine Pollution Bulletin 115:217–224.

Sutton, R., S. A. Mason, S. K. Stanek, E. Willis-Norton, I. F. Wren, and C. Box. 2016. Microplastic contamination in the San Francisco Bay, California, USA. Marine Pollution Bulletin 109:230–235.

Thompson, R. C., Y. Olsen, R. P. Mitchell, A. Davis, S. J. Rowland, A. W. John, D. McGonigle, and A. E. Russell. 2004. Lost at sea: where is all the plastic? Science 304:838–838.

Thomson, R. E. 1981. Oceanography of the British Columbia coast. Dept. of Fisheries and Oceans, Ottawa.

Tian, Z., H. Zhao, K. T. Peter, M. Gonzalez, J. Wetzel, C. Wu, X. Hu, J. Prat, E. Mudrock, R. Hettinger, A. E. Cortina, R. G. Biswas, F. V. C. Kock, R. Soong, A. Jenne, B. Du, F. Hou, H. He, R. Lundeen, A. Gilbreath, R. Sutton, N. L. Scholz, J. W. Davis, M. C. Dodd, A. Simpson, J. K. McIntyre, and E. P. Kolodziej. 2021. A ubiquitous tire rubber–derived chemical induces acute mortality in coho salmon. Science 371:185–189.

Toole, C. L. 1980. Intertidal recruitment and feeding in relation to optimal utilization of nursery areas by juvenile English sole (*Parophrys vetulus*: *Pleuronectidae*). Environmental Biology of Fishes 5:383–390.

Torre, M., N. Digka, A. Anastasopoulou, C. Tsangaris, and C. Mytilineou. 2016. Anthropogenic microfibres pollution in marine biota. A new and simple methodology to minimize airborne contamination. Marine Pollution Bulletin 113:55–61.

Van Melkebeke, M., C. R. Janssen, and S. De Meester. 2020. Characteristics and sinking behavior of typical microplastics including the potential effect of biofouling: implications for remediation. Environmental Science & Technology 54:668–8680.

Vinay Kumar, B. N., L. A. Löschel, H. K. Imhof, M. G. J. Löder, and C. Laforsch. 2020. Analysis of microplastics of a broad size range in commercially important mussels by combining FTIR and Raman spectroscopy approaches. Environmental Pollution:116147.

Walkinshaw, C., P. K. Lindeque, R. Thompson, T. Tolhurst, and M. Cole. 2020. Microplastics and seafood: lower trophic organisms at highest risk of contamination. Ecotoxicology and Environmental Safety 190:110066.

Wang, J., Z. Tan, J. Peng, Q. Qiu, and M. Li. 2016. The behaviors of microplastics in the marine environment. Marine Environmental Research 113:7–17.

Ward, E. J., and S. E. Shumway. 2004. Separating the grain from the chaff: particle selection in suspension- and deposit-feeding bivalves. Journal of Experimental Marine Biology and Ecology 300:83–130.

Ward, J. E., M. Rosa, and S. E. Shumway. 2019. Capture, ingestion, and egestion of microplastics by suspension-feeding bivalves: a 40-year history. Anthropocene Coasts 2:39–49.

Watanabe, K., F. Y. Bois, and L. Zeise. 1992. Interspecies extrapolation: a reexamination of acute toxicity data. Risk Analysis 12:301–310.

Watts, A. J. R., M. A. Urbina, S. Corr, C. Lewis, and T. S. Galloway. 2015. Ingestion of plastic microfibers by the crab *Carcinus maenas* and its effect on food consumption and energy balance. Environmental Science & Technology 49:14597–14604.

Welden, N. A., B. Abylkhani, and L. M. Howarth. 2018. The effects of trophic transfer and environmental factors on microplastic uptake by plaice, *Pleuronectes plastessa*, and spider crab, Maja squinado. Environmental Pollution 239:351–358.

Welden, N. A., and P. R. Cowie. 2017. Degradation of common polymer ropes in a sublittoral marine environment. Marine Pollution Bulletin 118:248–253.

Wentworth, C. K. 1922. A scale of grade and class terms for clastic sediments. The Journal of Geology 30:377–392.

Wieczorek, A. M., L. Morrison, P. L. Croot, A. L. Allcock, E. MacLoughlin, O. Savard, H. Brownlow, and T. K. Doyle. 2018. Frequency of microplastics in mesopelagic fishes from the northwest Atlantic. Frontiers in Marine Science 5:127.

Woodall, L. C., C. Gwinnett, M. Packer, R. C. Thompson, L. F. Robinson, and G. L. J. Paterson. 2015. Using a forensic science approach to minimize environmental contamination and to identify microfibres in marine sediments. Marine Pollution Bulletin 95:40–46.

Woodall, L. C., A. Sanchez-Vidal, M. Canals, G. L. J. Paterson, R. Coppock, V. Sleight, A. Calafat, A. D. Rogers, B. E. Narayanaswamy, and R. C. Thompson. 2014. The deep sea is a major sink for microplastic debris. Royal Society Open Science 1:140317.

Wright, S. L., and F. J. Kelly. 2017. Plastic and human health: a micro issue? Environmental Science & Technology 51:6634–6647.

Xu, X., C. Y. Wong, N. F. Y. Tam, H.-S. Lo, and S.-G. Cheung. 2020. Microplastics in invertebrates on soft shores in Hong Kong: influence of habitat, taxa and feeding mode. Science of The Total Environment 715:136999.

Yang, F., T. Yao, Z. Huo, Y. Zhang, X. Yan, and G. Zhang. 2010. Effects of starvation on growth, survival, and body biochemical composition among different sizes of Manila clam *Ruditapes philippinarum*. Acta Ecologica Sinica 30:135–140.

Zeytin, S., G. Wagner, N. Mackay-Roberts, G. Gerdts, E. Schuirmann, S. Klockmann, and M. Slater. 2020. Quantifying microplastic translocation from feed to the fillet in European sea bass *Dicentrarchus labrax*. Marine Pollution Bulletin 156:111210.

Zhang, F., X. Wang, J. Xu, L. Zhu, G. Peng, P. Xu, and D. Li. 2019a. Food-web transfer of microplastics between wild caught fish and crustaceans in East China Sea. Marine Pollution Bulletin 146:173–182.

Zhang, K., X. Xiong, H. Hu, C. Wu, Y. Bi, Y. Wu, B. Zhou, P. K. S. Lam, and J. Liu. 2017. Occurrence and characteristics of microplastic pollution in Xiangxi Bay of Three Gorges Reservoir, China. Environmental Science & Technology 51:3794–3801.

Zhang, L., Y. Xie, J. Liu, S. Zhong, Y. Qian, and P. Gao. 2020a. An overlooked entry pathway of microplastics into agricultural soils from application of sludge-based fertilizers. Environmental Science & Technology 54:4248–4255.

Zhang, S., J. Wang, X. Liu, F. Qu, X. Wang, X. Wang, Y. Li, and Y. Sun. 2019b. Microplastics in the environment: A review of analytical methods, distribution, and biological effects. TrAC Trends in Analytical Chemistry 111:62–72.

Zhang, X., Y. Leng, X. Liu, K. Huang, and J. Wang. 2019c. Microplastics pollution and risk assessment in an urban river: a case study in the Yongjiang River, Nanning City, south China. Exposure and Health.

Zhang, Z., H. Wu, G. Peng, P. Xu, and D. Li. 2020b. Coastal ocean dynamics reduce the export of microplastics to the open ocean. Science of The Total Environment 713:136634.

Zhu, J., Q. Zhang, Y. Huang, Y. Jiang, J. Li, J. J. Michal, Z. Jiang, Y. Xu, and W. Lan. 2021. Long-term trends of microplastics in seawater and farmed oysters in the Maowei Sea, China. Environmental Pollution:116450.

Zitouni, N., N. Bousserrhine, S. Belbekhouche, O. Missawi, V. Alphonse, I. Boughatass, and M. Banni. 2020. First report on the presence of small microplastics (≤ 3 μm) in tissue of the commercial fish *Serranus scriba* (Linnaeus. 1758) from Tunisian coasts and associated cellular alterations. Environmental Pollution 263:114576.

Appendices

Appendix A: Supplementary Material for Chapter Two

FTIR spectrometry identification

Due to limited equipment time, FTIR spectrometry was only conducted on a sub-sample of fibres. To determine the efficacy of visual identification qualitatively, 29 microfibres were randomly selected from one filter membrane each from the 1-L DB, 10-L DB, 1-L MBREF, and 10-L MBREF samples. The chosen samples were selected as representative of what was commonly found in each sampling type. The fibres were lifted from membranes using metal tweezers and placed on slides, which had been coated in a thin layer of 20% dextrose solution to allow for adhesion. Micro-ATR (attenuated total reflectance) FTIR spectroscopy was conducted on a Cary 660 FTIR spectrometer (Agilent Technologies Inc., Santa Clara, California, USA). Of the 29 fibres analysed, 20 successfully produced spectra whose composition could be identified. The identifications were made using the spectroscopy software Knowitall (Bio-Rad Laboratories Inc., Hercules, California, USA), which searched a library of 250,000 entries to match spectra identifications.

FTIR spectroscopy results

Micro-ATR FTIR spectroscopy demonstrated the presence of a number of fibre types (Fig. A1), including both natural and manufactured materials. The two polyamide (nylon) fibres and the single nylon-rayon blend fibre detected were the only particles that were positively identified as plastic out of the 20 particles tested. Five rayon fibres were detected, as well as nine other cellulosic fibres (which may have been regenerated or modified cellulose), and one cotton fibre. One blue fibre from the 1-L DB sample matched the physical characteristics of blue cotton fibres sourced from the coveralls worn by laboratory workers and was therefore likely due to sample contamination, although spectroscopy identified it as rayon or viscose. The two mineral fibres detected suggest building and/or boating materials like insulation and fibreglass as potential sources.

Of the 20 particles successfully analysed by micro-ATR FTIR spectroscopy, one clear fibre, one turquoise fibre, and one pink fibre were visually identified as putative microplastics. None of them were confirmed to be plastic. FTIR analysis identified the pink fibre as a mineral fibre, while the turquoise and clear fibres were an unknown type of regenerated or modified cellulose, and rayon or viscose, respectively. On the other hand, three clear fibres that were not visually identified as matching the structural requirements for microplastics were false negatives, two being spectroscopically identified as nylon and one as a blend of nylon and rayon. Interestingly, the FTIR analysis did not identify the three microfibres from the subsample that visually matched the physical characteristics of MPs as plastic polymers, although they were still manufactured materials. On the other hand, three microfibres not thought to visually match the known physical characteristics of microplastics were chemically identified as plastic by FTIR. It is hard to make any sound conclusions given the small sample size, but the presence of false positives/negatives supports the currently accepted view that studies must combine chemical identification methods with traditional visual identification (Elert *et al.*, 2017; Shim *et al.*, 2017).

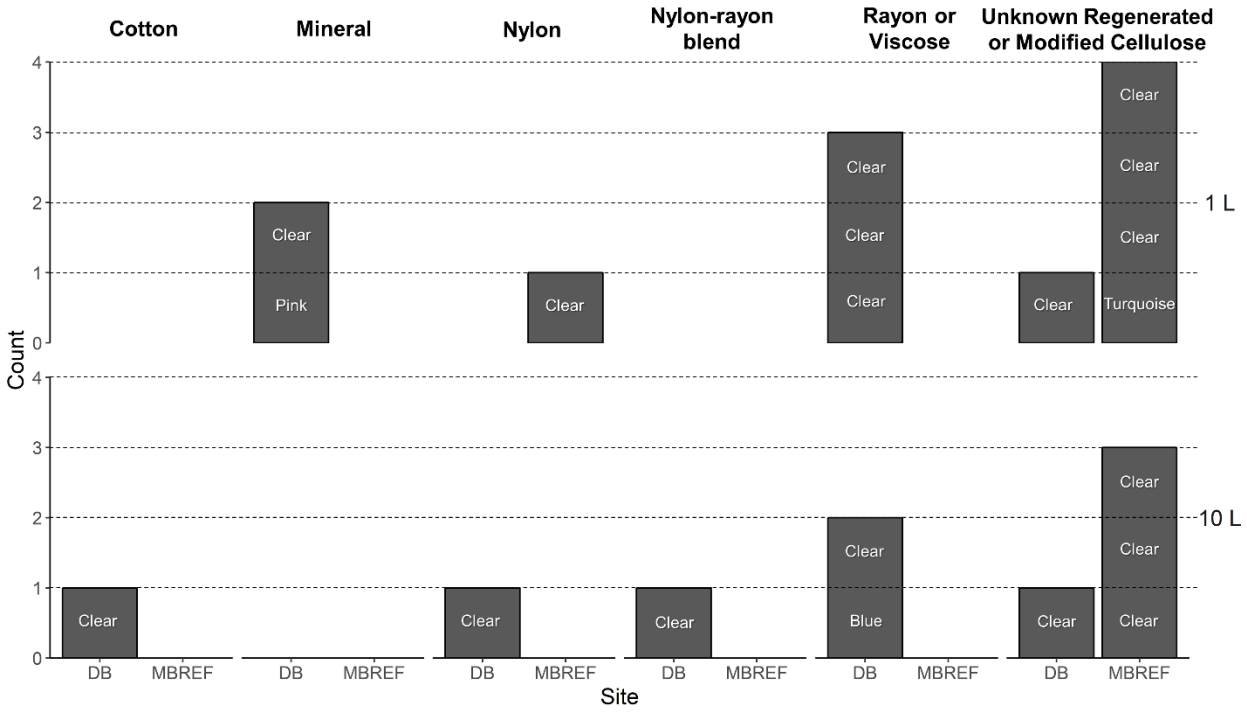

Figure A1: Number and type of particles as identified by micro-ATR FTIR for 20 fibres. Fibres were taken from DB and MBREF 1-L jar and 10-L bucket samples and filtered to a minimum mesh size of 8 and 63 µm, respectively. DB is an active shellfish aquaculture lease and MBREF is an unused stretch of beach located in front of a residential area. The colour of each fibre is indicated by text inset into each box. Site abbreviations are: DB=Deep Bay and MBREF=Mud Bay Reference.

Table A1: Comparison of 45 studies (including the present one, resulting in 58 data points) that measured microplastic particle (MP) concentrations in seawater in various locations, using various sampling methods and mesh sizes.

Study	Location	Sampling Method	Mesh Size (µm)	Mean MP Concentration (particles/ m^3)	Depth	Volume (L)
This study	North-east Pacific	Bucket and sieve	63	910	Surface	10
		Jar sample	8	4,780	Surface	1
Amélineau *et al.*, 2016	Greenland Sea	Vertical tow	500	1.69	Epipelagic	
Aytan *et al.*, 2016	South-east Black Sea	Neuston net	200	900	Surface	
Barrows *et al.*, 2017		Neuston net	335	5	Surface	791,730

	North-west Atlantic Ocean	Jar sample	0.45	5,900	Surface	1
Barrows *et al.*, 2018	Global Oceans	Jar sample	0.45	11,800	Surface	1
Cai *et al.*, 2018	South China Sea	Bongo net	333	0.045	Epipelagic	5,789
		Pump	44	2,569	Surface	3,000
Castillo *et al.*, 2016	Persian Gulf	Plankton tow	120	0.71	Surface	3,499
Castro *et al.*, 2016	South-east Atlantic Ocean	Plankton tow	150	16.4	Surface	
Chae *et al.*, 2015	South-east Yellow Sea	Surface tension	0.75	1,972	Surface	2.57
		Plankton net	330	0.08	Surface	100
		Hand-net	20	6.92	Surface	100
Cincinelli *et al.*, 2017	Ross Sea	Pump	1	0.17	Epipelagic	
Cole *et al.*, 2015	Western English Channel	Plankton net	200	0.27	Surface	69,100
Collignon *et al.*, 2012	North-west Mediterranean Sea	Manta-trawl	333	0.116	Surface	
Courtene-Jones *et al.*, 2017	Rockall Trough, Northeast Atlantic Ocean	Niskin bottles	80	70.8	Abyssalpelagic	10
de Lucia *et al.*, 2014	Mediterranean	Manta-trawl	500	0.15	Surface	614,000
Desforges *et al.*, 2014	North-east Pacific Ocean	Pump	62.5	2,080	Epipelagic	
Di Mauro *et al.*, 2017	Northern Gulf of Mexico	Bongo net	335	6	Epipelagic	45,975
		Neuston net	335	11.1	Surface	23,650

		Niskin bottles	0.7	102,000	Epipelagic	5
Dubaish and Liebezeit, 2013	Southern North Sea	Bottles	1.2	76,000	Surface	6
Frère *et al.*, 2017	Celtic Sea	Manta-trawl	335	0.24	Surface	
Gajšt *et al.*, 2016	Northern Adriatic Sea	Neuston net	300	6.29	Surface	
Gewert *et al.* 2017	North-east Atlantic	Manta-trawl	335	1.37	Surface	
Gray *et al.*, 2018	Western Atlantic Ocean	Sea surface microlayer sampling apparatus	63	18,700	Surface	4
Isobe *et al.*, 2015	Sea of Japan, East China Sea, North-west Pacific Ocean	Neuston net	350	3.7	Surface	
Isobe *et al.*, 2017	Southern Ocean	Neuston net	350	0.031	Surface	415,800
Ivar do Sul *et al.*, 2013	Equatorial Atlantic	Plankton net	300	0.01	Surface	
Ivar do Sul *et al.*, 2014	South-west Atlantic Ocean	Manta-trawl	300	0.028	Surface	938
Kang *et al.*, 2015a	South-west Sea of Japan	Manta-trawl	330	3.71	Surface	
		Hand-net	50	753.77	Surface	100
Kang *et al.*, 2015b	South-west Sea of Japan	Manta-trawl	330	3.72	Surface	
Kanhai *et al.*, 2017	Atlantic Ocean	Pump	250	1.15	Epipelagic	2,000
Kanhai *et al.*, 2018	Arctic Ocean	Pump	250	0.97	Epipelagic	2,000
		Niskin bottles	250	46.5	Full water column	

Kooi *et al.* 2016	North Atlantic	Multi-level trawl	500	0.68	Surface	
		Multi-level trawl	500	0.11	Epipelagic	
Lima *et al.*, 2014	South-west Atlantic Ocean	Plankton net	300	0.022	Epipelagic	350
Lusher *et al.*, 2014	North-east Atlantic Ocean	Pump	250	2.46	Epipelagic	2,000
Lusher *et al.*, 2015	Arctic Ocean	Manta-trawl	333	0.34	Surface	
		Pump	250	2.68	Epipelagic	2,000
Maes *et al.*, 2017	North-east Atlantic Ocean	Manta-trawl	333	0.14	Surface	
Panti *et al.*, 2015	Western Mediterranean Sea	Plankton net	200	0.17	Surface	945
Sadri and Thompson, 2014	North-west English Channel	Manta-net	300	0.028	Surface	278
Setälä *et al.*, 2016	Gulf of Finland	Manta-trawl	333	0.2	Surface	2,000
		Pump	300	0.6	Surface	2,000
		Pump	100	1.3	Surface	2,000
Song *et al.*, 2015	South-west Sea of Japan	Surface-tension	0.75	88,000	Surface	2.6
Tamminga *et al.*, 2018	Baltic sea	Manta trawl	300	0.07	Surface	156,400
		Integrated water sampler	300	1,030	Epipelagic	5
Tang *et al.*, 2018	South China Sea	Manta trawl	330	514.3	Surface	309

Tsang *et al.*, 2017	Northern South China Sea	Plankton tow	153	46.62	Surface	
van der Hal *et al.*, 2017	Eastern Mediterranean	Manta-trawl	333	7.68	Surface	111
Wang *et al.*, 2018	Yellow Sea	Neuston net	333	0.33	Surface	
Zhang *et al.*, 2017	North-west Pacific	Manta-trawl	330	0.33	Surface	
Zhao *et al.*, 2014	North-west Pacific	Pump	32	4,137	Surface	16.6
	North-west Pacific	Neuston net	333	0.167	Surface	158,000
Zhao *et al.*, 2015	North-west Pacific	Pump	330	960.47	Surface	20
Zhu *et al.*, 2018	North Yellow Sea	Niskin bottles	30	545	Surface	25

Table A2. Coefficient estimates, standard error (SE) of coefficients, *z* values, and *p* values for all covariates, including interactions, for Poisson GLM comparing MP concentrations as predicted by site, sampling method, and the interaction between site and sampling method. Coefficient values are set to 0 for the covariates 'DB' and '1-L sample'.

Covariate	**Coefficient**	**SE of Coefficient**	***z* value**	***p* value**
DBREF	-1.792	0.624	-2.87	0.004
MB	-0.325	0.364	-0.894	0.371
MBREF	0.544	0.296	1.834	0.067
SP	-0.251	0.356	-0.705	0.481
SPREF	-0.118	0.344	-0.343	0.732
10-L sample	-9.325	0.364	-25.621	< 0.001
DBREF x 10-L sample	2.661	0.706	3.770	< 0.001
MB x 10-L Sample	1.589	0.481	3.305	0.001
MBREF x 10-L Sample	-0.113	0.463	-0.243	0.808
SP x 10-L Sample	1.448	0.478	3.037	0.002
SPREF x 10-L Sample	-0.049	0.535	-0.092	0.927

Site abbreviations are: DB=Deep Bay, DBREF=Deep Bay Reference, MB=Mud Bay, MBREF=Mud Bay Reference, SP=Ships Point, and SPREF=Ships Point Reference.

Table A3. Coefficient estimates, standard error of coefficients, *z* values, and *p* values for all levels of site, for two Poisson GLMs comparing MP concentrations using (A) the 1-L samples and (B) the 10-L samples. Coefficient values are set to 0 for 'DB'.

Covariate	Coefficient	Std. Error of Coefficient	*z* value	*p value*
(A)				
DBREF	-1.792	0.624	-2.872	0.004
MB	-0.325	0.364	-0.894	0.371
MBREF	0.544	0.296	1.834	0.067
SP	-0.251	0.356	-0.705	0.481
SPREF	-0.118	0.344	-0.343	0.732
(B)				
DBREF	-0.869	0.330	2.630	0.009
MB	1.2637	0.314	4.023	<0.001
MBREF	0.4308	0.356	1.209	0.227
SP	1.1963	0.317	3.779	<0.001
SPREF	-0.167	0.410	-0.408	0.683

Site abbreviations are: DB=Deep Bay, DBREF=Deep Bay Reference, MB=Mud Bay, MBREF=Mud Bay Reference, SP=Ships Point, and SPREF=Ships Point Reference.

Table A4. Coefficient estimates, standard error of coefficients, *t* values, and *p* values for linear model fit to data from 30 studies in the literature, with microplastic concentration as the response, and mesh size, sample volume, and the interaction between mesh size and sample volume as predictors.

Covariate	Coefficient	Std. Error of Coefficient	*t* value	*p value*
Mesh size	-0.023	0.006	9.753	<0.001
ln(volume)	-0.973	0.257	-3.788	<0.001
Mesh size * ln(volume)	0.002	0.001	2.106	0.042

References

Amélineau, F., Bonnet, D., Heitz, O., Mortreux, V., Harding, A.M.A., Karnovsky, N., Walkusz, W., Fort, J., Grémillet, D., 2016. Microplastic pollution in the Greenland Sea: Background levels and selective contamination of planktivorous diving seabirds. Environ. Pollut. 219, 1131–1139. https://doi.org/10.1016/j.envpol.2016.09.017

Aytan, U., Valente, A., Senturk, Y., Usta, R., Esensoy Sahin, F.B., Mazlum, R.E., Agirbas, E., 2016. First evaluation of neustonic microplastics in Black Sea waters. Mar. Environ. Res. 119, 22–30. https://doi.org/10.1016/j.marenvres.2016.05.009

Barrows, A.P.W., Cathey, S.E., Petersen, C.W., 2018. Marine environment microfiber contamination: Global patterns and the diversity of microparticle origins. Environ. Pollut. 237, 275–284. https://doi.org/10.1016/j.envpol.2018.02.062

Barrows, A.P.W., Neumann, C.A., Berger, M.L., Shaw, S.D., 2017. Grab vs. neuston tow net: a microplastic sampling performance comparison and possible advances in the field. Anal. Methods 9, 1446–1453. https://doi.org/10.1039/C6AY02387H

Cai, M., He, H., Liu, M., Li, S., Tang, G., Wang, W., Huang, P., Wei, G., Lin, Y., Chen, B., Hu, J., Cen, Z., 2018. Lost but can't be neglected: Huge quantities of small microplastics hide in the South China Sea. Sci. Total Environ. 633, 1206–1216. https://doi.org/10.1016/j.scitotenv.2018.03.197

Castillo, A.B., Al-Maslamani, I., Obbard, J.P., 2016. Prevalence of microplastics in the marine waters of Qatar. Mar. Pollut. Bull. 111, 260–267. https://doi.org/10.1016/j.marpolbul.2016.06.108

Castro, R.O., Silva, M.L., Marques, M.R.C., de Araújo, F.V., 2016. Evaluation of microplastics in Jurujuba Cove, Niterói, RJ, Brazil, an area of mussels farming. Mar. Pollut. Bull. 110, 555–558. https://doi.org/10.1016/j.marpolbul.2016.05.037

Chae, D.-H., Kim, I.-S., Kim, S.-K., Song, Y.K., Shim, W.J., 2015. Abundance and Distribution Characteristics of Microplastics in Surface Seawaters of the Incheon/Kyeonggi Coastal Region. Arch. Environ. Contam. Toxicol. 69, 269–278. https://doi.org/10.1007/s00244-015-0173-4

Cincinelli, A., Scopetani, C., Chelazzi, D., Lombardini, E., Martellini, T., Katsoyiannis, A., Fossi, M.C., Corsolini, S., 2017. Microplastic in the surface waters of the Ross Sea (Antarctica): Occurrence, distribution and characterization by FTIR. Chemosphere 175, 391–400. https://doi.org/10.1016/j.chemosphere.2017.02.024

Cole, M., Webb, H., Lindeque, P.K., Fileman, E.S., Halsband, C., Galloway, T.S., 2015. Isolation of microplastics in biota-rich seawater samples and marine organisms. Sci. Rep. 4. https://doi.org/10.1038/srep04528

Courtene-Jones, W., Quinn, B., Gary, S.F., Mogg, A.O.M., Narayanaswamy, B.E., 2017. Microplastic pollution identified in deep-sea water and ingested by benthic invertebrates in the Rockall Trough, North Atlantic Ocean. Environ. Pollut. 231, 271–280. https://doi.org/10.1016/j.envpol.2017.08.026

de Lucia, G.A., Caliani, I., Marra, S., Camedda, A., Coppa, S., Alcaro, L., Campani, T., Giannetti, M., Coppola, D., Cicero, A.M., Panti, C., Baini, M., Guerranti, C., Marsili, L., Massaro, G., Fossi, M.C., Matiddi, M., 2014. Amount and distribution of neustonic micro-plastic off the western Sardinian coast (Central-Western Mediterranean Sea). Marine Environmental Research, Large marine vertebrates as sentinels of GES in the European MSFD 100, 10–16. https://doi.org/10.1016/j.marenvres.2014.03.017

Desforges, J.-P.W., Galbraith, M., Dangerfield, N., Ross, P.S., 2014. Widespread distribution of microplastics in subsurface seawater in the NE Pacific Ocean. Mar. Pollut. Bull. 79, 94–99. https://doi.org/10.1016/j.marpolbul.2013.12.035

Di Mauro, R., Kupchik, M.J., Benfield, M.C., 2017. Abundant plankton-sized microplastic particles in shelf waters of the northern Gulf of Mexico. Environ. Pollut. 230, 798–809. https://doi.org/10.1016/j.envpol.2017.07.030

Dubaish, F., Liebezeit, G., 2013. Suspended Microplastics and Black Carbon Particles in the Jade System, Southern North Sea. Water. Air. Soil Pollut. 224, 1352. https://doi.org/10.1007/s11270-012-1352-9

Elert, A.M Dubaish, F., Liebezeit, G., 2013. Suspended Microplastics and Black Carbon Particles in the Jade System, Southern North Sea. Water. Air. Soil Pollut. 224, 1352. https://doi.org/10.1007/s11270-012-1352-9., Becker, R., Duemichen, E., Eisentraut, P.,

Falkenhagen, J., Sturm, H., Braun, U., 2017. Comparison of different methods for MP detection: What can we learn from them, and why asking the right question before measurements matters? Environ. Pollut. 231, 1256–1264. https://doi.org/10.1016/j.envpol.2017.08.074

Frère, L., Paul-Pont, I., Rinnert, E., Petton, S., Jaffré, J., Bihannic, I., Soudant, P., Lambert, C., Huvet, A., 2017. Influence of environmental and anthropogenic factors on the composition, concentration and spatial distribution of microplastics: A case study of the Bay of Brest (Brittany, France). Environ. Pollut. 225, 211–222. https://doi.org/10.1016/j.envpol.2017.03.023

Gajšt, T., Bizjak, T., Palatinus, A., Liubartseva, S., Kržan, A., 2016. Sea surface microplastics in Slovenian part of the Northern Adriatic. Mar. Pollut. Bull. 113, 392–399. https://doi.org/10.1016/j.marpolbul.2016.10.031

Gewert, B., Ogonowski, M., Barth, A., MacLeod, M., 2017. Abundance and composition of near surface microplastics and plastic debris in the Stockholm Archipelago, Baltic Sea. Marine Pollution Bulletin 120, 292–302. https://doi.org/10.1016/j.marpolbul.2017.04.062

Gray, A.D., Wertz, H., Leads, R.R., Weinstein, J.E., 2018. Microplastic in two South Carolina Estuaries: Occurrence, distribution, and composition. Mar. Pollut. Bull. 128, 223–233. https://doi.org/10.1016/j.marpolbul.2018.01.030

Isobe, A., Uchida, K., Tokai, T., Iwasaki, S., 2015. East Asian seas: A hot spot of pelagic microplastics. Mar. Pollut. Bull. 101, 618–623. https://doi.org/10.1016/j.marpolbul.2015.10.042

Isobe, A., Uchiyama-Matsumoto, K., Uchida, K., Tokai, T., 2017. Microplastics in the Southern Ocean. Mar. Pollut. Bull. 114, 623–626. https://doi.org/10.1016/j.marpolbul.2016.09.037

Ivar do Sul, J.A., Costa, M.F., Barletta, M., Cysneiros, F.J.A., 2013. Pelagic microplastics around an archipelago of the Equatorial Atlantic. Mar. Pollut. Bull. 75, 305–309. https://doi.org/10.1016/j.marpolbul.2013.07.040

Ivar do Sul, J.A., Costa, M.F., Fillmann, G., 2014. Microplastics in the pelagic environment around oceanic islands of the Western Tropical Atlantic Ocean. Water. Air. Soil Pollut. 225, 2004. https://doi.org/10.1007/s11270-014-2004-z

Kang, J.-H., Kwon, O.Y., Lee, K.-W., Song, Y.K., Shim, W.J., 2015a. Marine neustonic microplastics around the southeastern coast of Korea. Mar. Pollut. Bull. 96, 304–312. https://doi.org/10.1016/j.marpolbul.2015.04.054

Kang, J.-H., Kwon, O.-Y., Shim, W.J., 2015b. Potential Threat of Microplastics to Zooplanktivores in the Surface Waters of the Southern Sea of Korea. Arch. Environ. Contam. Toxicol. 69, 340–351. https://doi.org/10.1007/s00244-015-0210-3

Kanhai, L.D.K., Gårdfeldt, K., Lyashevska, O., Hassellöv, M., Thompson, R.C., O'Connor, I., 2018. Microplastics in sub-surface waters of the Arctic Central Basin. Mar. Pollut. Bull. 130, 8–18. https://doi.org/10.1016/j.marpolbul.2018.03.011

Kanhai, L.D.K., Officer, R., Lyashevska, O., Thompson, R.C., O'Connor, I., 2017. Microplastic abundance, distribution and composition along a latitudinal gradient in the Atlantic Ocean. Mar. Pollut. Bull. 115, 307–314. https://doi.org/10.1016/j.marpolbul.2016.12.025

Kooi, M., Reisser, J., Slat, B., Ferrari, F.F., Schmid, M.S., Cunsolo, S., Brambini, R., Noble, K., Sirks, L.-A., Linders, T.E.W., Schoeneich-Argent, R.I., Koelmans, A.A., 2016. The effect of particle properties on the depth profile of buoyant plastics in the ocean. Scientific Reports 6, 33882. https://doi.org/10.1038/srep33882

Lima, A.R.A., Costa, M.F., Barletta, M., 2014. Distribution patterns of microplastics within the plankton of a tropical estuary. Environ. Res. 132, 146–155. https://doi.org/10.1016/j.envres.2014.03.031

Lusher, A.L., Burke, A., O'Connor, I., Officer, R., 2014. Microplastic pollution in the Northeast Atlantic Ocean: Validated and opportunistic sampling. Mar. Pollut. Bull. 88, 325–333. https://doi.org/10.1016/j.marpolbul.2014.08.023

Lusher, A.L., Tirelli, V., O'Connor, I., Officer, R., 2015. Microplastics in Arctic polar waters: the first reported values of particles in surface and sub-surface samples. Sci. Rep. 5. https://doi.org/10.1038/srep14947

Maes, T., Meulen, V. der, D, M., Devriese, L.I., Leslie, H.A., Huvet, A., Frère, L., Robbens, J., Vethaak, A.D., 2017. Microplastics Baseline Surveys at the Water Surface and in Sediments of the North-East Atlantic. Front. Mar. Sci. 4. https://doi.org/10.3389/fmars.2017.00135

Panti, C., Giannetti, M., Baini, M., Rubegni, F., Minutoli, R., Fossi, M.C., 2015. Occurrence, relative abundance and spatial distribution of microplastics and zooplankton NW of Sardinia in the Pelagos Sanctuary Protected Area, Mediterranean Sea. Environ. Chem. Online Collingwood 12, 618–626. http://dx.doi.org/10.1071/EN14234

Sadri, S.S., Thompson, R.C., 2014. On the quantity and composition of floating plastic debris entering and leaving the Tamar Estuary, Southwest England. Mar. Pollut. Bull. 81, 55–60. https://doi.org/10.1016/j.marpolbul.2014.02.020

Setälä, O., Magnusson, K., Lehtiniemi, M., Norén, F., 2016a. Distribution and abundance of surface water microlitter in the Baltic Sea: A comparison of two sampling methods. Mar. Pollut. Bull. https://doi.org/10.1016/j.marpolbul.2016.06.065

Shim, W.J., Hong, S.H., Eo, S.E., 2017. Identification methods in microplastic analysis: a review. Anal. Methods 9, 1384–1391. https://doi.org/10.1039/C6AY02558G

Song, Y.K., Hong, S.H., Jang, M., Han, G.M., Shim, W.J., 2015. Occurrence and Distribution of Microplastics in the Sea Surface Microlayer in Jinhae Bay, South Korea. Arch. Environ. Contam. Toxicol. 69, 279–287. https://doi.org/10.1007/s00244-015-0209-9

Tamminga, M., Hengstmann, E., Fischer, E.K., 2018. Microplastic analysis in the South Funen Archipelago, Baltic Sea, implementing manta trawling and bulk sampling. Mar. Pollut. Bull. 128, 601–608. https://doi.org/10.1016/j.marpolbul.2018.01.066

Tang, G., Liu, M., Zhou, Q., He, H., Chen, K., Zhang, H., Hu, J., Huang, Q., Luo, Y., Ke, H., Chen, B., Xu, X., Cai, M., 2018. Microplastics and polycyclic aromatic hydrocarbons (PAHs) in Xiamen coastal areas: Implications for anthropogenic impacts. Sci. Total Environ. 634, 811–820. https://doi.org/10.1016/j.scitotenv.2018.03.336

Tsang, Y.Y., Mak, C.W., Liebich, C., Lam, S.W., Sze, E.T.-P., Chan, K.M., 2017. Microplastic pollution in the marine waters and sediments of Hong Kong. Mar. Pollut. Bull. 115, 20–28. https://doi.org/10.1016/j.marpolbul.2016.11.003

van der Hal, N., Ariel, A., Angel, D.L., 2017. Exceptionally high abundances of microplastics in the oligotrophic Israeli Mediterranean coastal waters. Mar. Pollut. Bull. 116, 151–155. https://doi.org/10.1016/j.marpolbul.2016.12.052

Wang, T., Zou, X., Li, B., Yao, Y., Li, J., Hui, H., Yu, W., Wang, C., 2018. Microplastics in a wind farm area: A case study at the Rudong Offshore Wind Farm, Yellow Sea, China. Mar. Pollut. Bull. 128, 466–474. https://doi.org/10.1016/j.marpolbul.2018.01.050

Zhang, W., Zhang, S., Wang, J., Wang, Y., Mu, J., Wang, P., Lin, X., Ma, D., 2017. Microplastic

pollution in the surface waters of the Bohai Sea, China. Environmental Pollution 231, 541–548. https://doi.org/10.1016/j.envpol.2017.08.058

Zhao, S., Zhu, L., Wang, T., Li, D., 2014. Suspended microplastics in the surface water of the Yangtze Estuary System, China: First observations on occurrence, distribution. Marine Pollution Bulletin 86, 562–568. https://doi.org/10.1016/j.marpolbul.2014.06.032

Zhao, S., Zhu, L., Li, D., 2015. Microplastic in three urban estuaries, China. Environmental Pollution 206, 597–604. https://doi.org/10.1016/j.envpol.2015.08.027

Zhu, L., Bai, H., Chen, B., Sun, X., Qu, K., Xia, B., 2018. Microplastic pollution in North Yellow Sea, China: Observations on occurrence, distribution and identification. Sci. Total Environ. 636, 20–29. https://doi.org/10.1016/j.scitotenv.2018.04.182

Appendix B: Supplementary Material for Chapter Three

Table B1

A. Effect of site type (aquaculture vs. reference) on MP concentrations in clams

Formula: glmmadmb(sum ~ site.type + (1 | site/quad) + offset(log(error * tiss.dry.weight)), family = "poisson", link = "log", zeroInflation = TRUE)

	Coefficient estimate	SE	z value	p
Intercept	-1.521	0.197	-7.95	<0.001
site.type = non-aquaculture	-0.241	0.271	-0.89	0.37

n=170; site=17; site:quad =51

B. Effect of site type (aquaculture vs. reference) on MP concentrations in oysters

Formula: glmmadmb(sum ~ site.type + (1 | site/quad) + offset(log(error * tiss.dry.weight)), family = "poisson", link = "log", zeroInflation = TRUE)

	Coefficient estimate	SE	z value	p
Intercept	-3.167	0.151	-20.97	<0.001
site.type = non-aquaculture	-0.114	0.197	-0.58	0.56

n=189; site=19; site:quad=57

C. Effect of region on MP concentrations in clams

Model 1: sum ~ 1 + offset(log(error * tiss.dry.weight))
Model 2: sum ~ region + offset(log(error * tiss.dry.weight))

Model	Log-likelihood	Difference in degrees of freedom	Deviance	p
1	-266.83			
2	-261.55	5	10.56	0.06

D. Effect of region on MP concentrations in oysters

Model 1: sum ~ 1 + offset(log(error * tiss.dry.weight))
Model 2: sum ~ region + offset(log(error * tiss.dry.weight))

Model	Log-likelihood	Difference in degrees of freedom	Deviance	p
1	-327.27			
2	-322.61	5	9.33	0.10

E. Effect of distance to nearest shellfish aquaculture site on MP concentrations in clams

Formula: glmmadmb(sum ~ aqua_nearest_km + offset(log(error * tiss.dry.weight)) + (1 | site/quad), family = "poisson", link = "log", zeroInflation = TRUE)

	Coefficient estimate	SE	z value	p
Intercept	-1.570	0.199	-7.87	<0.001
aqua_nearest_km	-0.304	0.699	-0.44	0.66

n=170; site=17; site:quad=51

F. Effect of distance to nearest shellfish aquaculture site on MP concentrations in oysters

Formula: glmmadmb(sum ~ aqua_nearest_km + offset(log(error * tiss.dry.weight)) + (1 | site/quad), family = "poisson", link = "log", zeroInflation = TRUE)

	Coefficient estimate	SE	z value	p
Intercept	-3.148	0.140	-22.91	<0.001
aqua_nearest_km	-0.491	0.551	-0.89	0.37

n=189; site=19; site:quad=57

G. Effect of site type (aquaculture vs. reference) on MP concentrations in seawater

Formula: glmmadmb(sum ~ site.type + (1 | site) + offset(log(error)), family = "poisson", zeroInflation = TRUE)

	Coefficient estimate	SE	z value	p
Intercept	-0.951	0.309	-3.08	0.002
site.type = non-aquaculture	0.193	0.419	0.46	0.65

n=44; site=16

H. Effect of region on MP concentrations in seawater

Model 1: sum ~ 1 + offset(log(error))
Model 2: sum ~ region + offset(log(error))

Model	Log-likelihood	Difference in degrees of freedom	Deviance	p

1	-107.13			
2	-103.04	3	8.18	0.04

I. Effect of distance to nearest shellfish farm on MP concentrations in seawater

Formula: glmmadmb(sum ~ aqua_nearest_km + offset(log(error)) + (1 | site), family = "poisson", link = "log", zeroInflation = TRUE)

	Coefficient estimate	SE	z value	p
Intercept	-0.639	0.272	-2.35	0.02
aqua_nearest_km	-1.256	1.102	-1.14	0.25

n=44; site=16

J. Effect of MP concentrations in seawater on MP concentrations in clams

Formula: glmmadmb(sum ~ wat.av + (1 | site/quad) + offset(log(error * tiss.dry.weight)), family = "poisson", link = "log", zeroInflation = FALSE)

	Coefficient estimate	SE	z value	p
Intercept	-1.852	0.298	-6.21	<0.001
water.av	-0.095	0.337	-0.28	0.78

n=118; site=12, site:quad=36

K. Effect of MP concentrations in seawater on MP concentrations in oysters

Formula: glmmadmb(sum ~ wat.av + (wat.av | site/quad) + offset(log(error * tiss.dry.weight)), family = "poisson", link = "log", zeroInflation = FALSE)

	Coefficient estimate	SE	z value	p
Intercept	-5.350	0.321	-16.65	<0.001
water.av	-0.175	0.458	0.38	0.7

n=68; site=10, site:quad=20

L. Effect of site type (aquaculture vs. reference) on MP concentrations in sediment

Formula: glmmadmb(formula = sum ~ site.type + (1 | site) + offset(log(error)), family = "poisson", zeroInflation = TRUE)

	Coefficient estimate	SE	z value	p
Intercept	-0.883	0.182	-4.84	<0.001
site.type = non-aquaculture	-0.132	0.255	-0.52	0.60

n=93; site=16

M. Effect of region on MP concentrations in sediment

Model 1: sum ~ 1 + offset(log(error))

Model 2: sum ~ region + offset(log(error))

Model	Log-likelihood	Difference in degrees of freedom	Deviance	p
1	-220.00			
2	-216.55	3	6.89	0.08

N. Effect of distance to nearest shellfish farm on MP concentrations in sediment

Formula: glmmadmb(sum ~ aqua_nearest_km + offset(log(error)) + (1 | site), family = "poisson", link = "log", zeroInflation = TRUE)

	Coefficient estimate	SE	z value	p
Intercept	-0.843	0.165	-5.12	<0.001
aqua_nearest_km	-0.676	0.690	-0.98	0.33
n=93; site=16				

O. Effect of beach slope and sediment grain size on MP concentrations in clams

Formula: glmmadmb(sum ~ beach.slope.deg + PC1 + PC2 + offset(log(error * tiss.dry.weight)) + (1 | site/quad), family = "poisson", link = "log", zeroInflation = TRUE)

	Coefficient estimate	SE	z value	p
Intercept	-1.557	0.220	-7.09	<0.001
beach.slope.deg	-0.023	0.056	-0.42	0.68
PC1	0.114	0.094	1.21	0.23
PC2	0.134	0.136	0.99	0.32
n=148; site=15, site:quad=45				

P. Effect of beach slope and sediment grain size on MP concentrations in oysters

Formula: glmmadmb(sum ~ beach.slope.deg + PC1 + PC2 + offset(log(error * tiss.dry.weight)) + (1 | site/quad), family = "poisson", link = "log", zeroInflation = TRUE)

	Coefficient estimate	SE	z value	p
Intercept	-3.315	0.110	-30.15	<0.001
beach.slope.deg	-0.006	0.032	0.20	0.84
PC1	-0.010	0.047	-0.21	0.83
PC2	-0.184	0.066	-2.78	0.01
n=163; site=17, site:quad=50				

Q. Effect of beach slope and sediment grain size on MP concentrations in water

Formula: glmmadmb(sum ~ beach.slope.deg + PC1 + PC2 + offset(log(error)) + (1 | site), family = "poisson", link = "log", zeroInflation = FALSE)

	Coefficient estimate	SE	z value	p
Intercept	-0.925	0.284	-3.26	0.001
beach.slope.deg	0.038	0.082	0.47	0.64
PC1	-0.158	0.147	-1.07	0.28
PC2	0.085	0.175	0.49	0.63
n=41; site=15				

R. Effect of beach slope and sediment grain size on MP concentrations in sediment

Formula: glmmadmb(sum ~ beach.slope.deg + PC1 + PC2 + offset(log(error)) + (1 | site), family = "poisson", link = "log", zeroInflation = FALSE)

	Coefficient estimate	SE	z value	p
Intercept	-1.219	0.155	-7.86	<0.001
beach.slope.deg	-0.048	0.044	1.08	0.28
PC1	0.079	0.048	1.66	0.10
PC2	0.009	0.059	-0.15	0.88
n=91; site=16				

S. Effect of amount of plastic on site on MP concentrations in clams

Model 1: sum ~ 1 + offset(log(error * tiss.dry.weight))
Model 2: sum ~ plastic + offset(log(error * tiss.dry.weight))

Model	Log-likelihood	Difference in degrees of freedom	Deviance	p
1	-266.83			
2	-265.15	3	3.37	0.34

T. Effect of amount of plastic on site on MP concentrations in sediment

Model 1: sum ~ 1 + offset(log(error))
Model 2: sum ~ plastic + offset(log(error))

Model	Log-likelihood	Difference in degrees of freedom	Deviance	p
1	-223.36			
2	-220.51	3	5.70	0.13

U. Effect of amount of plastic on site on MP concentrations in seawater

Model 1: sum ~ 1 + offset(log(error))
Model 2: sum ~ plastic + offset(log(error))

Model	Log-likelihood	Difference in degrees of freedom	Deviance	p
1	-116.27			
2	-115.21	3	2.13	0.55

V. Effect of amount of plastic on site on MP concentrations in oysters

Model 1: sum ~ 1 + offset(log(error * tiss.dry.weight))
Model 2: sum ~ plastic + 1 + offset(log(error * tiss.dry.weight))

Model	Log-likelihood	Difference in degrees of freedom	Deviance	p
1	-333.96			
2	-324.63	4	18.65	<0.001

W. Model output from Model 2 (from V)

Formula: glmmadmb(sum ~ plastic + 1 + (1 | site/quad) + offset(log(error * tiss.dry.weight)), family = "poisson", link = "log", zeroInflation = TRUE)

	Coefficient estimate	SE	z value	p
Intercept	-3.640	0.275	-13.25	<0.001
plastic-Low	0.305	0.312	0.98	0.33
plastic-Medium	0.539	0.313	1.72	0.09
plastic-High	0.711	0.337	2.11	0.04

n=189; site=19; site:quad=57

Appendix C: Supplementary Material for Chapter Four

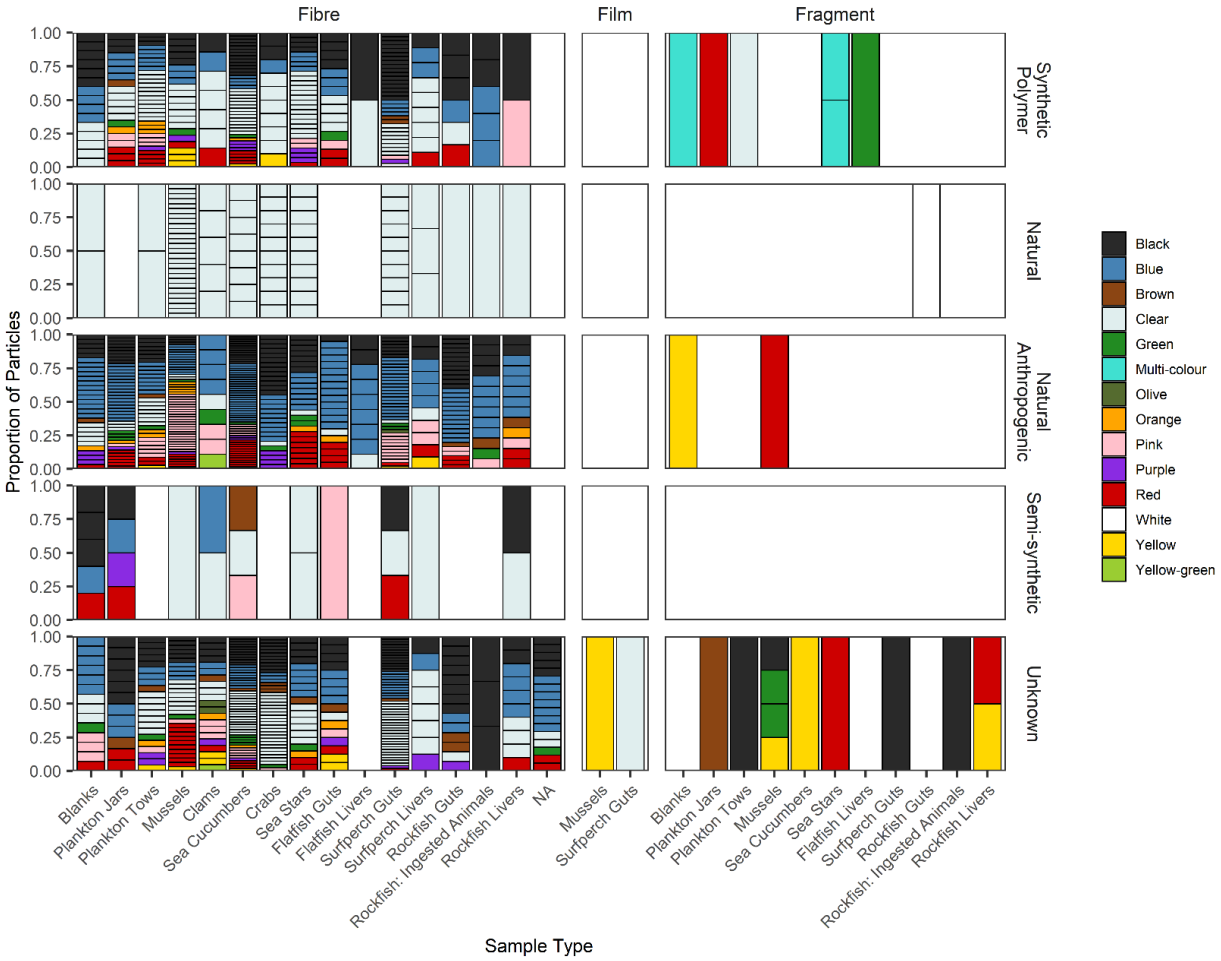

Figure C1: Colours of all potential microplastic particles, by sample type, particle class, and particle shape.

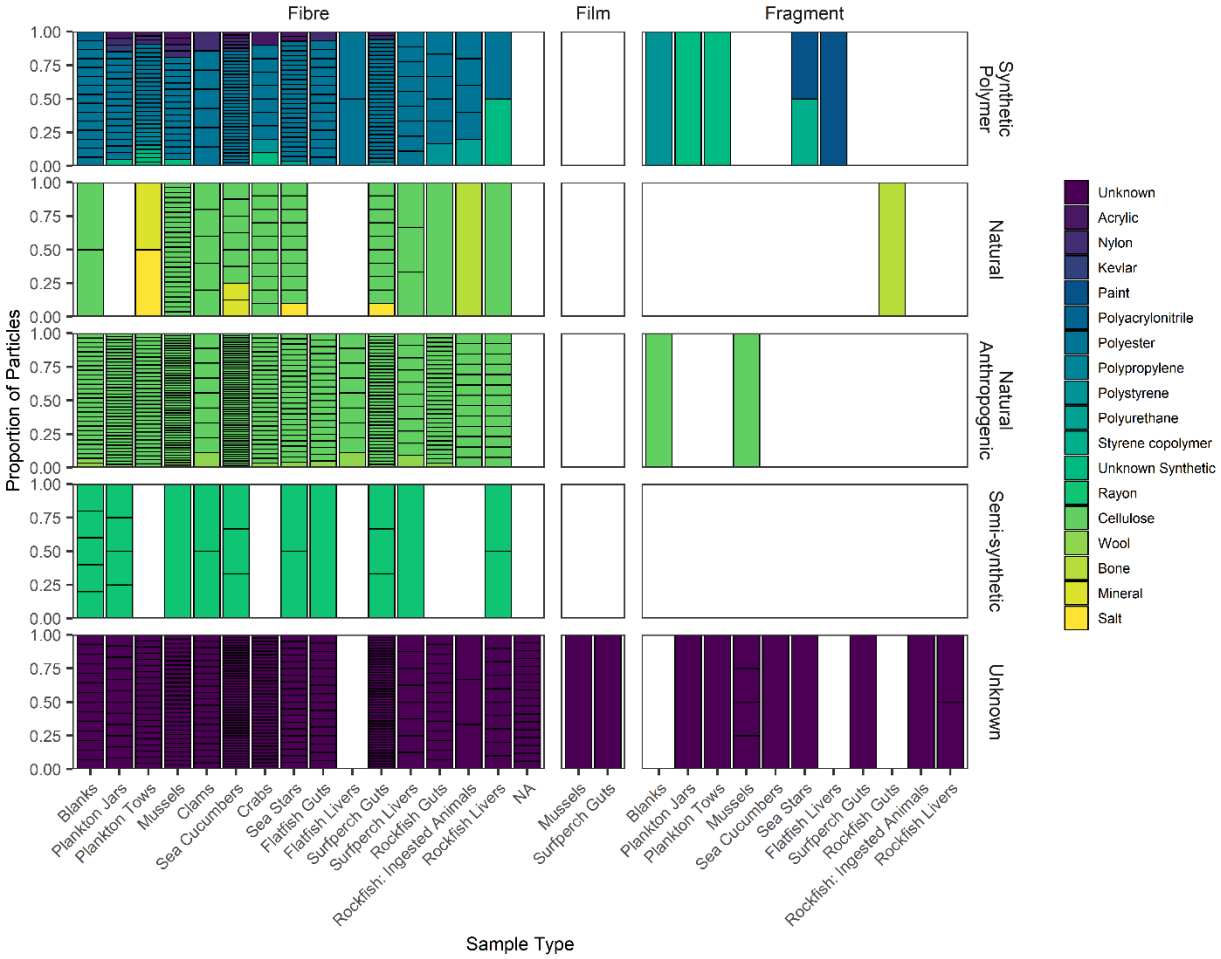

Figure C2: Particle classifications for the 882 particles identified by Raman spectroscopy. Of these particles, 779 were classified as synthetic polymer (microplastics), natural (salt, bone, mineral, or clear cellulose), natural anthropogenic (dyed cellulose or wool), semi-synthetic (rayon) particles.

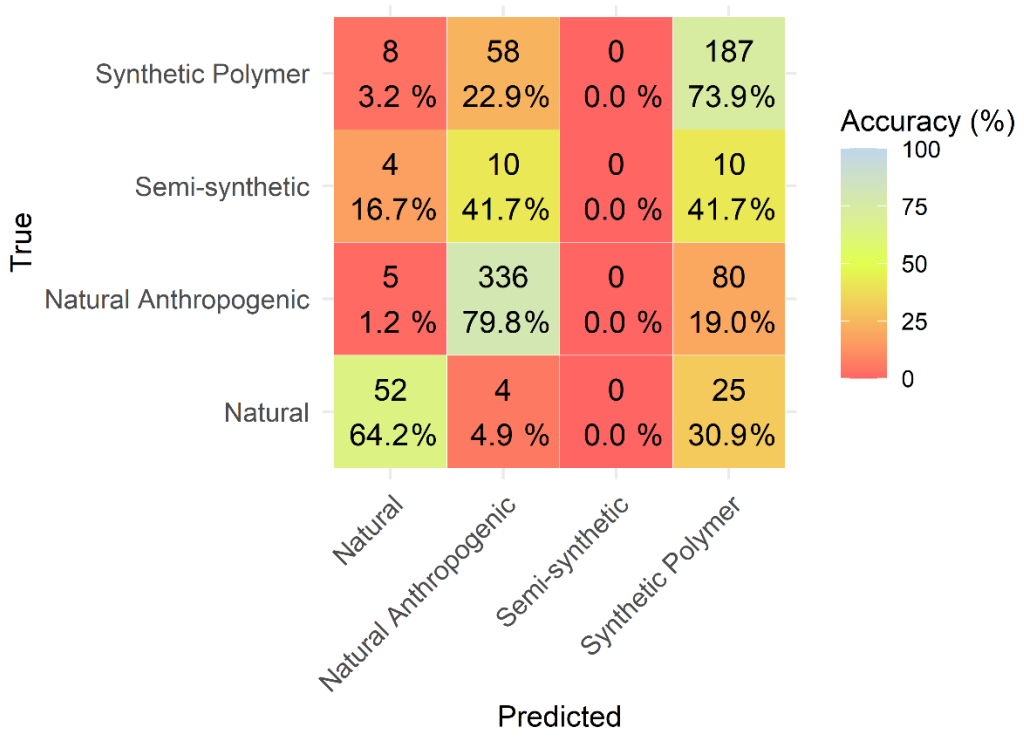

Figure C3: Confusion matrix from the random forest model. Each box contains the number of particles that were correctly or incorrectly classified into each category and the percent of each particle type that were classified into each group. The boxes are coloured according to these percentage values.

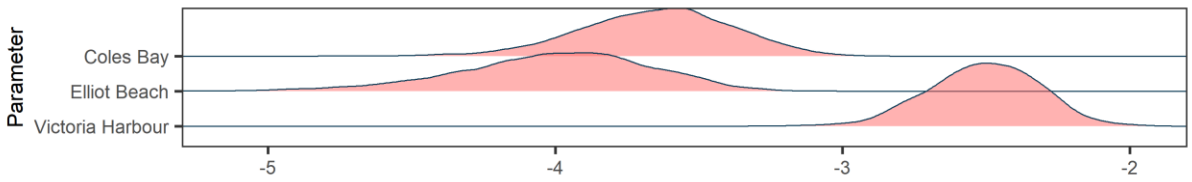

Figure C4: Parameter posteriors for the plankton tow GLMM with microplastic count in each sample as the response variable, site as a predictor, and sample volume as an offset term. Parameter estimates are on the link function (log-scale).

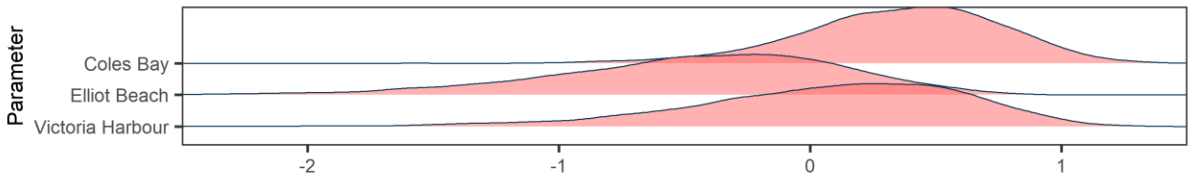

Figure C5: Parameter posteriors for the seawater jar sample GLMM with microplastic count in each sample as the response variable and site as a fixed effect. Parameter estimates on are on the scale of the link function (log-scale).

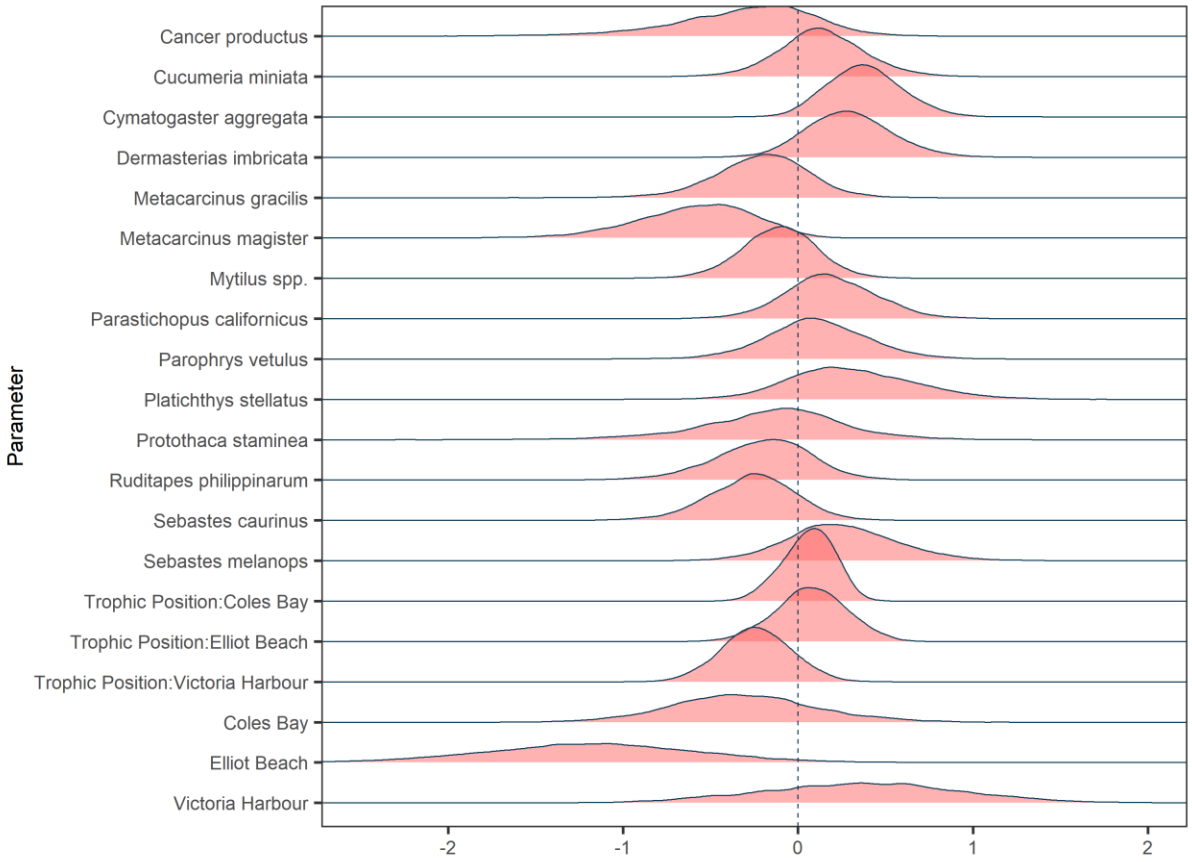

Figure C6: Parameter posteriors for the animal digestive tracts GLMM with number of microplastics in each digestive tract as the response variable, site and the interaction between site and trophic position as fixed effects, and species as a random effect. Parameter estimates on are on the scale of the link function (log-scale).

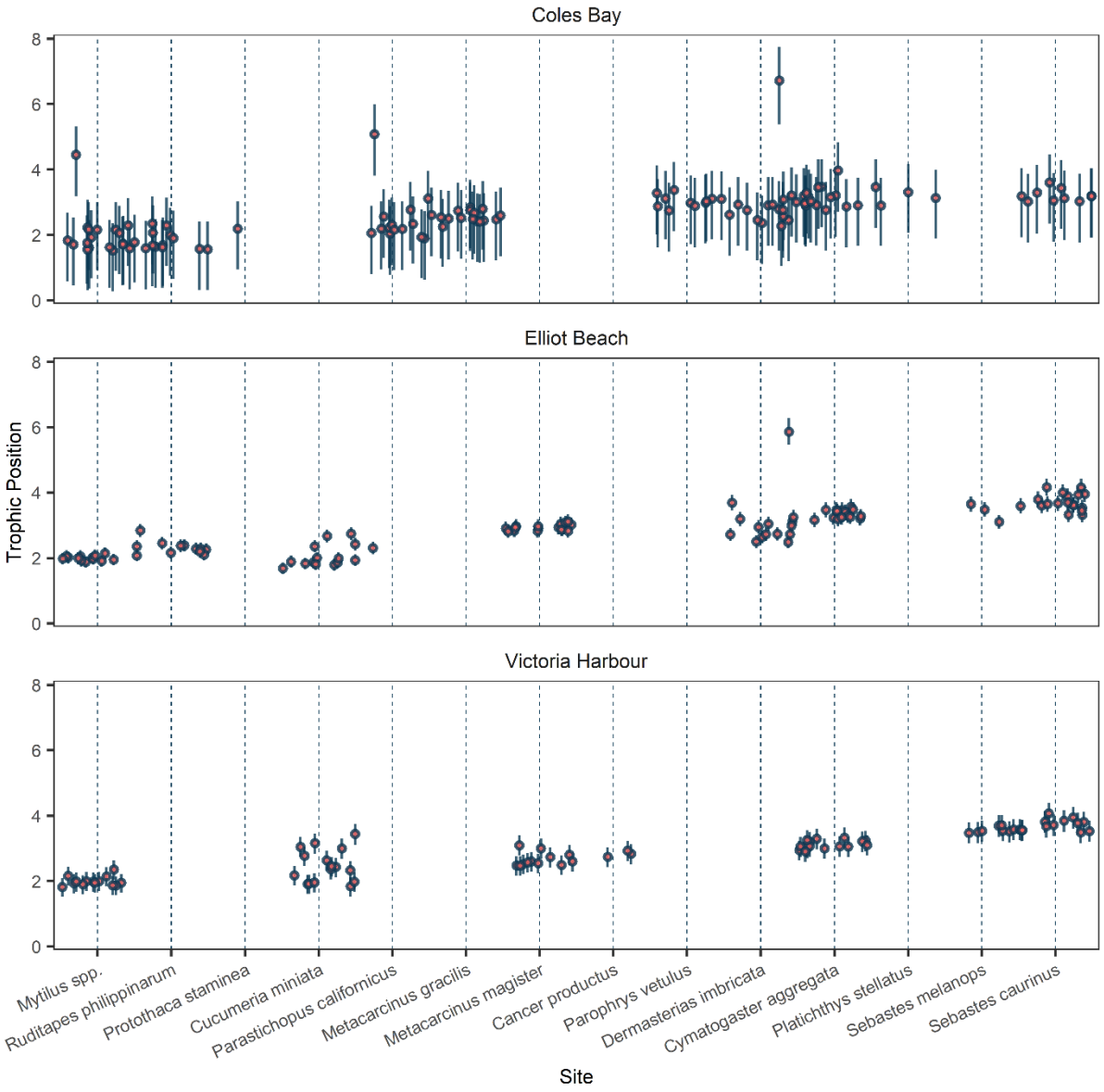

Figure C7: Predicted trophic position for each sampled individual according to the digestive tracts and trophic position GLMM. The points represent the mean of the posterior predictive samples and the lines the 95% credibility interval for each individual of each species.

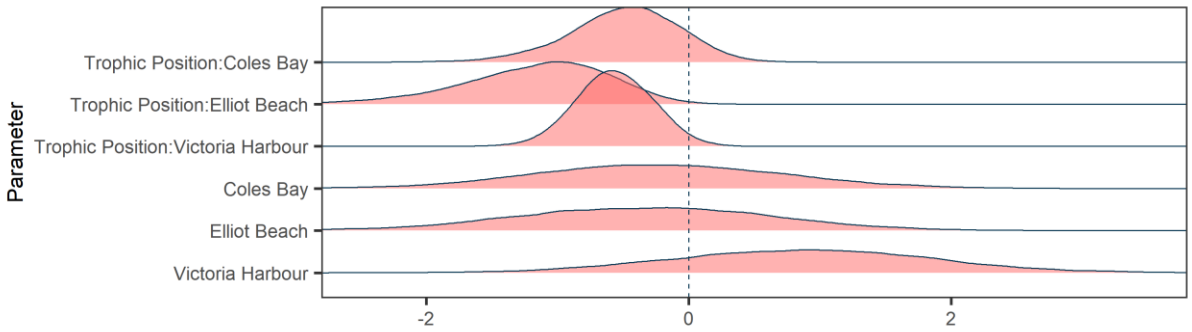

Figure C8: Posteriors for the fish liver GLMM with number of microplastics in a liver as the response variable and site and the interaction between site and trophic position as fixed effects. Parameter estimates on are on the scale of the link function (log-scale).

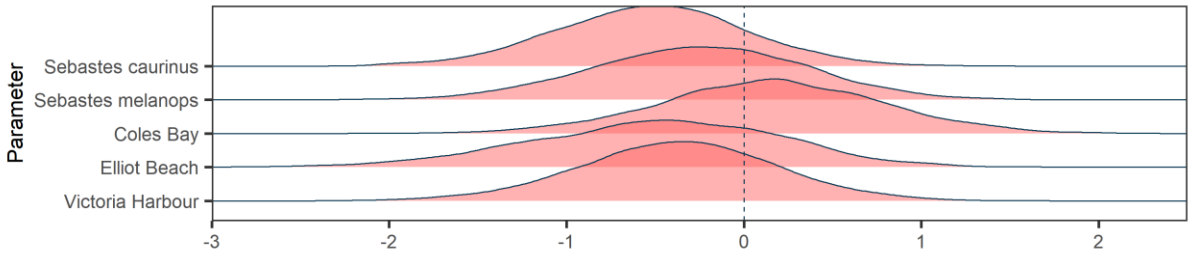

Figure C9: Posteriors for the GLMM quantifying microplastics in animals ingested by the rockfish with number of microplastics in a sample as the response variable and site and species as fixed effects. Parameter estimates on are on the scale of the link function (log-scale).

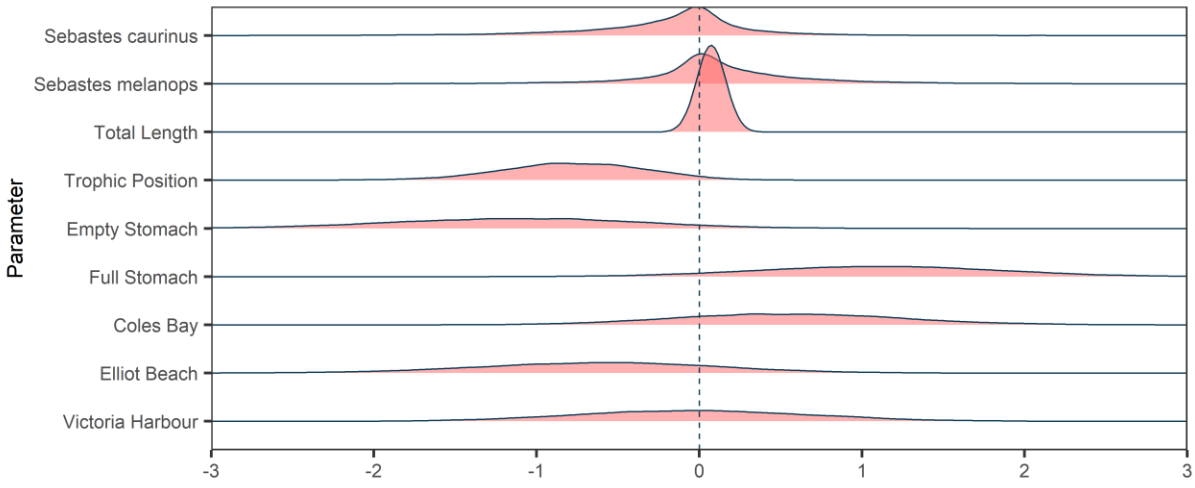

Figure C10: Posteriors for the rockfish digestive tracts GLMM with number of microplastics in a digestive tract as the response variable and fish total length, trophic position, stomach fullness (empty or full), and site as fixed effects and species as a random effect. Parameter estimates on are on the scale of the link function (log-scale).